

Fall 2015

Asymmetric Transfer Hydrogenation of Secondary Allylic Alcohols

Christopher Olugbenga Olusegun Shoola
christopher.shoola@student.shu.edu

Follow this and additional works at: <https://scholarship.shu.edu/dissertations>



Part of the [Organic Chemistry Commons](#)

Recommended Citation

Shoola, Christopher Olugbenga Olusegun, "Asymmetric Transfer Hydrogenation of Secondary Allylic Alcohols" (2015). *Seton Hall University Dissertations and Theses (ETDs)*. 2118.
<https://scholarship.shu.edu/dissertations/2118>

Asymmetric Transfer Hydrogenation of Secondary Allylic Alcohols

*A dissertation submitted in partial fulfillment of the requirements
for the degree of Doctor of Philosophy*

By

Christopher Olugbenga Olusegun Shoola

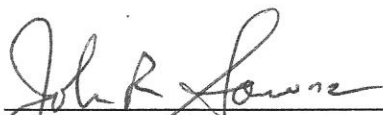
Seton Hall University
Department of Chemistry and Biochemistry
South Orange, New Jersey USA

December, 2015

© 2015 Christopher Olugbenga Olusegun Shoola

We certify that we have read this thesis and that in our opinion it is adequate in scientific scope and quality as a dissertation for the degree of Doctor of Philosophy.

APPROVED



John R. Sowa, Jr., Ph.D.
Research Advisor and Reader



David Sabatino, Ph.D.
Member of Dissertation Committee



Cecilia Marzabadi, Ph.D.
Member of Dissertation Committee



Nicholas Snow, Ph.D.
Chairperson, Department of Chemistry and Biochemistry

Abstract

This dissertation highlights the developments and optimization of a new reaction method that transforms racemic secondary allylic alcohols into optically active secondary alcohols. The key step in this methodology occurs through a ruthenium catalyzed tandem isomerization and asymmetric transfer hydrogenation reaction. This reaction is a one pot, two-step process, which utilizes the unique ability of a transition metal catalyst to effect a combined reduction of the C-C double bond and the carbonyl group in a selected class of secondary allylic alcohols.

With α -vinyl benzyl alcohol as substrate, the optimal catalyst for this reaction was generated *in situ* from a di- μ -chlorobis[(*p*-cymene)chlororuthenium (II)] complex and the chiral ligand (*S,S*)-*TsDPEN* in the presence of potassium hydroxide as a base to afford yields of up to 97% and up to 93% enantiomeric excess (ee) for the desired chiral secondary benzyl alcohol.

Moreover, a series of substituted α -vinyl benzyl alcohols with electron-donating groups (EDG) and electron withdrawing groups (EWG) were tested under the optimized asymmetric transfer hydrogenation (ATH) conditions in order to explore their effects on chemical reactivity. Interestingly, the *ortho*-methyl substituent in α -vinyl tolyl alcohol and the sterically encumbered internal alkene in *trans*-1,3-diphenyl-2-propen-1-ol had the most adverse effects on chemical reactivity (77-86% yields) and enantioselectivities (30-40% ee). Both EWG and EDG at the *para*-positions were found to be well tolerated and exhibited good product yields (>80%)

and enantioselectivities (>90%) underscoring the influence of steric crowding on the reactivity of starting materials.

The mechanism for the isomerization and ATH reaction was proposed to proceed through the transposition of the allylic double bond to generate a carbonyl compound. This reactive intermediate was then reduced to the corresponding chiral secondary alcohol through a metal-ligand bifunctional pathway.

Taken altogether, this thesis describes an important development in the isomerization and ATH reaction of the challenging secondary allylic alcohols. This discovery is not only an essential contribution to this broad reaction class but also in its application towards the synthesis of important targets, such as the LTD₄ antagonist currently marketed as Singulair™.

Dedication

*To all my **TEACHERS**, at every level of my education, your great work has brought me this far.*

I remain forever grateful.

Acknowledgements

My profound gratitude goes to Prof. John R. Sowa Jr. for his commitment, encouragement, and selfless contribution toward my academic development. I am fortunate to have him as my mentor and research advisor.

I thank Prof. David Sabatino for being the chair of my matriculation examination committee, and a member of my dissertation committee, and importantly, for reviewing each chapter of this thesis and providing useful comments.

I also thank Prof. Cecilia Marzabadi for being a member of my dissertation committee and for her support and guidance at various times during my research work.

I thank Profs. Stephen Kelty, Sergiu Gorun and Suliya de-Silva of the College of Science and Mathematics at Montclair State University, Montclair, NJ. They were members of my matriculation examination committee, and provided useful comments early on in my research work.

I thank all the faculty members and the secretaries at the Department of Chemistry and Biochemistry at Seton Hall University, South Orange, NJ for their support and inspirations.

I thank the members of the Sowa research group for their support and good wishes.

I am very grateful to my wife, Imelda, whose support and understanding all through the years of my studies have been my greatest source of inspiration and strength to accomplish this degree.

Likewise, I am very thankful for the birth of our son, Luke, whose presence in our lives has crowned all my efforts towards this degree with brilliant success.

Table of Contents

Abstract	
Dedication	6
Acknowledgements	7
Table of Contents	8
List of Figures	11
List of Schemes	12
List of Tables	15
Abbreviations	16
Chapter One: Transfer Hydrogenation Reactions	18
1.1: Introduction	18
1.2: Reaction Variables in Transfer Hydrogenation	22
1.2.1: Organic Hydrogen Atom Donor	22
1.2.2: Effect of Solvents	23
1.2.3: Effect of Temperature	24
1.2.4: Effect of Promoters	25
1.3: Catalysts in Transfer Hydrogenation	26
1.4: Asymmetric Transfer Hydrogenation (ATH)	28
1.5: Mechanisms of TH and ATH	32
1.6: Ligands for ATH	37
1.7: Catalytic Hydrogenation of Allylic Alcohols	39
1.8: Conclusions	42
References	43

Chapter Two: Accounts of Chemical Research from the Sowa Group

on the ATH of Allylic Alcohols	46
2.1: ATH of primary allylic alcohols	46
2.1.1: Introduction	46
2.1.2: Isomerization-Hydrogenation mechanism – the discovery of ATH reaction of allylic alcohols	48
2.1.3: The development of ATH reaction of allylic alcohols	52
2.1.4: Mechanistic Studies of ATH of allylic alcohols	57
2.1.5: Summary and Outlook	61
2.2. Research objectives of ATH reaction of secondary allylic alcohols	62
2.2.1: Research Objectives	62
2.3: Conclusions	66
References	67

Chapter Three: Development and Optimization of the ATH Reaction of Secondary Allylic Alcohols

3.1: Development of the ATH reaction of secondary allylic alcohols	70
3.2: Optimization of the ATH reaction of secondary allylic alcohols	77
3.3: Postulated mechanism of ATH reaction of secondary allylic alcohols	82
3.2: ATH reaction of derivatives of α -vinyl benzyl alcohol	84
3.3: Evaluation of the Electronic Effects	88
3.4: Conclusions	89
3.5: Experimental Section	90
3.5.1: General Information	90
3.5.2: Procedure for Isomerization/Asymmetric Transfer	

Hydrogenation of Model Substrate	92
3.5.3: Procedure for Synthesis of Allylic Alcohols Derivatives	93
3.6: Experimental Data	94
3.6.1: ATH Product of Model Substrate – α -vinylbenzyl alcohol	94
3.6.2: Synthesis of Intermediates – Derivatives of the model substrate	95
3.6.3: Isomerization/Asymmetric Transfer Hydrogenation Products	98
References	102
Chapter Four: Conclusions and Future Work	103
4.1: General Conclusions	103
4.2: Mechanistic Rationale	105
4.3: Future Work	106
4.4: Publication and Presentations	110
Reference	111
Appendix	113

List of Figures

Figure 1.1. Representative structures of Noyori's ATH catalysts, 1.17-1.19.

Figure 1.2. Representative concerted transition state mechanism of the MPV reduction process.

Figure 1.3. Transition states representing chiral recognition in ATH.

Figure 1.4. C_2 -symmetry representation of privileged ligands.

Figure 1.5. Examples of C_2 -symmetrical ligands used for ATH.

Figure 3.1. Chiral separation of the first attempted ATH reaction of secondary allylic alcohol.

Figure 3.2. Structures of precatalyst, ligand, and presumed metal-ligand catalyst complex.

Figure 3.3. Plot of enantioselectivity vs. energy difference of the diastereomeric transition states.

Figure 3.4. Chiral separation of products of isomerization/ATH reaction of secondary allylic alcohol.

Figure 3.5. ^1H NMR spectrum of 1-phenyl-1-propanol (3.5).

Figure 3.5. FT-IR spectrum of 1-phenyl-1-propanol (3.5).

Figure 3.6. *trans*-1,3-diphenyl-2-propen-1-ol.

Figure 3.7. Comparative trend of relative rates of ATH reaction of secondary allylic alcohols.

List of Schemes

Scheme 1.1. Hydrogen atom transfer of (+)-reynosin, 1.2.

Scheme 1.2. Hydrogen disproportionation reactions of benzaldehyde.

Scheme 1.3. General reaction scheme of a concerted transfer hydrogenation.

Scheme 1.4. First observation of transfer hydrogenation of dimethyl 1,4-dihydroterephthalate, 1.7 into dimethyl terephthalate, 1.8, and dimethyl hexahydroterephthalate.

Scheme 1.5. Aromatization reaction via transfer hydrogenation of cyclohexane and benzene derivatives.

Scheme 1.6. General scheme for the MPV transfer hydrogenation process.

Scheme 1.7. Transfer hydrogenation of acetophenone.

Scheme 1.8. The ATH reactions of aromatic carbonyl compounds, 1.20, to their corresponding chiral secondary alcohols, 1.20-1.28 using IPA as hydrogen atom donor.

Scheme 1.9. The ATH reactions of aromatic carbonyl compounds, 1.20, to their corresponding chiral alcohols, 1.29-1.40 using formic acid as hydrogen atom donor.

Scheme 1.10. Mechanism of hydride transfer from a donor source to acceptor.

Scheme 1.11. Conventional mechanism of transfer hydrogenation with IPA.

Scheme 1.12. ATH mechanism with chiral ruthenium-diamine catalyst complex.

Scheme 1.13. Asymmetric hydrogenation of a chiral allylic alcohol.

Scheme 1.14. Two-point binding of ruthenium complex to allylic substrate.

Scheme 1.15. Asymmetric hydrogenation of geraniol.

Scheme 2.1. Redox isomerization of allylic alcohol to carbonyl compound.

Scheme 2.2. Postulated reaction mechanism for the transformation of secondary allylic alcohols to their corresponding secondary alcohols.

Scheme 2.3. Isomerization-hydrogenation mechanism.

Scheme 2.4. Proposed mechanism for isomerization of geraniol to γ -geraniol.

Scheme 2.5. ATH reaction of geraniol under optimized conditions.

Scheme 2.6. ATH reaction of nerol under optimized conditions.

Scheme 2.7. ATH reaction of 3-phenyl-2-buten-1-ol, 2.9, under optimized conditions.

Scheme 2.8. ATH reaction of geraniol using commercial catalyst complex.

Scheme 2.9. ATH of geraniol without IPA.

Scheme 2.10. ATH reaction of geraniol with deuterated IPA.

Scheme 2.11. ATH reaction of geraniol with mono deuterated IPA.

Scheme 2.12. ATH reaction of deuterated geraniol.

Scheme 2.13. Proposed mechanism of the ATH reaction of primary allylic alcohols.

Scheme 2.14. Proposed model reaction for the ATH reaction of secondary allylic alcohols.

Scheme 2.15. Representative substrate of interest in our investigation.

Scheme 2.16. Evaluation of electronic effects in the ATH of α -vinyl benzylic alcohols 2.21-2.24.

Scheme 2.17. Secondary allylic alcohols of interest in our investigation.

Scheme 3.1. Optimized reaction conditions for primary allylic alcohols.

Scheme 3.2. First attempted ATH reaction of secondary allylic alcohols.

Scheme 3.3. Enantioselective isomerization/transfer hydrogenation mechanism of geraniol.

Scheme 3.4. Isomerization/ATH of secondary allylic alcohol.

Scheme 3.5. Optimized conditions for isomerization/ATH reaction of secondary allylic alcohol.

Scheme 3.6. Proposed mechanism for isomerization/ATH reaction of secondary allylic alcohol.

Scheme 3.7. Charge distribution in the transition state via H-bonding.

Scheme 3.8. Synthesis of derivatives 3.15-3.18 of α -vinyl benzyl alcohol.

Scheme 3.9. Evaluation of electronic effects using competition experiments.

Scheme 4.1. Substituent (a) EWG and (b) EDG effects on the rate of reaction for the ATH of substituted α -vinyl benzyl alcohols.

Scheme 4.2. Proposed mechanism of the chiral ATH of α -vinyl benzyl alcohols.

Scheme 4.3. Proposed synthesis of ibuprofen.

Scheme 4.4. Stereoselective synthesis step for the LTD4 antagonist.

List of Tables

Table 2.1. ATH of geraniol in different hydrogen donors/solvents.

Table 2.2. ATH of geraniol with different chiral ligands.

Table 3.1. Study of the catalytic activity and selectivity.

Table 3.2. Derivatives of α -vinyl benzyl alcohols.

Table 3.3. Isomerization/ATH of substrates under the optimized conditions.

Abbreviations

ATH	-	Asymmetric Transfer Hydrogenation
BINAP	-	2,2'- <i>bis</i> (diphenylphosphino)-1,1'-binaphthyl
BINOL	-	[1,1'-binaphthalene]-2,2'-diol
BIPYRIDINES	-	(S)-6-(sec-butyl)-2,2'-bipyridine
BOX	-	(4S,4'S)-4,4'-diisopropyl-4,4',5,5'-tetrahydro-2,2'-bioxazole
DH	-	Direct Hydrogenation
DIOP	-	[(4S,5S)-2,2-dimethyl-1,3-dioxolane-4,5-diyl] <i>bis</i> (diphenylphosphine)
DOI	-	Digital Object Identifier
ee	-	enantiomeric excess
EDG	-	Electron donating group
equiv.	-	Equivalent
EWG	-	Electron withdrawing group
FA	-	Formic acid
GC-MS	-	Gas Chromatography – Mass Spectroscopy
HPLC	-	High Pressure Liquid Chromatography
IPA, i-PrOH	-	Isopropyl alcohol
i-Pr-DuPHOS	-	1,2- <i>bis</i> ((2S,5S)-2,5-di-i-propylphospholano)benzene
LTD ₄	-	Leukotriene D ₄
mmol	-	Millimole
MeDuPHOS	-	1,2- <i>bis</i> ((2S,5S)-2,5-dimethylphospholano)benzene

mol	-	Mole
M-S	-	Metal–solvent complex
<i>m/z</i>	-	mass to charge ratio
OD-RH	-	Chiracel reverse phase column
PHANEPHOS	-	(S)-4,12- <i>bis</i> (diphenylphosphino)-[2.2]-paracyclophane
R	-	8.3144 g mol ⁻¹ K ⁻¹
RT	-	room temperature
RuCl ₂ -(<i>p</i> -cymene)	-	di-μ-chloro <i>bis</i> [(<i>p</i> -cymene)chlororuthenium (II)] complex
Ru/MeO-BIPHEP	-	Ruthenium complex of (S)-(+)-2,2'- <i>bis</i> [di(3,5-di- <i>t</i> -butyl-4-methoxyphenyl)phosphino]-6,6'-dimethoxy-1,1'-biphenyl,
Ru(OOCCF ₃) ₂ /BINAP	-	Ruthenium <i>bis</i> -trifluoroacetic complex of 2,2'- <i>bis</i> (diphenylphosphino)-1,1'-binaphthyl
SALEN	-	2,2'-Ethylene <i>bis</i> (nitrilomethylidene)diphenol, N,N'-ethylene <i>bis</i> (salicylimine)
T	-	Temperature
TEMPO	-	(2,2,6,6-Tetramethylpiperidin-1-yl)oxyl
TH	-	Transfer Hydrogenation
THF	-	Tetrahydrofuran
TLC	-	Thin Layer Chromatography
TMS	-	Tetramethylsilane
tol-BINAP	-	(S)-2,2'- <i>bis</i> (di- <i>p</i> -tolylphosphosphino)-1,1'-binaphthyl
TsDPEN	-	N- <i>p</i> -toluenesulfonyldiphenylethylenediamine
UV	-	Ultraviolet
ΔΔG [‡]	-	Free energy difference in the transition state

Chapter One: Transfer Hydrogenation Reactions

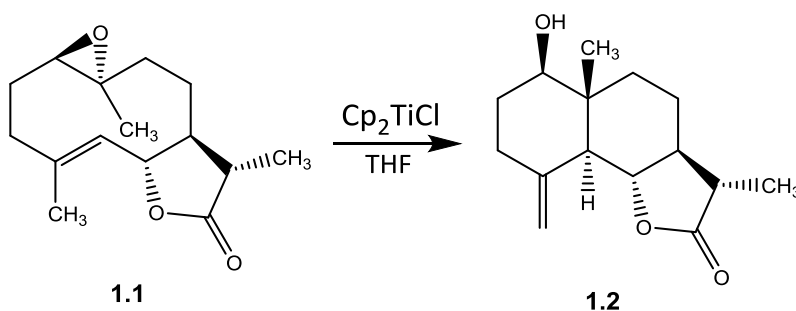
1.1: Introduction

Hydrogenation is a process by which hydrogen atoms are added to an unsaturated organic compound, usually in the presence of a metal catalyst. This addition takes place across the π -bond of unsaturated compounds such as acetylenes, olefins, carbonyls, imines and nitriles. Since usable hydrogenation reactions require the presence of an organometallic catalyst, studies on hydrogenation has long been interwoven with that of catalysis. For example, the first commercialized hydrogenation processes dates back to the seminal works of Dobereiner, applied in the generation of hydroplatinic lamps in 1823 and that of Paul Sabatier in 1897 which led to the production of margarine.¹ These examples have been used as historical reference points in the studies of heterogeneous catalytic hydrogenation processes. Thus, hydrogenation of unsaturated organic compounds is one of the most fundamental classes of reactions in organic chemistry that has been employed in the synthesis of commodity and fine chemicals, with widespread applications in the petrochemical, perfumery, pharmaceutical, functional material and food industries.²

The strategies for hydrogenation are divided into two categories: direct hydrogenation and transfer hydrogenation.³ Direct hydrogenation (DH) is the reduction of multiple bonds using pressurized hydrogen gas as the source of hydrogen atoms – a technique that is very familiar to all organic chemists. Transfer hydrogenation (TH) is the addition of hydrogen atoms to unsaturated compounds using an organic molecule as a hydrogen atom donor in the presence

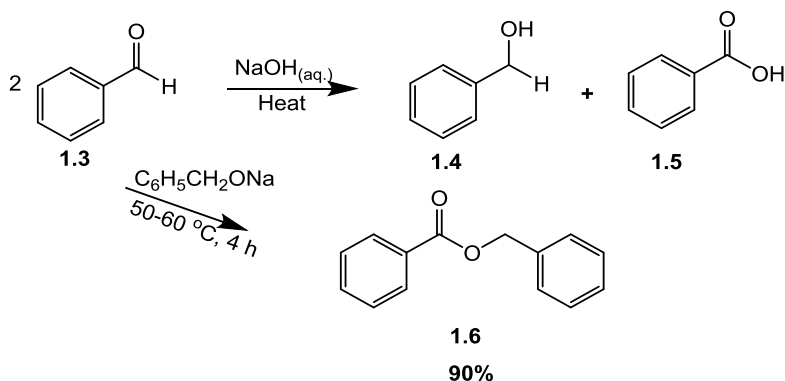
of a catalyst. This technique is commonly referred to as catalytic transfer hydrogenation or simply, TH. It is one of the possible methods of hydrogen atom transfer reactions aptly classified by Braude and Linstead in 1954, into three main categories:⁴

a. Hydrogen atom migrations, occurring within one molecule. For example, thermal mediated hydride shifts in carbocation rearrangements or transition metal mediated radical cyclization reactions.⁵



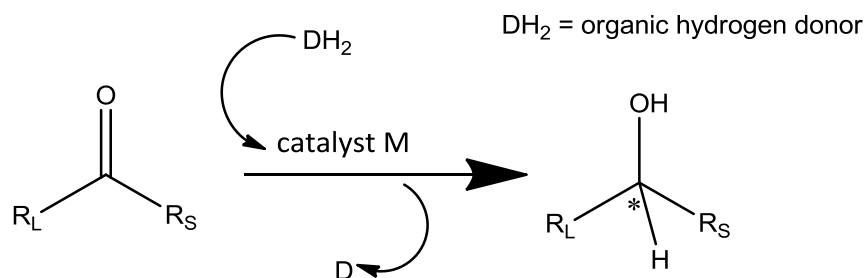
Scheme 1.1. Hydrogen atom transfer of (+)-reynosin, **1.2**.⁵

b. Hydrogen atom disproportionation, involving hydrogen atom transfer between two identical donor and acceptor molecules, for example, the Cannizzaro reaction or the Tishchenko reaction.⁶



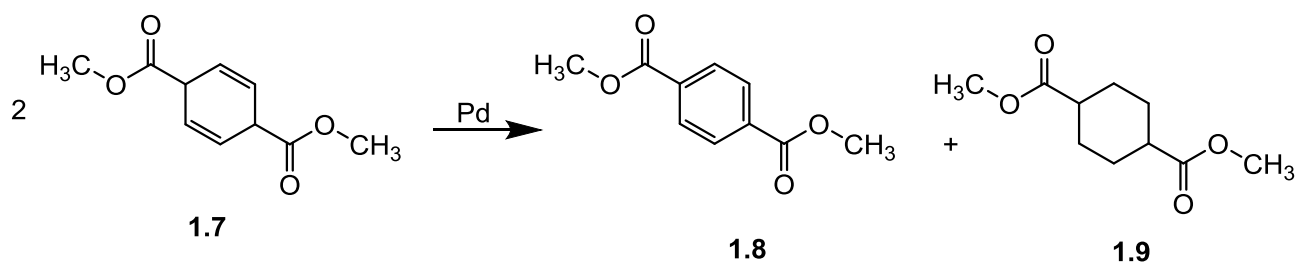
Scheme 1.2. Hydrogen disproportionation reactions of benzaldehyde.⁶

c. Hydrogen atom transfer during a concerted transfer hydrogenation - dehydrogenation processes between two different donor and acceptor molecules, mediated by a metal catalyst complex.



Scheme 1.3. General reaction scheme of a concerted transfer hydrogenation.⁷

This TH reaction was first observed by Knoevenagel in 1903, during the transformation of dimethyl 1,4-dihydroterephthalate into dimethyl terephthalate and hexahydroterephthalate in the presence of palladium black.⁸



Scheme 1.4. First observation of transfer hydrogenation of dimethyl 1,4-dihydroterephthalate, **1.7** into dimethyl terephthalate, **1.8**, and dimethyl hexahydroterephthalate.⁸

Subsequent studies by Wieland and others including the trio of Meerwein-Ponndorf-Verley further confirmed this observation.⁹ Systematic studies of the TH reaction was undertaken by Braude and co-workers, who then suggested in 1952, that catalytic hydrogen

transfer from an organic donor molecule to a variety of organic acceptors might be possible under *mild* conditions. It also demonstrated the practicality of this reaction through the discovery that multiple bonds of ethylenic and acetylenic systems could be reduced in high yield and purity by refluxing with cyclohexene in tetrahydrofuran at 65 °C in the presence of palladium black.¹⁰ Studies following this discovery further established the scope of this reaction as several functional groups including nitro, azo, nitrile and carbonyl groups were reduced.⁴

Since then, transfer hydrogenation became an important and attractive area of research, with diverse subsets of reactions being developed. These were based on the type of catalyst and other variables such as the nature of the organic hydrogen atom donor, solvent effects, temperature, as well as the nature of the functional groups to be reduced.⁴ Each of these variables must be carefully studied in order to develop an efficient transfer hydrogenation process.

The operational simplicity and convenience of TH has made the methodology a powerful alternative to DH, as it does not require the hazardous pressurized hydrogen gas and specialized experimental equipment for reactivity. The availability of the organic alcohol, as hydrogen atom donor coupled with their inexpensive cost and ease of handling have made this reaction widely applicable to a broad range of substrates. Moreover, the side products may be recycled into usable materials and moisture sensitive catalysts have made TH reactions a more advantageous and safer alternative than the DH reactions.¹¹ As a drawback, large amounts of solvent is typically required for this reaction in order to overcome unfavorable thermodynamics, especially, when the alcohol is used as both solvent and hydrogen atom donor.¹²

1.2: Reaction Variables in Transfer Hydrogenation

1.2.1: Organic Hydrogen Atom Donor

An organic compound with a sufficiently low oxidation potential would be a good hydrogen atom donor in a TH reaction under mild conditions. However, at higher temperature and in the presence of a suitable catalyst, almost any organic compound can donate hydrogen atoms – a process referred to as catalytic cracking. Nonetheless, this would be a wasteful and dangerous effort due the difficulty associated with the uncontrolled reactivity of certain classes of organic compounds.⁴ The choice of organic donor, is therefore, generally determined by the reactivity, (that is, the ease of the donor to release hydrogen atom) and availability. Hence, organic donors tend to be hydroaromatics (ability to become aromatic upon releasing hydrogen atoms), unsaturated terpenes, alcohols and triethyl ammonium formate (TEAF). Early research work identified cyclohexene as the preferred hydrogen donor and one of the most frequently employed organic hydrogen donors because of its reactivity and availability. Also frequently used are tetralin, limonene, terpinolene and α -phellandrene.¹³

Moreover, increasing the degree of unsaturation in hydroaromatics leads to a rapid rate of reaction. Therefore, dienes are more reactive than alkenes, while saturated hydrocarbons react more slowly or may not react at all under the TH conditions. Limonene and α -phellandrene are considered more reactive donors given their shorter reaction times.¹³ Also, increasing substituent bulk on the organic donors has been found to reduce reaction rates, particularly when using cyclohexene is used as donor molecule. An activating substituent such as phenyl is noted to increase reaction rates due to its electron-rich π -system. For example, 1-

phenylcyclohexene was found to release hydrogen atoms more quickly than 1-ethylcyclohexene and unsubstituted cyclohexene.¹⁴

Recent studies have shown that the use of alcohols (2-propanol – IPA), formic acid (FA) and triethyl ammonium formate (TEAF) as the hydrogen atom donor and *solvent* have overtaken the use of hydroaromatics, with significant acceleration in reaction rates.³ The hydrogen donor, TEAF in particular, has proven to be a good hydrogen atom donor because of its solubility in many organic solvents. Moreover, dehydrogenation of FA derivatives provides the energetics for TH, since the transfer of hydrogen atom from the formic acid derivative is an irreversible and exothermic process.^{3, 12} Thus, TEAF is the usual alternative hydrogen donor for FA, in a system where unfavorable thermodynamic tendencies of transfer hydrogenations may be expected.¹⁵

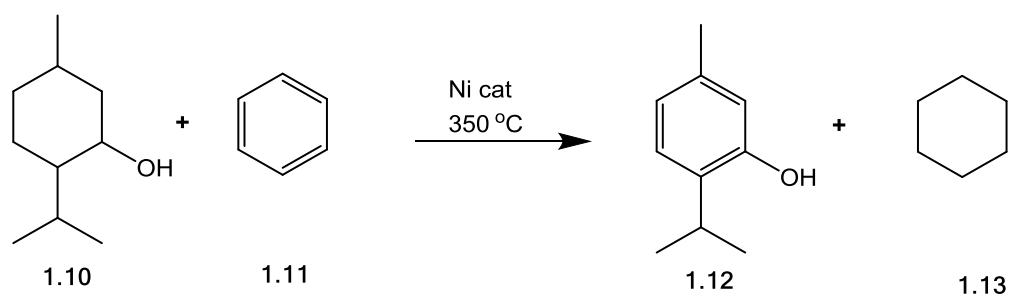
1.2.2: Effect of Solvents

The effect of a solvent on TH is largely limited to its ability to effectively solubilize the reacting species, except in a system where the solvent is also the organic donor.⁴ Early investigation did not find any significant effects of solvent on TH, other than varied reaction times depending on the system under study. Transfer hydrogenation, therefore, showed a wide tolerance for a number of common organic solvents in normal or supercritical states, ionic liquids and recently more common aqueous solvents.¹⁶ The aqueous solvents are becoming increasingly popular because of their green chemistry advantages, good water solubility of commonly employed hydrogen donors, and importantly, in the design and synthesis of efficient water-soluble catalyst complexes. Although, transition metal catalysts tend to be sensitive to

the pH conditions³ (requiring slightly basic pH), a careful balance of the reaction and solvent conditions can enhance selectivity and reduce possible side reactions. Notwithstanding the necessity of aqueous solvents, *pure* alcohols still remain the leading organic solvents for effective TH reactions. For example, isopropyl alcohol (IPA), in particular has been widely employed as hydrogen atom donor and solvent especially, in the TH of carbonyl and imine compounds.¹⁷ The alcohol, IPA is stable, easy to handle, relatively volatile (bp 82 °C), environmentally friendly (nontoxic), inexpensive and dissolves many organic compounds which facilitates reactivity. Furthermore, IPA generates acetone as a by-product, which can be readily removed and recycled for consumption.¹⁷

1.2.3: Effect of Temperature

The reaction temperature is a critical variable in transfer hydrogenation reactions. Early studies have employed hydrogen atom transfer at higher temperatures (usually > 150 °C), particularly, in hydrogen transfer leading to aromatization reactions. For example, the transformation of benzene, **1.11**, to cyclohexane, **1.13** in the presence of a heterogeneous nickel catalyst (Scheme 1.5).¹⁸ Nevertheless, with the advances in the design and synthesis of efficient homogeneous transition metal catalysts coupled with effective hydrogen atom donors, much lower temperatures have been used for effective TH of many organic compounds. The work of Chowdhury and Backvall in the 1990s, particularly made TH reactions possible over a mild range of temperatures; including ambient to refluxing temperatures with noted increased rates of reactions.¹⁹



Scheme 1.5. Aromatization reaction via transfer hydrogenation of cyclohexane and benzene derivatives.¹⁸

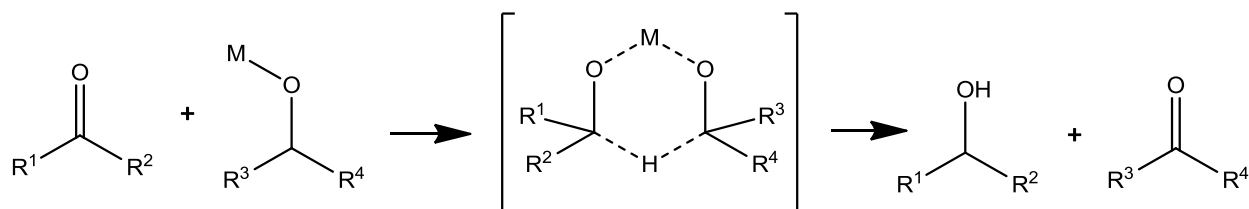
1.2.4: Effect of Promoters

Reaction promoters include strong bases such as potassium hydroxide (KOH), potassium carbonate (K_2CO_3), potassium t-butoxide (KO^tBu), cesium carbonate (Cs_2CO_3), sodium hydroxide (NaOH), sodium alkoxides, and several other inorganic bases like potassium hexamethyldisilazane (KHMDs) and potassium phosphate (K_3PO_4) have all shown to produce beneficial effects on the rates of reaction in TH.^{3, 4, 19} Their influence in the catalytic efficiencies of homogeneous transition metal catalysts is exerted through their role as catalyst preactivation agents. Their presence in the reaction mixture affords a highly active and reproducible catalyst system for effective transfer of hydrogen atoms. For example, in the reduction of ketones with IPA as hydrogen donor, KOH is the usual promoter and its addition is essential, as no reaction occurs in its absence or in low concentrations.^{15a} Nonetheless, TH has recently been shown to occur without the addition of the base in a few cases using iridium and ruthenium based catalysts.²⁰ It is suspected that the dissociated ligands in these cases may be acting as the reaction promoters.

1.3: Catalysts in Transfer Hydrogenation

The presence of a catalyst is a key requirement for a successful TH reaction. Prior to the pioneering MPV reduction of carbonyl compounds in 1925, TH reactions have only been effective with heterogeneous palladium and nickel catalysts albeit at high temperatures. Other known catalysts such as platinum and rhodium did not work.⁴

In the advent of homogeneous catalysis and decades after the publication of the MPV process over an aluminum catalyst, direct transfer hydrogenation via the MPV process have been explored. These were found to occur through the concerted formation of the a cyclic six-membered ring transition state, with other catalysts such as zirconium, lanthanum, cerium, samarium and ytterbium (Scheme 1.6).²¹

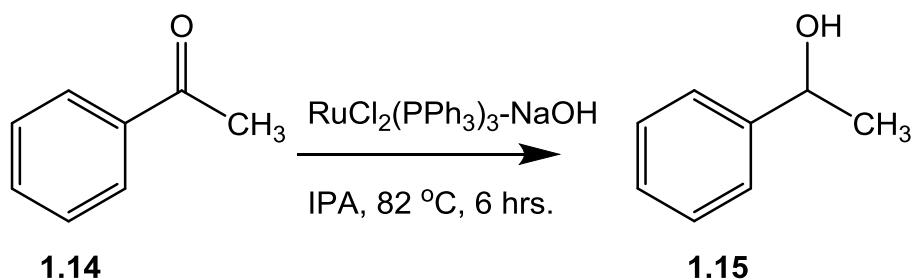


Scheme 1.6. General scheme for the MPV transfer hydrogenation process.²¹

The MPV process has also been reported with the use of heterogeneous Lewis acidic or basic catalysts such as supported aluminum alkoxides, magnesium oxide, hydrotalcites, hydrous zirconia, and supported zirconium complexes, as well as zeolites, and grafted lanthanide alkoxides. Despite its extensive use, this reaction is limited to the ketones and it is not *a truly catalytic* process given the stoichiometry requirement of the reagents, sensitivity of the aluminum catalyst to air and moisture, and the undesirable side products. However, the MPV

process is the harbinger of the successful TH reactions of many varieties of organic compounds today.

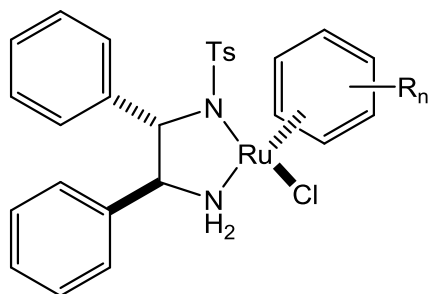
Transfer hydrogenation, therefore, truly became a viable research endeavor with the discovery of organic solvents, and soluble catalyst complexes of late transitional metals such as Fe, Ru, Os, Co, Rh, Ir, Ni, Pd, Pt, Cu, Ag, and Au. These homogeneous catalyst complexes, particularly, complexes of iridium, ruthenium and rhodium showed significant efficient capacity in the TH of carbonyl compounds.³ In the 1960s, Henbest and co-workers demonstrated the efficiency of iridium-hydride in catalyzing the reductions (transfer hydrogenations) of cyclohexanone and α,β -unsaturated ketones to their corresponding alcohols, with IPA as hydrogen atom donor and solvent.²² Sasson and Blum's contribution in the early 1970s showed dichloro*tris*(triphenylphosphine)ruthenium(II) $[\text{RuCl}_2(\text{PPh}_3)_3]$ as an active catalyst in the homogeneous transfer hydrogenations of α,β -unsaturated carbonyl compounds with formyl and IPA donors at high temperatures.²³ This concept was later improved by the work Chowdhury and Backvall in the 1990s, when the duo discovered a significant acceleration in the rate of transfer hydrogenation reactions upon addition of catalytic amounts of NaOH as a co-catalyst.¹⁹ This discovery paved the way for the transfer hydrogenation reaction to be conducted at much lower reaction temperature – room temperature to reflux, leading into the asymmetric transfer hydrogenation (ATH) reaction with chiral ligands.



Scheme 1.7. Transfer hydrogenation of acetophenone.²³

1.4: Asymmetric Transfer Hydrogenation (ATH)

The first example of an ATH reaction was first demonstrated by Doering and Young in 1950 via a partially asymmetric MPV reduction.^{24a} In the beginning of the 1980s, Bianchi and co-workers reported the practical viability of ATH in contemporary chemistry with the use of chiral ruthenium complexes.^{24b,c} Thereon, the ATH reaction became the research focus of several groups and in 1992, Gladiali and co-workers^{15a} reviewed the advances in ATH reactions catalyzed by homogeneous transition metals catalysts with *C*₂-symmetrical chiral ligands. They concluded that ATH reactions rival the classical asymmetric hydrogenation (AH), given the impressive asymmetric induction achieved with chiral iridium, rhodium and ruthenium catalyst complexes in the reduction of carbonyl compounds.¹⁵ A major breakthrough in ATH was reported by Noyori and co-workers in 1995, with the development of ruthenium complexes using chiral diamine ligands (the Noyori-Ikariya catalysts, **1.17-1.19**) Figure 1.1.^{12a}



Ts = SO₂C₆H₄-*p*-CH₃, **1.17**

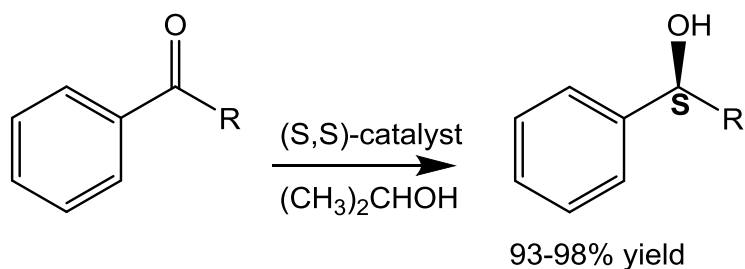
R_n = 1-CH₃-4-CH(CH₃)₂ - *p*-cymene, **1.18**

= 1,3,5-(CH₃)₃ - mesitylene, **1.19**

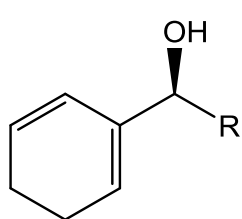
Figure 1.1. Representative structures of Noyori's ATH catalysts, **1.17-1.19**.^{12a}

The efficiency of this catalyst and many of its variants made the ATH one of the most powerful methods for asymmetric reduction of carbonyl compounds. The substrate scope was also extended to other unsaturated substrates such as alkenes, imines and heteroarenes, efficiently converting them to their corresponding *saturated* chiral compounds. Highlights of the ATH reactions with Noyori's class of catalysts are presented in Figure 1.2. Reactions were separately performed using IPA and formic acid as both hydrogen atom donors and solvents.¹⁷

The success of these catalysts in the reduction of a wide range of unsaturated organic compounds and their applications in the syntheses of important bioactive compounds such as carbonic anhydrase inhibitors and LTD₄ antagonists, has not only made the ATH a powerful reaction, but has also elevated the transition metal ruthenium to the level of most classic and popular types of catalysts for highly efficient asymmetric reduction processes.^{12c}

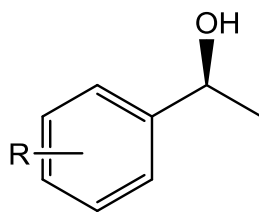


(S,S)-catalyst = $[\text{RuCl}_2(p\text{-cymene})]_2$ - (S,S)-TsDPEN-KOH (mole ratio 1:2:5)



R = CH₃ 97% ee, **1.20**

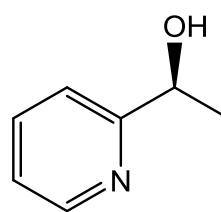
R = C₂H₅ 97% ee, **1.21**



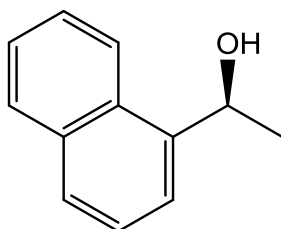
R = *m*-Cl 98% ee, **1.22**

R = *p*-Cl 93% ee, **1.23**

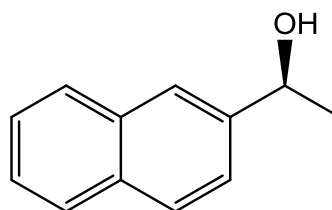
R = *m*-OCH₃ 96% ee, **1.25**



>97% yield, 95% ee, **1.26**

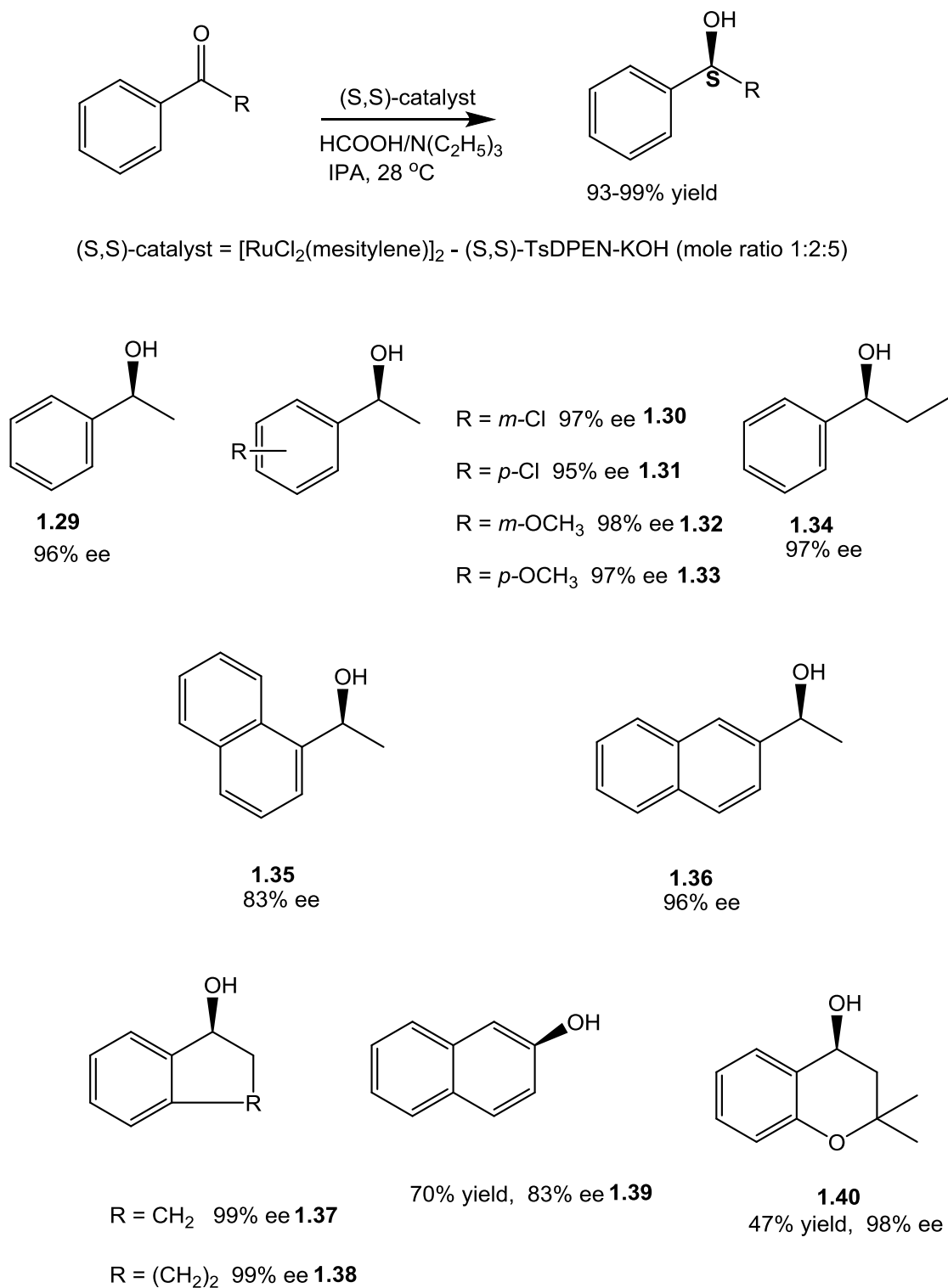


93% ee, **1.27**



98% ee, **1.28**

Scheme 1.8. The ATH reactions of aromatic carbonyl compounds, **1.20**, to their corresponding chiral secondary alcohols, **1.20-1.28** using IPA as hydrogen atom donor.^{12c}



Scheme 1.9. The ATH reactions of aromatic carbonyl compounds, **1.20**, to their corresponding chiral alcohols, **1.29-1.40** using formic acid as hydrogen atom donor.^{12c}

1.5: Mechanisms of TH and ATH

Transfer hydrogenation has long been presumed to operate by two discrete mechanisms, depending on the nature of the metal catalyst and the hydrogen source, both of which have been extensively studied.²⁵ The first mechanism involves a concerted process with direct hydrogen atom transfer occurring in a six-membered transition state that begins with the MPV reduction of carbonyls (Figure 1.2). In this mechanism, the hydrogen donor and acceptor are concertedly coordinated to a metal center, for example, rhodium or iridium to facilitate hydrogen transfer from the donor to the acceptor.

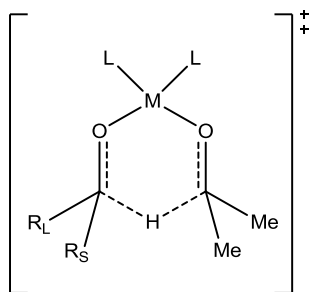
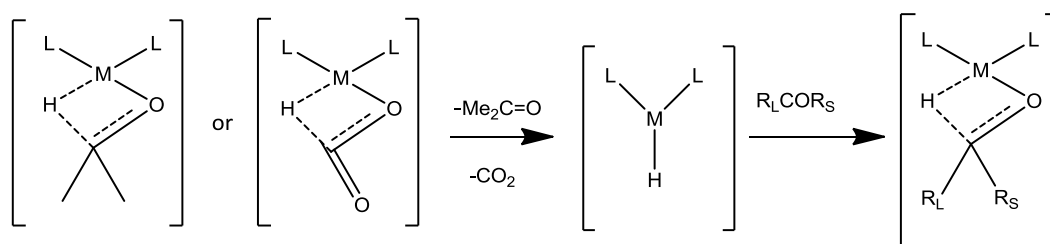


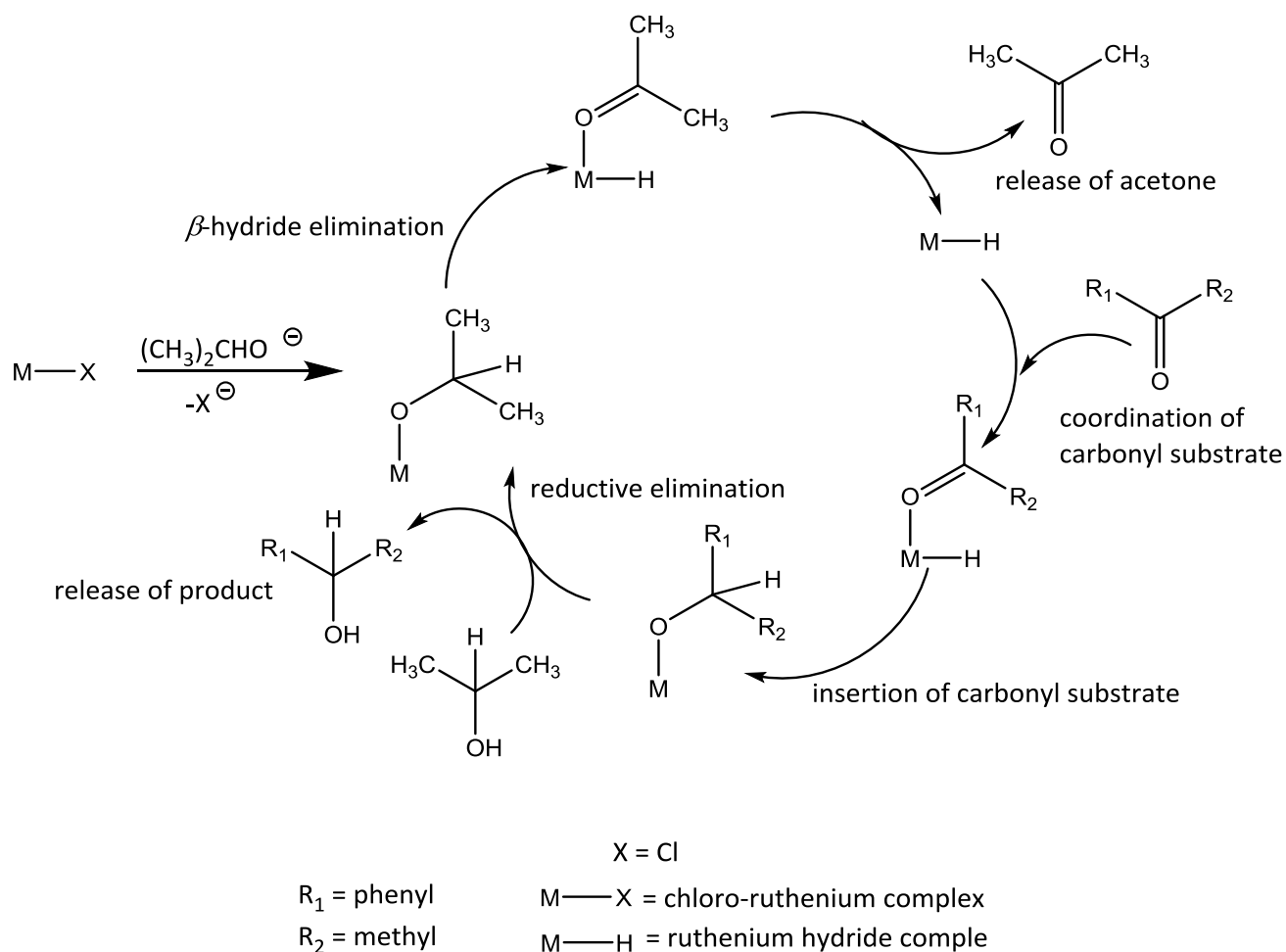
Figure 1.2. Representative concerted transition state mechanism of the MPV reduction process.²⁵

The other proposed mechanism involves a stepwise process via the formation of a metal-hydride complex (Scheme 1.10). The hydrogen atom donor (2-propanol or formic acid) first coordinates to the metal catalyst, followed by the elimination of acetone or carbon-dioxide to generate a metal hydride which then coordinates with the substrate to effect hydride transfer.²⁵



Scheme 1.10. Mechanism of hydride transfer from a donor source to acceptor.²⁵

Both pathways are regarded as inner-sphere mechanisms since the donor and acceptor remain coordinated to the metal center at some point of the *catalytic* cycle. The metal-hydride pathway is considered to be the more conventional mechanism for TH reactions involving transition metal catalysts.²⁶



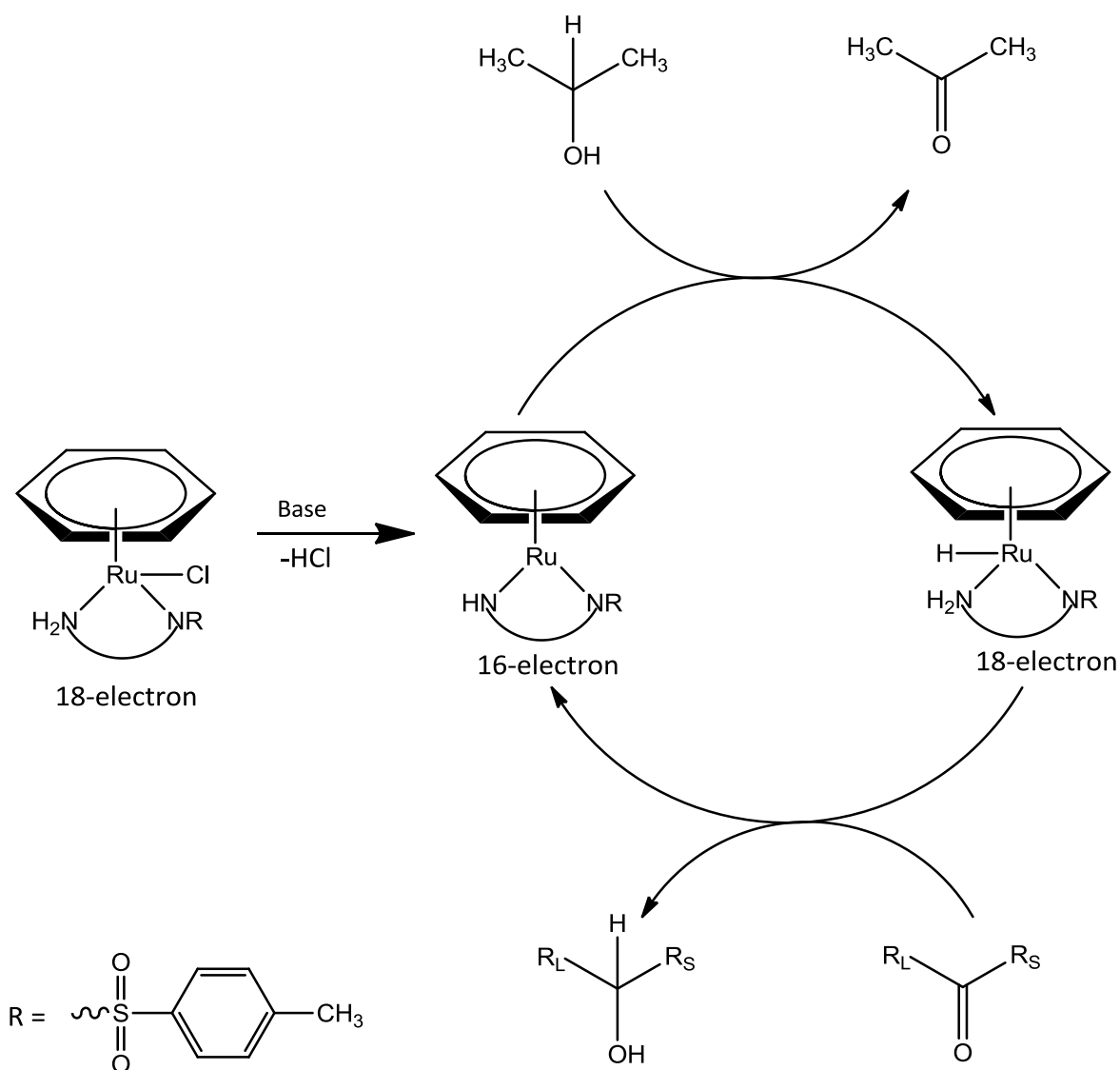
Scheme 1.11. Conventional mechanism of TH with IPA.²⁶

The catalytic cycle of the TH reaction with IPA begins with base (KOH) deprotonation of IPA forming the alkoxide intermediate which coordinates with the dechlorinated metal complex, initially a chloro-ruthenium complex. The β -hydride elimination reaction of the coordinated complex generates the ruthenium metal hydride species which coordinates to the carbonyl substrate. The carbonyl substrate is then inserted into the metal hydride complex via migratory hydride transfer onto the carbonyl carbon of the substrate forming the metal alkoxide complex. Protonation by the incoming hydrogen source releases the alcohol product and the metal

complex via reductive elimination. The metal complex re-enters the catalytic cycle and regenerates the active metal hydride to begin another catalytic cycle. This mechanism has been reasonably explained by Noyori and co-workers, through a combination of known stoichiometry reactions where each elementary step has been well established with model compounds.^{26a, 29}

The mechanism involving formic acid as hydrogen donor with or without trimethylamine as a base has not been clearly stated. Many literature reports have shown the success of transfer hydrogenation with this hydrogen donor over a mild range of temperatures (rt to 70 °C) and using standard operating conditions.²⁷ However, only a few reports have described the use of autoclaves, due to the large increases in reaction pressures observed from production of hydrogen gas and carbon dioxide at higher temperatures (> 125 °C).²⁸ This decomposition of formic acid was also noted under catalytic conditions, and is inconsequential to the process, because the gaseous hydrogen generated does not participate in the alcohol formation.^{15c} The reaction mechanism may be resolved through detailed mechanistic studies by deuterium labeling experiments involving formic acid/triethylamine as the hydrogen donor and solvent.

The excellent performance of Noyori's catalysts introduced a new mechanistic perspective, the outer-sphere mechanism in which the substrate does not interact with the metal center.^{26a} This mechanism is described as a bifunctional metal-ligand mechanism and has been established for the ATH reactions with nitrogen containing ligands. This mechanism involves the critical participation of the ligand's basic amido group of the chiral ruthenium-diamine complex in the hydrogen atom transfer.²⁹



Scheme 1.12. ATH mechanism with chiral ruthenium-diamine catalyst complex.²⁹

The critical role of the ligand amido group begins with the base initiated nucleophilic attack of the 18-electron ruthenium-diamine complex generating a 16-electron ruthenium-amido complex. This step activates the amido nitrogen which is nucleophilic enough to deprotonate IPA with concomitant hydride transfer to the adjacent ruthenium metal center and reestablishes the 18-electron saturated complex. This reactive complex is activated via a highly ordered cyclic transition state with alternate charge distribution (Figure 1.3), which favors a

concerted hydride transfer from the complex to the ketone substrate to afford the alcohol product and catalytic turnover.²⁹ Moreover, this highly ordered cyclic transition state provides the platform for asymmetric induction. This is due to the chiral ruthenium-diamine complex which serves as the source of both the proton and hydride species, thereby allowing the prochiral ketone substrate to orient itself in its most energy minimal geometry in order to induce chiral recognition.

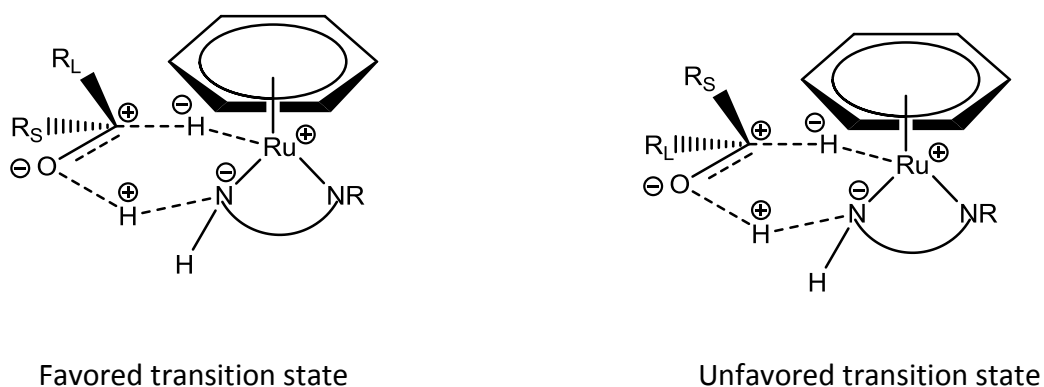


Figure 1.3. Transition states representing chiral recognition in ATH.²⁹

1.6: Ligands for ATH

Over the years, chiral bidentate ligands with C_2 -symmetry have provided excellent stereoselectivity in asymmetric hydrogenation and asymmetric transfer hydrogenation reactions.³⁰ These ligands are regarded as “privileged”, because of their structural characteristics, such as, ease of modification and formation of rigid chiral pockets that facilitate the proximity of the substrate’s prochiral center to the metal coordination site, thereby ensuring

a strong metal substrate binding. The symmetry axes of these ligands create chiral fences around the metal center, thereby narrowing the path towards the metal center. This reduces the number of possible diastereomeric transition states, thus, enhancing asymmetric induction (Figure 1.4). Also, the metal-ligand complexes facilitate substrate-catalyst complex studies, thus, simplifying mechanistic and structure reactivity experiments.³¹ Chiral phosphine ligands remain popular in hydrogen atom transfer reactions, particularly AH involving gaseous hydrogen, with iridium, rhodium and ruthenium metal complexes.^{15a} Chiral ligands containing nitrogen atoms, not phosphorus, are the most used in the field of ATH. This may be due to the less polarizable nature of the nitrogen atom compared to the phosphorus atom, and the ability of the nitrogen atom to localize electron density that may be involved in catalysis. For example, in the bifunctional metal ligand mechanism proposed by Noyori and co-workers,²⁹ the critical role of the amido group can be ascribed to the *nucleophilicity* of the nitrogen atom through its ability to sustain the electron pair in the 16-electron intermediate complex (Scheme 1.12). This results in high catalytic activity as displayed by the chiral ruthenium-diamine complexes.

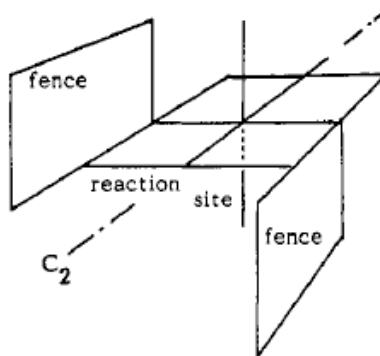


Figure 1.4. C₂-symmetry representation of privileged ligands.

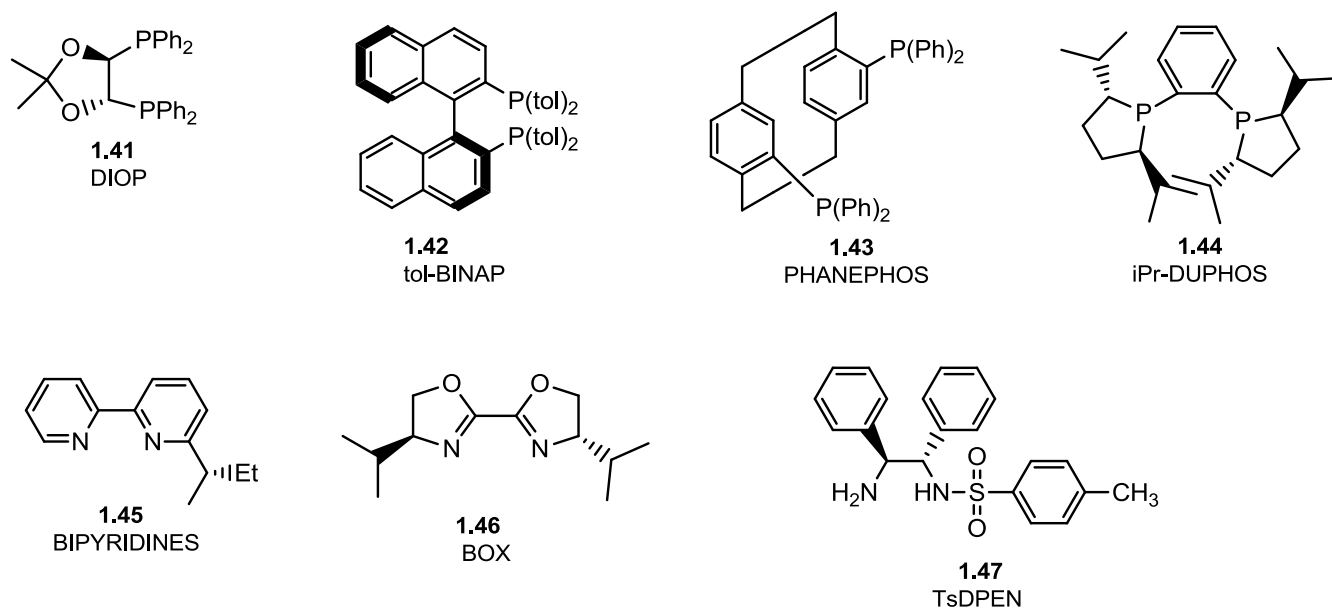


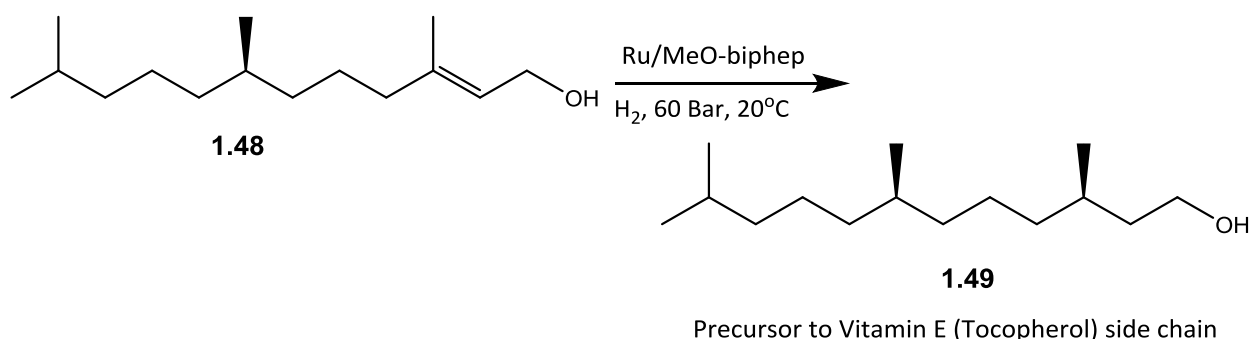
Figure 1.5. Examples of C_2 -symmetrical ligands used for ATH.

1.7: Catalytic Hydrogenation of Allylic Alcohols

Hydrogenation of allylic alcohols often promotes formation of carbonyl compounds due to a thermodynamically favorable process that ensures *almost* exclusive formation of carbonyl compounds as products from allylic alcohols.³² This is because, the addition of a metal hydride to an allylic alcohol causes the transposition of the double bond and generates an enol intermediate which tautomerizes to a carbonyl. This process is energetically favored by about 125 kJ mol^{-1} due to the relative strengths of the C-C, and C=O bonds formed in the product compared to the C-O, and C=C bonds of the reactant.³³ Rhodium, iridium and ruthenium catalysts are suitable DH catalysts for carbonyl compounds, and have been shown to cause

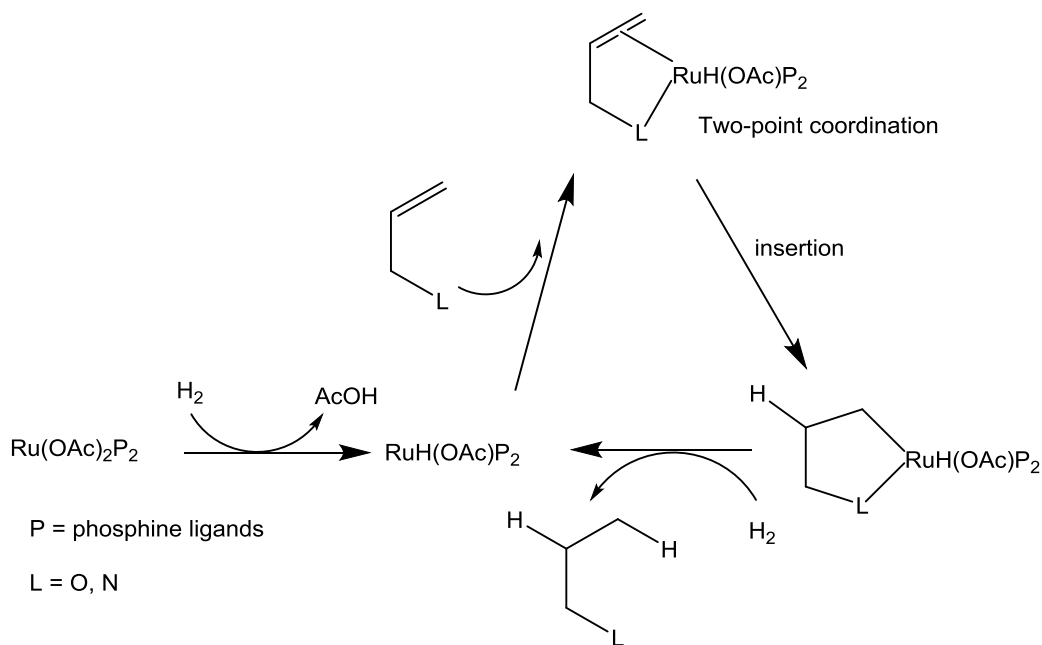
further reduction of the carbonyl compounds generated from primary allylic alcohols under gaseous hydrogenation reactions. In this way, a straightforward access to saturated alcohols is possible with these catalysts, particularly, ruthenium complexes.

Many investigations reporting the hydrogenation of allylic alcohols have been carried out with cyclic and acyclic allylic systems, particularly, geraniol with various transition metals including rhodium, iridium and ruthenium catalysts. The development of chiral ruthenium-BINAP catalysts has made reduction of primary allylic alcohols possible under asymmetric gaseous hydrogenation with high efficiencies (Scheme 1.13). These reactions have led to both applications in the synthesis of fragrances and vitamins.³⁴



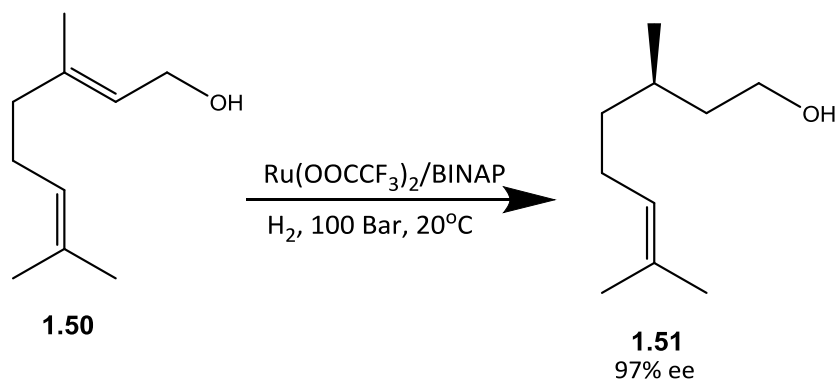
Scheme 1.13. Asymmetric hydrogenation of a chiral allylic alcohol, **1.49**.³⁴

Preliminary mechanistic studies have suggested a two-point binding of the ruthenium complex to the allylic substrate involving coordination of the hydroxyl oxygen and the alkenyl moiety to the metal complex, leading to high stereoselectivity, with the $\text{Ru}(\text{BINAP})(\text{OAc})_2$ catalyst.^{34b} Complexes of iridium containing P,N ligands have also shown similar selectivity.^{34a}



Scheme 1.14. Two-point binding of ruthenium complex to allylic substrate.^{34b}

Geraniol, a primary allylic alcohol, gives (S) or (R)-citronellol in nearly quantitative yields with excellent enantioselectivity (97 %ee) on the reduction of the allylic double bond without affecting the double bond at the C₆ and C₇ positions of the substrate.³⁵ This reduction requires high hydrogen pressures in order to obtain high enantioselectivities, as low pressure causes racemization of the product.



Scheme 1.15. Asymmetric hydrogenation of geraniol.³⁵

1.8: Conclusions

Hydrogenation of unsaturated organic compounds is an important fundamental reaction in organic chemistry. Of the two strategies used for hydrogenation, TH and ATH have been established as essential classes of reactions in modern synthetic chemistry. This is due to their operational simplicity, safety and green chemistry advantages. With the advances in the design and synthesis of more homogeneous catalysts and controllable reaction variables and conditions, the field of ATH has evolved into a powerful research area and safe alternative to the *gaseous* AH. The widening scope of ATH and its tolerance of other functional groups in a variety of organic solvents have made it a choice reaction in the asymmetric synthesis of bioactive compounds and functional materials.

References

1. (a) Rylander, P. N. "Hydrogenation and Dehydrogenation" in *Ullmann's Encyclopedia of Industrial Chemistry*, Wiley-VCH, Weinheim, **2005**. (b) Wisniak, J. *Ind. J. Chem. Tech.*, Vol. 12, **2005**, 232-243.
2. (a) Cervený, L., Ed. *Catalytic Hydrogenation*; Elsevier: Amsterdam, **1986**. (b) de Vries, J. G., Elsevier, C. J., Eds. *The Handbook of Homogeneous Hydrogenation*; Wiley-VCH: Weinheim, **2007**. (c) Andersson, P. G., Munslow, I. J., Eds. *Modern Reduction Methods*; Wiley-VCH Verlag GmbH & Co. KGaA: Weinheim, **2008**.
3. Wang, D., Astruc, D. *Chem. Rev.* **2015**, 115, 6621-6686.
4. Brieger, G.; Nestrück, T. J. *Chem. Rev.* **1974**, 74, 567–580.

5. Barrero, A. F., Oltra, J. E., Cuerva, J. M. and Rosales, A. *J. Org. Chem.*, **2002**, 67, 2566–2571.
6. (a) Cannizzaro, S. *Liebigs Annalen*, **1853**, 88, 129–130. (b) Tishchenko, V. *J. Russ. Phys. Chem. Soc.*, **1908**, 38, 355–402.
7. Palmer, M. J. and Wills, M. *Tetrahedron: Asymmetry*, 10, **1999**, 2045–2061.
8. Knoevenagel, E.; Bergdolt, B. *Chem. Ber.* **1903**, 36, 2857–2860.
9. (a) Wieland, H. *Chem. Ber.* **1912**, 45, 484–493. (b) Verley, A. *Bull. Soc. Chim. Fr.* **1925**, 37, 537–542. (c) Meerwein, H.; Schmidt, R. *Liebigs Ann. Chem.* **1925**, 444, 221–238. (d) Ponndorf, W. *Angew. Chem.* **1926**, 39, 138.
10. Braude, E. A.; Linstead, R. P. *J. Chem. Soc.* **1954**, 3544–3547.
11. (a) Wang, C.; Wu, X.; Xiao, J. Broader, *Chem. Asian. J.* **2008**, 3, 1750–1770. (b) Gladiali, S.; Alberico, E. *Chem. Soc. Rev.* **2006**, 35, 226–236.
12. (a) Hashiguchi, S.; Fujii, A.; Takehara, J.; Ikariya, T.; and Noyori, R. *J. Am. Chem. Soc.* **1995**, 117, 7562–7563. (b) Everaere, K.; Mortreux, A.; *Adv. Synth. Catal.* **2003**, 345, 67–77. (c) Ikariya, T.; Blacker, A. J. *Acc. Chem. Res.* **2007**, 40, 1300–1308.
13. Kindler, K and Luhrs, K. *Liebigs Ann. Chem.*, **1965**, 685, 36.
14. Scribe, P. and Pallaud, R., *Chem. Rev. Acad. Sci.*, **1963**, 256, 1120.
15. (a) Zassinovich, G.; Mestroni, G.; Gladiali, S. *Chem. Rev.* **1992**, 92, 1051–1069. (b) Noyori, R.; Hashiguchi, S. *Acc. Chem. Res.* **1997**, 30, 97–102. (C) Fujii, A.; Hashiguchi, S.; Uematsu, N.; Ikariya, T. and Noyori, R. *J. Am. Chem. Soc.* **1996**, 118, 2521–2522.
16. (a) Mao, J.; Wan, B.; Wu, F. and Lu, S. *Tetrahedron Letters*, **2005**, 46, 7341–7344. (b) Li, X.; Wu, X.; Chen, W.; Hancock, F. E.; King, F. and Xiao, J. *Org. Lett.*, **2004**, 6, 3321–3324.
17. Noyori, R. and Hashiguchi, S. *Acc. Chem. Res.* **1997**, 30, 97–102.
18. Atkins, H.; Richards, L. M. and Davis, J. W. *J. Am. Chem. Soc.*, **1941**, 63, 1320.
19. Chowdhury, R.; Bäckvall, J. *J. Chem. Soc., Chem. Commun.* **1991**, 1063–1064.
20. Carrion, M. C.; Sepulveda, F.; Jalon, F. A. and Manzano, B. R. *Organometallics*, **2009**, 28, 3822–3833.
21. (a) Chuah, G. K.; Jaenicke, S.; Zhu, Y. Z.; Liu, S. H. *Curr. Org. Chem.* **2006**, 10, 1639–1654. (b) de Graauw, C. F.; Peters, J. A.; van Bakkum, H.; Huskens, J. *Synthesis*, **1994**, 10, 1007–1017. (c)

Evans, D.; Nelson, S.; Gagne, M.; Muci, A. *J. Am. Chem. Soc.* **1993**, *115*, 9800. (d) Cohen, R.; Graves, C. R.; Nguyen, S. T.; Martin, J. M. L.; Ratner, M. A. *J. Am. Chem. Soc.* **2004**, *126*, 14796–14803.

22. (a) Haddad, Y. M. Y.; Henbest, H. B.; Husbands, J.; Mitchell, T. R. *Proc. Chem. Soc.*, **1964**, 361–365. (b) Trochagr, J.; Henbest, H. B. *Chem. Commun.* **1967**, 544–544. (c) McPartli, M.; Mason, R. *Chem. Commun.* **1967**, 545–546.

23. (a) Sasson, Y.; Blum, J. *Tetrahedron Lett.* **1971**, *12*, 2167–2170. (b) Blum, J.; Sasson, Y.; Iflah, S. *Tetrahedron Lett.* **1972**, *13*, 1015–1018. (c) Sasson, Y.; Blum, J. *J. Org. Chem.* **1975**, *40*, 1887–1896.

24. (a) Doering, W. E.; Young, R. W. *J. Am. Chem. Soc.* **1950**, *72*, 631–631. (b) Bianchi, M.; Matteol, U.; Menchi, G.; Frediani, P.; Pratesi, U.; Piacenti, F.; Botteghi, C. *J. Organomet. Chem.* **1980**, *198*, 73–80. (c) Matteoli, U.; Frediani, P.; Bianchi, M.; Botteghi, C.; Gladiali, S. *J. Mol. Catal.* **1981**, *12*, 265–319.

25. Palmer, M. J. and Wills, M. *Tetrahedron: Asymmetry*, *10*, **1999**, 2045–2061.

26. (a) Noyori, R.; Yamakawa, M.; Hashiguchi, S. *J. Org. Chem.*, **2001**, *66*, 7931-7944. (b) Mizushima, E.; Yamaguchi, M.; Yamagishi, T. *Chem. Lett.*, **1997**, 237.

27. (a) Murata, K.; Okano, K.; Miyagi, M.; Iwane, H.; Noyori, R.; Ikariya, T. *Org. Lett.*, **1999**, *1*, 1119. (b) Yamada, I.; Noyori, R. *Org. Lett.*, **2000**, *2*, 3425.

28. (a) Wagner, K. *Angew. Chem. Int. Edit.* **1970**, *9*, 50. (b) Watanabe, Y.; Ohta, T.; Tsuji, Y. *Bull. Chem. Soc. Jpn.* **1982**, *55*, 2441.

29. Yamakawa, M.; Ito, H. and Noyori, R. *J. Am. Chem. Soc.* **2000**, *122*, 1466-1478.

30. (a) Dang, T. P. and Kagan, H. B. *J. Chem. Soc. D*, **1971**, 481-481. (b) Nishiyama, H.; Sakaguchi, H.; Nakamura, T.; Horihata, M.; Kondo, M. and Itoh, K. *Organometallics*, **1989**, *8*, 846–848.

31. (a) Seebach, D.; Beck, A. K.; Heckel, A. *Angew. Chem. Int. Ed.* **2001**, *40*, 92–138. (b) Katsuki, T. *Synlett*, **2003**, 281.

32. (a) van der Drift, R. C.; Bouwman, E. and Drent, E. *J. Organomet. Chem.*, **2002**, *650*, 1-24. (b) Uma, R.; Crevisy, C. and Gree, R. *Chem. Rev.* **2003**, *103*, 27-51.

33. Carey, F. A.; Sundberg, R. J.; Advanced Organic Chemistry. Part A: *Structure and Mechanisms*, Plenum Press, New York, **1991**, p. 12.

34. (a) Akutagawa, S. *Top. Catal.* **1997**, *4*, 271. (b) Tsuji, J.; Transition Metal Reagents and Catalysts; *Innovations in Organic Synthesis*, Wiley, **2002**.
35. Takaya, H.; Ohta, T.; Sayo, N.; Kumobayashi, H.; Akutagawa, S.; Inoue, S.; Kasahara, I.; Noyori, R. *J. Am. Chem. Soc.*, **1987**, *109*, 1596-1597.

Chapter Two: Accounts of Chemical Research from the Sowa Group on the ATH of Allylic Alcohols

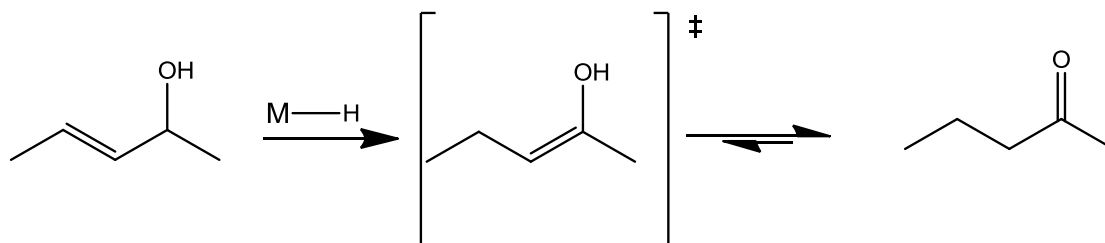
2.1: ATH of primary allylic alcohols

2.1.1: Introduction

The ATH reaction has emerged as a strong alternative to the gaseous AH reaction in the field of asymmetric synthesis. The methodology has been successfully applied to ketones, imines, heteroarenes and activated α,β -unsaturated carbonyls of olefinic and acetylenic moieties in excellent yields and enantioselectivities.¹ The advances in the design and synthesis of homogeneous catalyst complexes, particularly with the introduction of the Noyori-Ikariya chiral ruthenium-diamine catalysts and many of their analogues have provided an extended repertoire of useful chiral alcohols. Moreover, the practical applications of the ATH reaction on industrial scales have made the methodology a powerful chemical process.² However, the ATH appears to fall short in its applications to unsaturated compounds, such as the allylic alcohols, particularly, the secondary allylic alcohols. This is due to the perceived notion that the allylic bond is inactive towards reduction process involving transfer hydrogenation.⁴

It has been established from extensive studies conducted on catalytic hydrogenation of allylic alcohols with transition metals that the metal hydride species are the active catalytic components in the transformations of allylic alcohols into carbonyl compounds.³ This energetically favored transformation allowed the metal hydride to promote internal redox isomerization of the olefinic moiety of the allylic alcohol to form an enol intermediate which upon tautomerization affords the carbonyl compound (Scheme 2.1). This transformative

process has been very successful with catalyst complexes of iron, rhodium and ruthenium metals.⁴



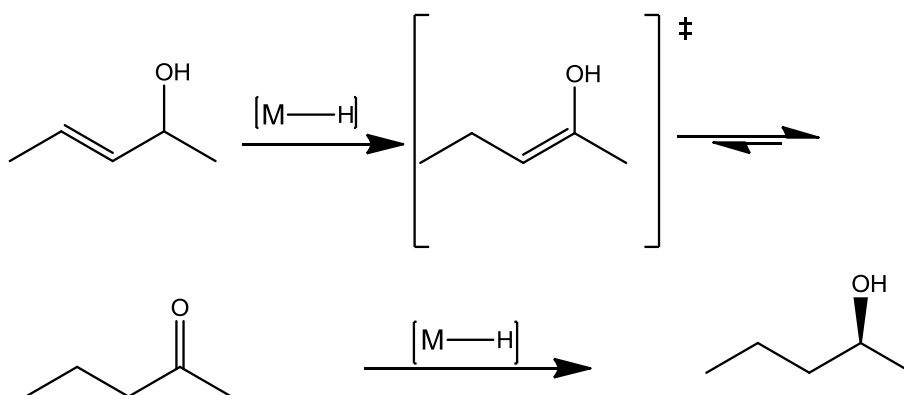
Scheme 2.1: Redox isomerization of allylic alcohol to carbonyl compound.³

Similarly, complexes of iridium, rhodium and ruthenium have been shown to reduce carbonyl compounds to their corresponding alcohols via the preformed or *in situ* generated metal hydrides. This process has been efficiently applied in transfer hydrogenation reactions using IPA as solvent and hydrogen source.^{3, 5}

Therefore, it is reasonable to hypothesize a one-pot, two-step process in which the *catalytic activities of the metal hydride* are effectively sustained under suitable reaction conditions. In this manner, effective reduction of the double bond and the carbonyl group occurs via transposition of the olefinic moiety (redox isomerization) and transfer hydrogenation of the carbonyl group, using IPA. This reaction mechanism was proven following the serendipitous discovery of the ATH reaction of allylic alcohols by the Sowa research group while investigating the effect of pressure changes on the AH of an allylic alcohol – geraniol.

The Sowa research group was able to demonstrate this hypothesis with an asymmetric induction using chiral ruthenium catalyst complexes and IPA. Enantioselection and good product

yields were observed in the isomerization step of primary allylic alcohols, and in the transfer hydrogenation step of secondary allylic alcohols (Scheme 2.2). The reactions with the secondary allylic alcohols not only showed the possibility of the ATH reaction with allylic alcohols, but also pioneered an emerging methodology to optically active secondary alcohols made directly from racemic secondary allylic alcohols under mild reaction conditions.¹⁷

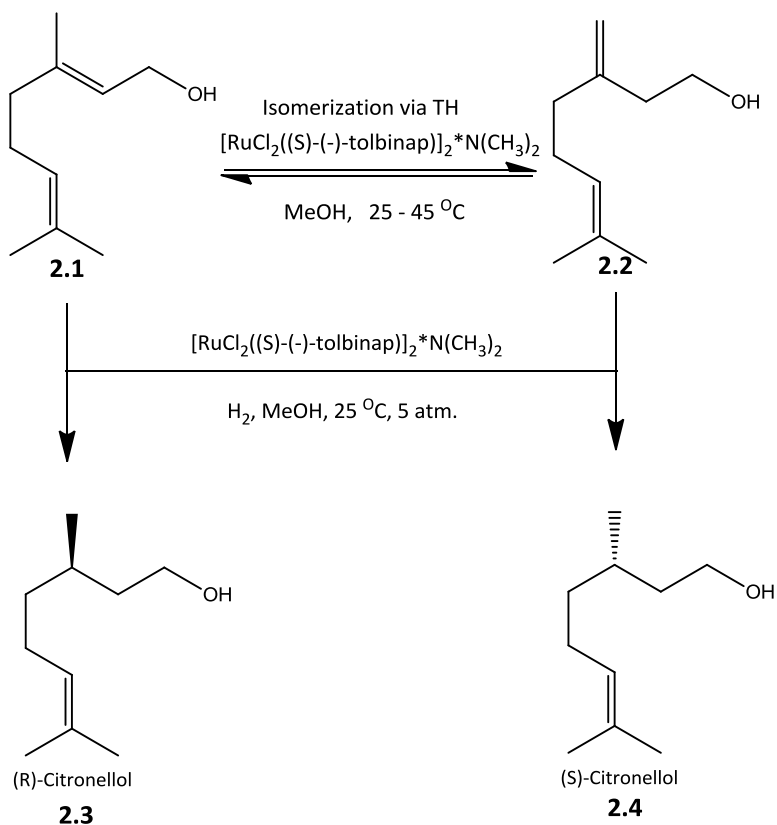


Scheme 2.2: Postulated reaction mechanism for the transformation of secondary allylic alcohols to their corresponding secondary alcohols.

2.1.2: Isomerization-Hydrogenation mechanism – the discovery of ATH reaction of allylic alcohols

In 1995, the Sowa research group was prompted to understand the rationale for the observed effects of hydrogen gas pressure on the enantioselectivity of the hydrogenation of geraniol. In the studies conducted, a striking inversion of stereochemistry became evident in the formation of the hydrogenated products between the initial and final conversions of geraniol mediated by the (S)-dichlororutheniumtol-BINAP catalyst in methanol. A close monitoring of the

reaction revealed an isomerization-hydrogenation mechanism (Scheme 2.3).⁶ The initial isomerization step involved an interconversion between the internal olefin in geraniol (**2.1**) and external olefin in γ -geraniol (**2.2**). This step was found to occur during the dissolution of the catalyst in a mixture of geraniol and methanol prior to the addition of hydrogen gas. This observation was rationalized by the confirmed presence of γ -geraniol in the reaction mixture according to ¹H NMR spectrum.^{6a} These prochiral olefin isomers then underwent hydrogenation reactions upon addition of hydrogen gas resulting in their respective citronellol isomers, **2.3**, and, **2.4** (Scheme 2.3).^{6a}

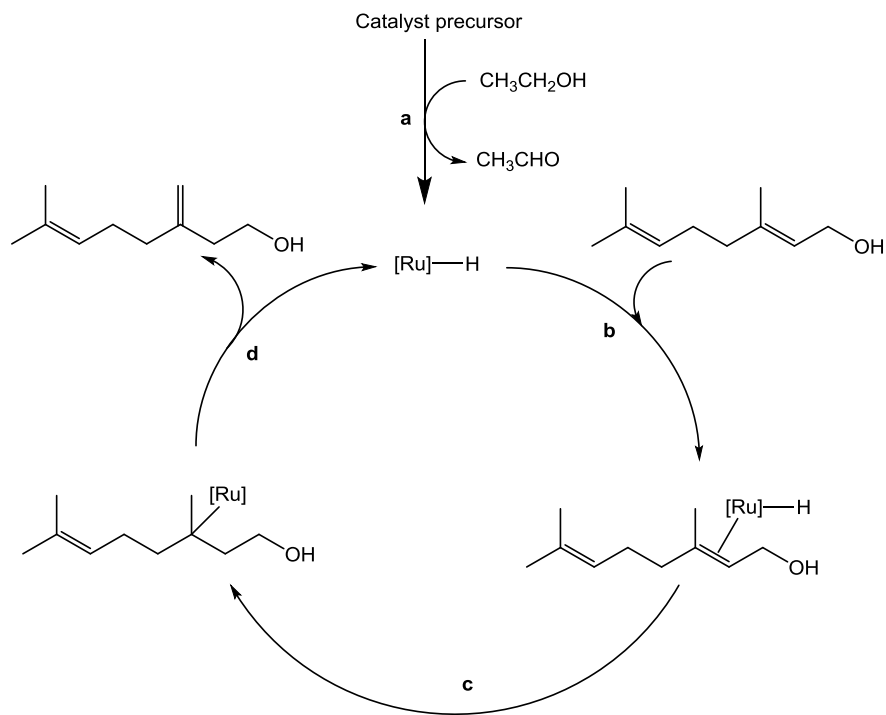


Scheme 2.3. Isomerization-hydrogenation mechanism.^{6a}

A temperature dependent study indicated an increase in the rate of isomerization reaction in between 25 °C and 45 °C with an increase in the concentration of γ -geraniol during the isomerization of geraniol. This is consistent with literature reports which suggested that a strongly competitive isomerization reaction is typically unavoidable in this type of procedure.⁷ It has also been suggested that the competitive isomerization may be suppressed by high hydrogen pressures in order to increase enantioselectivity.⁸ The effect of isomerization between **2.1** and **2.2** indicated that the rates of the interconversion and subsequent hydrogenation are key variables in determining the stereochemical outcome of asymmetric hydrogenation of the allylic alcohol substrate - geraniol.^{6a}

Based on these results, the Sowa research group investigated the isomerization (equilibration) process by NMR and chiral HPLC techniques. These experiments were based on the hypothesis that the hydrogen atom was being transferred by an *in situ* generated ruthenium hydride catalyst dissolved in methanol. This isomerization step also occurred in other oxidizable alcohol solvents such as ethanol and IPA, but failed to occur in *t*-butanol and *t*-butanol/water combination. This indicated that the hydrogen atom alpha to the hydroxyl group was being transferred from the alcohol solvent to the ruthenium metal via thermal oxidation or by an *auto-oxidation* process, to generate the required ruthenium hydride. This can be rationalized by the proposed mechanism highlighted in Scheme 2.4.^{6b} This presumed mechanism was postulated to begin with thermal or auto-oxidation of ethanol (**a**), generating the ruthenium hydride which coordinates with geraniol (**b**) via the hydroxyl allylic olefin moiety. This is followed by migratory insertion of the hydride into the olefin moiety (**c**). The β -elimination of the

ruthenium metal via external methyl group releases γ -geraniol and regenerates ruthenium hydride which cycles back into the isomerization process (d).



Scheme 2.4: Proposed mechanism for isomerization of geraniol to γ -geraniol.^{6b}

Moreover, a surprising result was obtained in an attempt to further understand the isomerization process in between geraniol and γ -geraniol. (R)-Citronellol was unexpectedly formed in 50 % ee and 27 % yield, among other products, when a mixture of geraniol, alcohol solvent and the catalyst were stirred at 140 °C for 72 hours. Surprisingly, γ -geraniol was not formed during this reaction process. This result ultimately changed the direction of the investigation. The formation of the optically active citronellol from geraniol indicated an

enantioselective isomerization-*transfer* hydrogenation process, that is, an ATH reaction of the allylic alcohol – a process that until then had not before been reported in the literature.^{6b}

2.1.3: The development of ATH reaction of allylic alcohols

Prior to the discovery of the ATH reaction of allylic alcohols by the Sowa group, allylic alcohols were considered inactive towards reduction reactions involving transfer hydrogenation procedures.⁴ Although some research was attempted with homogeneous and heterogeneous catalysts,⁹ no literature reports described transfer hydrogenation of allylic alcohols at the time. Thus, it became imperative to carefully study the key reaction parameters for the development and optimization of the ATH reaction of allylic alcohols using geraniol as a model substrate.

The notable hydrogen atom donors and solvents in the ATH reactions, such as IPA and formic acid, are cheap and readily available.¹⁰ Moreover, IPA is a safer, non-toxic and environmentally benign choice, however, it has an unfavorable thermodynamic equilibrium associated with its by product – acetone. This has been shown to effect reactivity and selectivity in the ketone substrates.¹¹ Nonetheless, the use of a large excess of solvent (IPA) can be employed to drive the equilibrium towards the desired product. In contrast, formic acid presents a better alternative to overcome the thermodynamic factors hindering the applications of IPA. However, the tendency of formic acid to decompose into hydrogen gas and carbon dioxide at elevated temperature results in elevated pressures which raises safety concerns.¹² Although, this has been suggested to not be a limiting issue,¹³ IPA was chosen as hydrogen atom donor for the development of ATH reactions of allylic alcohols.

Other alcohol compounds were examined as hydrogen atom donors and solvents, but IPA furnished better results (Table 2.1, entry 1).

Table 2.1. ATH of geraniol in different hydrogen donors/solvents.¹⁶

Entry	H-atom Donor/Solvent	Temp. (°C)	% Conversion ^b	ee ^c (R)
1	IPA	100	100	98
2	2-Pentanol	100	84	79
3	2-Pentanol	120	100	77
4	(S)-2-Pentanol	120	100	72
5	(R)-2-Pentanol	120	100	26
6	Cyclohexanol ^d	100	74	72
7	Cyclohexanol ^d	160	100	66

^aReaction time was 2 h. ^bConversions measured by GC. ^cee analysis measured with a RT-Beta

DEXsa 30 m x 0.32 mm ID x 0.25 µm GC Column. ^dReaction time was 4 h.

The long established efficiencies of the chiral ruthenium complexes in the AH and the ATH of ketones, along with the concept of bifunctional catalysis made the ruthenium metal well suited for the investigation of the ATH reactions of allylic alcohols. The ruthenium polymer - [Ru(COD)Cl₂]_n was chosen as the catalyst precursor and as a source of ruthenium because of its convenient reactivity in the formation of the pre-requisite metal-ligand complexes. Among the chiral bidentate ligands that were evaluated for the ATH of allylic alcohols, (S)-tol-BINAP, (R)-BINAP and (S,S)-iPr-DUPHOS showed very high catalyst activity with the ruthenium polymer

and yielded complete conversion of geraniol and significant enantioselectivities (up to 98% ee) of the desired product citronellol (Table 2.2, entry 5). The reaction was developed with (S)-tol-BINAP, because it offered the best results in substrate conversion and % ee.

Table 2.2. ATH of geraniol with different chiral ligands.¹⁶

Entry	Ligand	Time (h)	% Citronellol ^a (% Conversion ^a)	% ee, ^b (Configuration)
1	(S,S)-DIOP	20	31 (38)	0
2	(S)-PHANEPHOS	29	20 (24)	9, R
3	(S)-Me DUPHOS	2	80 (92)	75, R
4	(S,S)-Et BPE	2	56 (80)	31, R
5	(S)-tol-BINAP	2	98 (100)	98, R (78 %) ^c
6	(R)-BINAP	2	92 (100)	87, S
7	(S,S)-iPr DUPHOS	2	50 (100)	84, R
8 ^c	(S,S)-iPr DUPHOS	24	98 ^d (100)	90, R ^d

^aConversions and yields measured by GC. ^bee analysis measured on the (R)-Mosher ester on a

Chiralcel OJ-H column (Daicel, 250 mm x 4.6 mm). ^c78% isolated yield by column

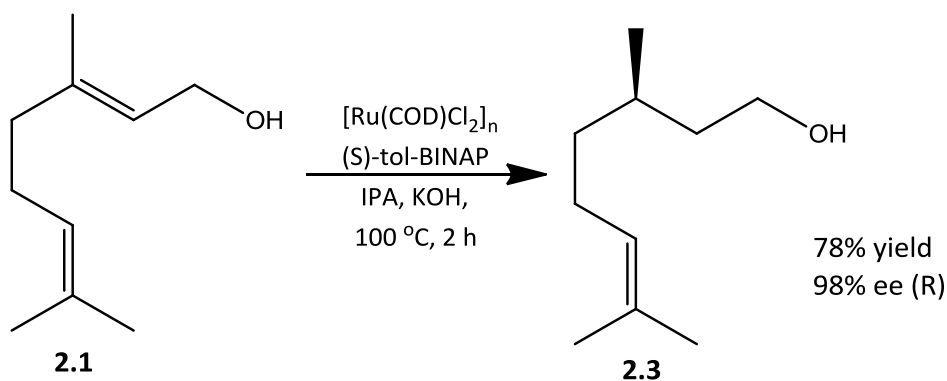
chromatography. ^dYield and ee of dihydrocitronellol, {geraniol-Ru(COD)Cl₂]_n-KOH-ligand molar ratio = 2/1/2/2}.

Backvall and Chowdhury had shown the importance of a base (NaOH, KOH) in increasing the rate of isomerization of allylic alcohols to carbonyl compounds.¹⁴ Noyori and co-workers also established the requirement of strong inorganic mineral bases as co-catalysts in the various

ATH reactions of ketones and imines.¹⁰ The base thus plays a critical role in the pre-activation of the catalyst, therefore, the presence of a base as reaction promoter for the ATH reaction of allylic alcohols was also examined. A two equivalent amount of KOH per Ru was found to be optimal, and lower amounts compromised reaction conversions and enantioselectivities.

Other reaction parameters that were examined included the reaction temperature, substrate/catalyst ratio and the reaction sensitivity to air and moisture. A temperature of 100 °C was selected for a 2 h reaction. Slightly lower temperatures of 83 °C were later determined to be optimum for the reaction.

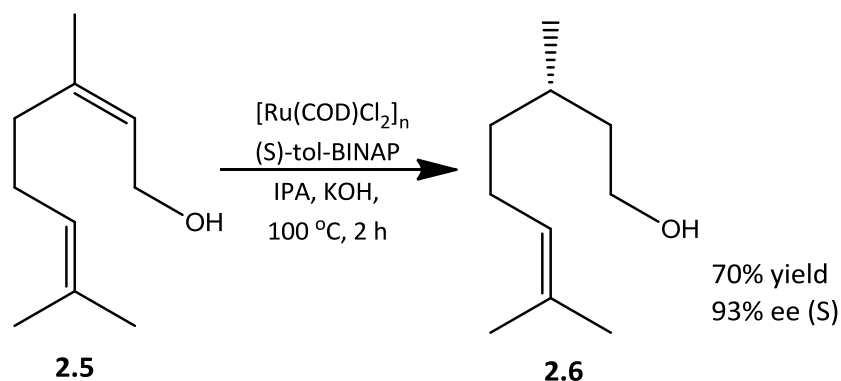
The substrate/catalyst (S/C) ratio was optimized at 10/1, which was found to enhance complete conversion of the substrate, while facilitating the purification of the product. This reaction was also found to be very sensitive to air and moisture, which led to the use of freeze-pump-thaw degassing procedures which protected the reaction from oxygen and water.



Scheme 2.5. ATH reaction of geraniol under optimized conditions.^{6b}

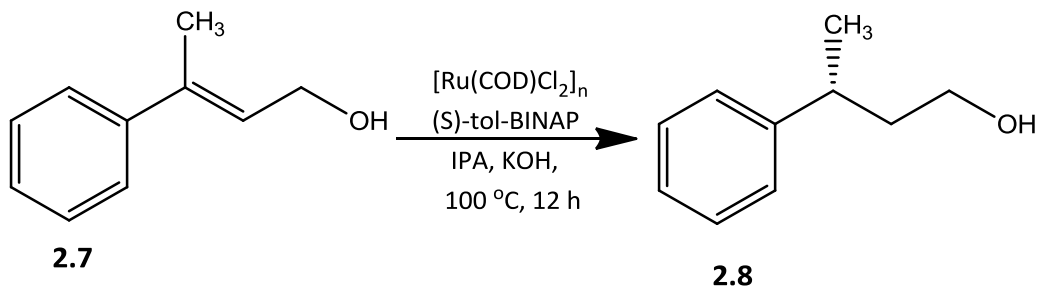
The ATH reaction of geraniol was later optimized with respect to the *cocktail* catalytic conditions. In this case, all the reacting species were added together and degassed through cycles of freeze-pump-thaw process before heating at 100 °C for 2 h (Scheme 2.5).^{6b}

An extension of this reaction to the Z-isomer of geraniol, nerol, gave 100% conversion and 70% yield of the isolated product, **2.8**, (S)- citronellol in 93% ee.



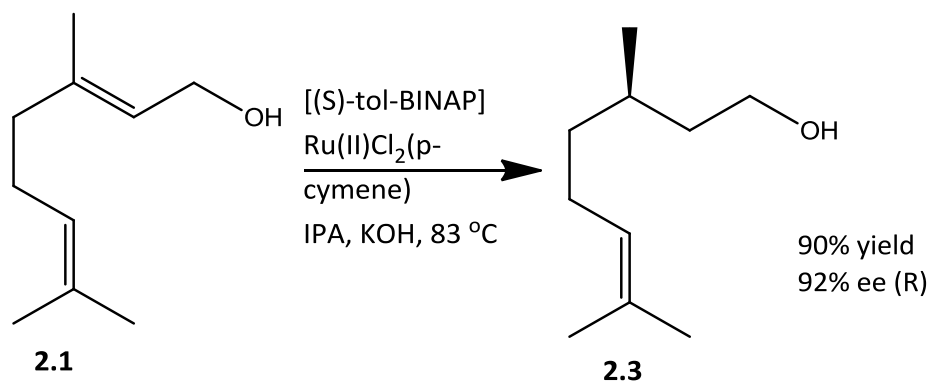
Scheme 2.6. ATH reaction of nerol under optimized conditions.^{6b}

Similarly, the use of 3-phenyl-2-buten-1-ol under these reaction conditions afforded 99% yield and 72% ee of **2.8**, in 12 h.



Scheme 2.7. ATH reaction of 3-phenyl-2-buten-1-ol, 2.9, under optimized conditions.^{6b}

Attempts at extending this reaction to γ -geraniol and α,β -unsaturated ketones gave very low yields and enantioselectivities, even at higher catalyst or base concentration.^{6b, 16} In contrast, gaseous hydrogenation of these substrates have afforded better results,¹⁵ this suggests that the ATH reaction of the allylic alcohols is operating under a specific mechanism which differs from the classical AH. This mechanism was investigated and published by the Sowa group in 2012.¹⁶ To evaluate the performance of this ATH reaction, studies were also conducted with commercially available *pure* catalyst - [(S)-tol-BINAP]Ru(II)Cl₂(p-cymene)]. Here, the reaction was efficient at a higher substrate concentration and a lower temperature of 83 °C affording a high yield and enantioselectivity.

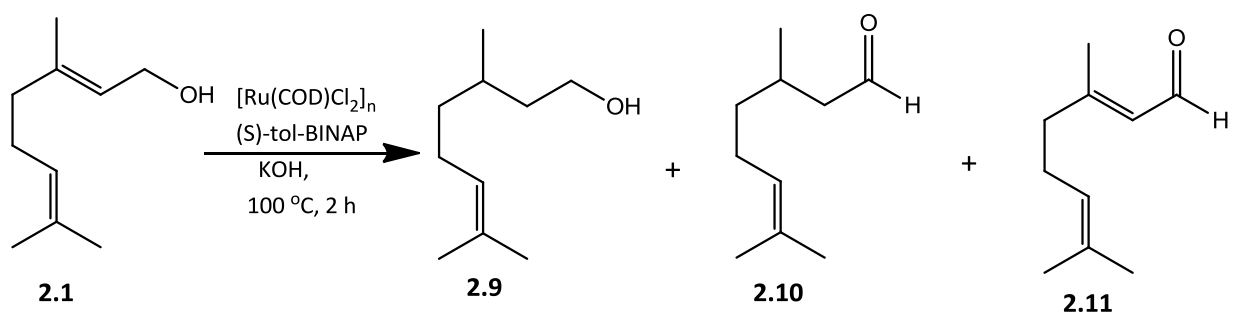


Scheme 2.8. ATH reaction of geraniol using commercial catalyst complex.¹⁶

2.1.4: Mechanistic Studies of ATH of allylic alcohols

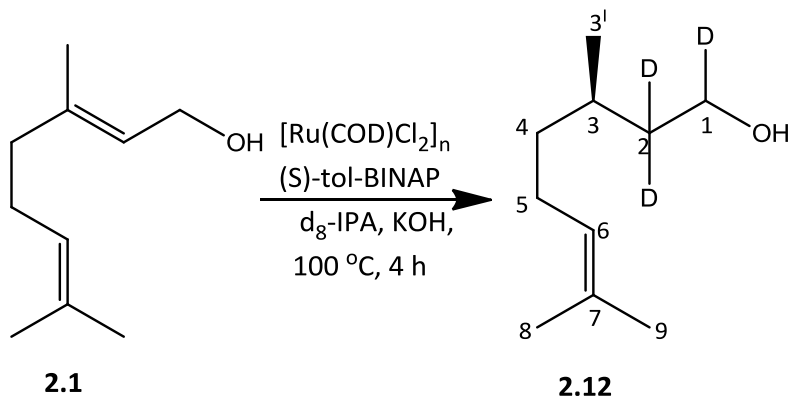
Considering that only a few literature reports of asymmetric isomerization of allylic alcohols exists,⁴ mechanistic studies of the ATH reaction of allylic alcohols were carefully performed by the Sowa group to ascertain the mechanism of reaction.

In the initial experiment conducted without IPA, the substrate geraniol served as the solvent and the hydrogen atom donor with 47% conversion, affording the hydrogenated product citronellol (13%) **2.9**, along with citronellal (21%) **2.10** and citral (13%) **2.11**. Interestingly, γ -geraniol was not formed, an indication that equilibration between geraniol and γ -geraniol did not occur at this elevated temperature.^{6b} Based on the isolated yields, citronellal was considered a reaction intermediate, as documented in literature reports on the transposition of allylic alcohols to carbonyl compounds.⁴



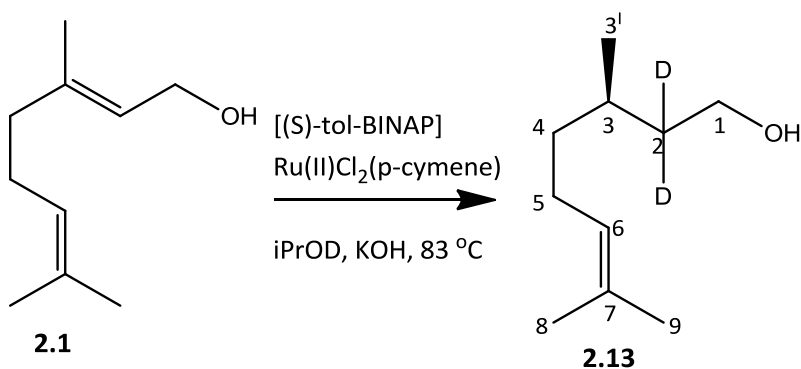
Scheme 2.9. ATH of geraniol without IPA.¹⁶

Subsequent deuterium labelling experiments were conducted with d_8 -IPA and confirmed the formation of d_3 -citronellol as the major product, with m/z of 159, according to GC/MS. ^1H NMR indicated one proton on C_1 and two deuterium atoms on C_2 , which was also confirmed according to ^{13}C NMR and HMQC analyses. This demonstrated that a different reaction mechanism other than the conventional mechanism of direct hydrogenation occurred in the ATH reaction of allylic alcohols.^{3,4}



Scheme 2.10. ATH reaction of geraniol with deuterated IPA.¹⁶

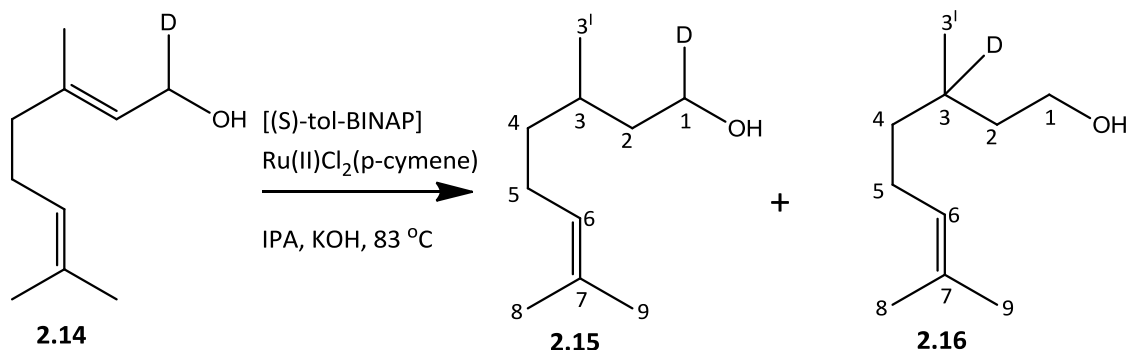
Further studies with mono deuterated IPA (iPrOD), showed d_2 -citronellol as the major product with m/z of 158. ^1H NMR, COSY and ^{13}C -DEPT 135 experiments also showed no hydrogen atoms on C_2 , with clear coupling between the C_2 and the deuterium atoms. This indicated that hydrogen atoms were being transferred from IPA to geraniol in the ATH reaction.



Scheme 2.11. ATH reaction of geraniol with mono deuterated IPA.¹⁶

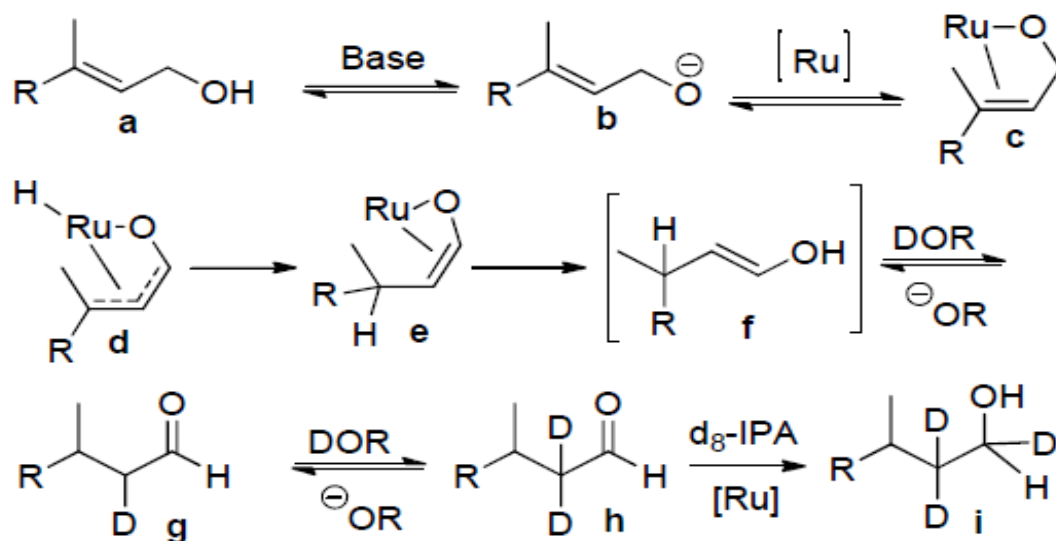
A clearer perspective of the mechanism emerged from the experiment with deuterated geraniol which showed the relocation of deuterium atom from C_1 to C_3 , in one of the mixed

deuterated citronellol products. Although, GC/MS analysis showed an m/z of 157 for the deuterated citronellol mixture, the identity of the second compound was confirmed by NMR experiments. ^2H NMR established the presence of a deuterium atom on C_3 . This strongly confirmed that a 1,3-hydride shift was occurring in the reaction mechanism.



Scheme 2.12. ATH reaction of deuterated geraniol.¹⁶

Based on these results, a mechanistic pathway was proposed for the ATH reduction reaction of allylic alcohols as highlighted in Scheme 2.13.¹⁶ This mechanism begins with base initiated generation of the allylic alkoxide (**b**) which coordinates to the metal (**a-c**). This is followed by a 1,3-hydride shift, that generates an enol which tautomerizes to a carbonyl intermediate (**d-g**), followed by hydrogen atom transfer to generate the alcohol (**h-i**).

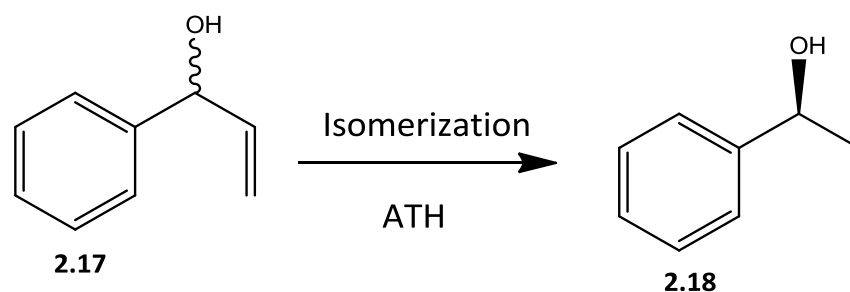


Scheme 2.13. Proposed mechanism of ATH reaction of primary allylic alcohols.¹⁶

2.1.5: Summary and Outlook

The ATH reaction of allylic alcohols and a thorough understanding of its mechanism of reaction using geraniol as model substrate was successfully developed in our laboratory. This reaction method afforded good yields and enantioselectivity, while promising in scope and versatility for a broad range of secondary allylic alcohols. The mechanism of the reaction was carefully investigated and found to involve an initial 1,3-hydride shift, which caused the transposition of the allylic double bond to generate a carbonyl intermediate via enol tautomerization. The carbonyl intermediate reacted further by the active metal hydride (inner-sphere) to afford the alcohol product. This mechanism is described as an enantioselective isomerization/transfer hydrogenation reaction, which translated into an efficient ATH reaction method.

Following these successful studies, our research group was prompted to apply the ATH reaction to a broader range of secondary allylic alcohols, including the prochiral benzyl alcohols. Using an α -vinyl benzylic alcohol as model substrate, my thesis objectives were based on the development of an efficient and enantioselective ATH reaction for this class of substrates (Scheme 2.14).



Scheme 2.14. Proposed model reaction for the ATH reaction of secondary allylic alcohols.

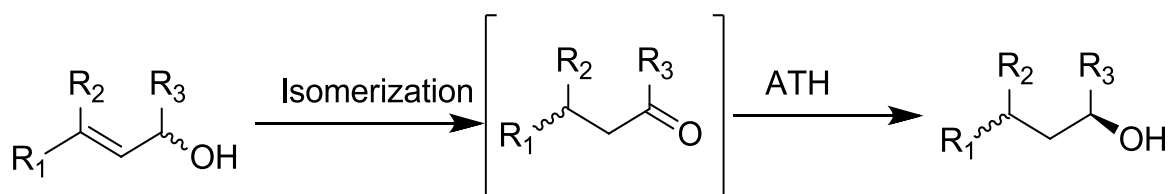
2.2. Research objectives of ATH reaction of secondary allylic alcohols

2.2.1: Research objectives

The ATH reaction has become an important synthetic tool and an increasingly attractive approach to the enantioselective reduction of unsaturated systems such as ketones, imines, olefins and heterocyclic aromatic compounds. Although, our laboratory has broadened the substrate scope of the ATH reaction with its application to geraniol; a primary allylic alcohol, the extension of this reaction to include another important class of the allylic alcohols; the secondary allylic alcohols is presented in this thesis. In this manner a *comprehensive* application of its versatility may be achieved, knowing that transition-metal hydrides such as, ruthenium-

hydride can be generated *in situ* and actively used to effect the redox-isomerization of the allylic alcohols to prochiral ketones. These can be subsequently reduced to chiral secondary alcohols, in this case, the conversion of α -vinyl benzyl alcohol, **2.17**, to a chiral benzyl alcohol, **2.18**, is proposed as the model reaction (Scheme 2.14).

As noted in sub-section 2.1.5, our laboratory was the first to report the asymmetric transfer hydrogenation of allylic alcohols via a combined enantioselective isomerization /transfer hydrogenation reaction mechanism. The reaction was found to occur, in excellent product yield and % ee, using primary allylic alcohols such as geraniol and nerol as substrates.¹⁶ *My research objectives related to this dissertation work are to further develop this reaction; to broaden the substrate scope to secondary allylic alcohols and to suggest further applications to the synthesis of useful bioactive compounds.*



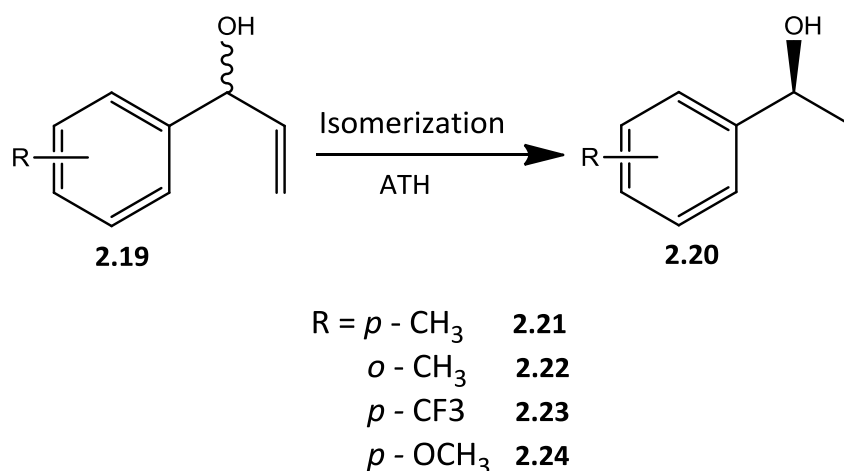
Scheme 2.15. Representative substrate of interest in our investigation.

In this regard, we propose a series of screening reactions, involving the conversion of racemic 1-phenyl-2-propen-1-ol (α -vinyl benzyl alcohol) to a single enantiomer as our model reaction (Figure 2.2). Here we will evaluate different *in situ* generated catalyst systems, using

ruthenium based precatalysts such as *di-μ-chlorobis*[(*p*-cymene)-chlororuthenium (II)], in combination with “privileged” chiral ligands such as (S)-(-)-2,2'-bis(*di-p*-tolylphosphino)-1-1'-binaphtyl [(S)-tol-BINAP], for optimal catalyst activity and selectivity. Through these studies, we will address the problems of low yields and lack of product enantioselectivity that was observed in the applications of the ATH reaction to secondary allylic alcohols studied in our preliminary investigations. Our aim will be to increase the enantioselectivity, propose the reaction mechanism and heuristically investigate the ruthenium-based precatalyst with a variety of chiral ligands.

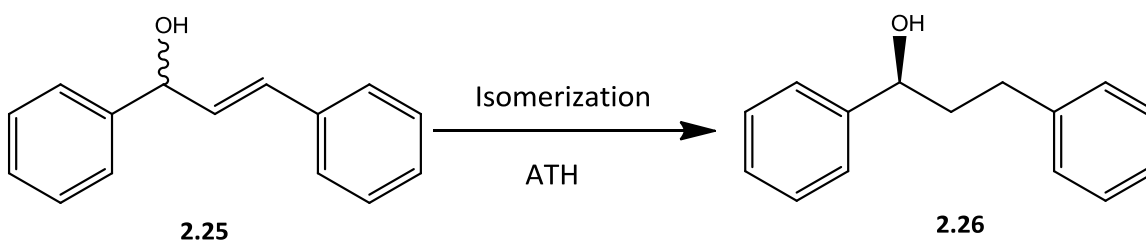
We will also monitor the reaction % ee over time by HPLC analysis. Monitoring the reaction over time may help us determine the point of asymmetric induction, product accumulation and possible racemization. Because the reaction is performed in isopropyl alcohol, it is ideally suitable for microwave synthesis.²⁵ In fact, it may also be possible to perform this reaction in isopropyl alcohol/water mixture. Thus, we will also carry out this reaction under microwave conditions to determine the potential of microwave technology to perform the ATH reaction.

Furthermore, we will study this reaction with various derivatives of α -vinyl benzyl alcohol, to evaluate the electronic effects of both electron withdrawing and electron donating groups on reactivity and enantioselectivity (Scheme 2.16).



Scheme 2.16. Evaluation of electronic effects in the ATH of α -vinyl benzylic alcohols 2.21-2.24.

Moreover, 1,3-diphenyl-2-propen-1-ol (Scheme 2.17), an important core component in the synthesis of LTD₄ antagonist Singulair™ (Merck Inc.) will also be examined in the optimized ATH process.



Scheme 2.17. Secondary allylic alcohols of interest to our investigation.

Similarly, we will explore competition reactions of the ATH technique between equimolar amounts of the model substrate and its derivatives to qualitatively determine the rate of tautomerization of the enol intermediate on the overall rate of the reaction.

We believe the reaction proceeds with a mechanism similar to the one elucidated by our colleagues in the ATH reaction of primary allylic alcohols as enantioselective isomerization/transfer hydrogenation reaction published in 2012.¹⁶ However, we suspect that the keto-enol intermediate presumed to be involved in the secondary allylic alcohol could be reacting under a different reduction mechanism, possibly through an outer-sphere bifunctional catalysis mechanism in which a highly ordered six-membered ring transition state is formed to afford the alcohol product. In this regard, this hypothesis may be studied in future applications by deuterium labeling experiments using GC/MS and NMR. These techniques in addition to computational density functional theory (DFT) and molecular orbital (MO) calculations may be used to determine the origin of the hydrogen atom transfer and to rationalize the orientation of the ketone intermediate during the reduction step.

2.3: Conclusions

The objective of this thesis as described above applies the ATH reaction developed in our laboratory to secondary allylic alcohols. This includes making necessary modifications towards addressing the problems of low yields and limited enantioselectivity under the optimized cocktail conditions developed for the primary allylic alcohols. We believe we can achieve higher yields and enantiomeric excesses through well-studied and optimized reaction conditions; catalyst, ligands, base and temperature. As presented in this thesis, a better understanding of the ATH reaction and its mechanism is applied to secondary allylic alcohols.

References

1. (a) Samec, J. S.; Backvall, J. E.; Andersson, P. G.; Brandt, P. *Chem. Soc. Rev.* **2006**, *35*, 237 – 248; (b) Krische, M. J.; Sun, Y.-K. *Acc. Chem. Res.* **2007**, *40*, 1237 – 1419. (c) Ikariya, T.; Blacker, A. J. *Acc. Chem. Res.* **2007**, *40*, 1300 – 1308.
2. (a) Noyori, R.; Hashiguchi, S. *Acc. Chem. Res.* **1997**, *30*, 97 – 102. (b) Noyori, R. *Asymmetric Catalysis in Organic Synthesis*, John Wiley, NewYork, **1994**. (c) Noyori, R. *Angew. Chem. Int. Ed.* **2002**, *41*, 2008 – 2022.
3. (a) Clapman, S. E.; Hadzovic, A.; Morris, R. H. *Coord. Chem. Rev.* **2004**, *248*, 2201. (c) Gladiali, S.; Alberico, E. *Chem. Soc. Rev.* **2006**, *35*, 226–236.
4. (a) Uma, R.; Crevisy, C.; Gree, R. *Chem. Rev.* **2003**, *103*, 27-51. (b) van der Drift, R. C.; Bouwman, E.; Drent, E. *J. Organomet. Chem.*, **2002**, *650*, 1-24. (c) Shabatai, J.; Lazar, R.; Biron, E. *J. Mol. Catalysis* **1984**, *27*, 35.
5. Baratta, W.; Chelucci, G.; Gladiali, S.; Siega, K.; Toniutti, M.; Zanette, M.; Zangrando, E; Rigo, R. *Angew. Chemie. Int. Ed.*, **2005**, *44*, 6214
6. Sun, Y.; LeBlond, C.; Wang, J.; Blackmond, D. G.; Laquidara, J.; Sowa, Jr., J. R. *J. Am. Chem. Soc.*, **1995**, *117*, 12647-12648. (b) Laquidara, J. *Asymmetric Transfer Hydrogenation of Allylic Alcohols*, Ph.D. Thesis, **2003**.
7. (a) Takaya, H.; Ohta, T.; Inoue, S.-I.; Tokunaga, M.; Kitamura, M.; Noyori, R. *Org. Synth.* **1993**, *72*, 74. (b) Saburi, M.; Tsukahara, T.; Ishii, Y.; Ikariya, T., Takahashi, T.; Uchida, Y. *J. Organomet. Chem.* **1992**, *428*, 155.
8. (a) Brown, J. M.; Naik, R. G. *J. Chem Soc., Chem. Commun.* **1982**, 348. (b) Evans, D. A. Morrissey, M. M. *J. Am. Chem. Soc.* **1984**, *106*, 3866.
9. (a) Shabatai, J.; Lazar, R.; Biron, E. *J. Mol. Catalysis* **1984**, *27*, 35. (b) Aramendia, M. A.; Borau, V.; Jimenez, C.; Marinas, J. M.; Ruiz, J. R.; Urbano, F. *J. Applied Catalysis A: General* **2001**, *206*, 95.
10. Ikariya, T.; Blacker, A. J. *Acc. Chem. Res.* **2007**, *40*, 1300–1308.
11. Hashiguchi, S.; Fujii, A.; Haack, K.-J.; Matsumura, K.; Ikariya, T.; Noyori, R. *Angew. Chem., Int. Ed. Engl.* **1997**, *36*, 288–290.

12. (a) Wagner, K. *Angew. Chem. Int. Edit.* **1970**, 9, 50. (b) Watanabe, Y.; Ohta, T.; Tsuji, Y. *Bull. Chem. Soc. Jpn.* **1982**, 55, 2441.
13. Fujii, A.; Hashiguchi, S.; Uematsu, N.; Ikariya, T.; Noyori, R. *J. Am. Chem. Soc.* **1996**, 118, 2521–2522.
14. Chowdhury, R.; Bäckvall, J. J. *Chem. Soc., Chem. Commun.* **1991**, 1063-1064.
15. (a) Kitamura, M.; Kasahara, I.; Manabe, K.; Noyori, R.; Takaya, H. *J. Org. Chem.* **1988**, 53, 710 – 712. (b) Noyori, R. *Angew. Chem. Int. Ed.* **2002**, 41, 2008 –2022;
16. Wu, R.; Beauchamps, M. G.; Laquidara, J. M.; Sowa, Jr. J. R. *Angew. Chem. Int. Ed.*, **2012**, 51, 1-6.
17. Shoola, C. O.; DelMastro, T.; Wu, R.; Sowa, Jr., J. R. *Eur. J. Org. Chem.*, **2015**, 1670-1673.
18. (a) Fürstner, A.; Hannen, P. *Chem. Eur. J.*, **2006**, 12, 3006-3019. (b) Hett, R.; Fang, Q. K.; Gao, Y.; Hong, Y.; Butler, H. T.; Nie, X.; Wald, S. *Tetrahedron Lett.*, **1997**, 38, 1125-1128.
19. (a) Yang, Z.-H. ; Zeng, R.; Yang, G.; Wang, Y.; Li, L-Z.; Lv, Z-S.; Yao, M.; Lai, B. *J. Ind. Micro. and Biotech.* **2002**, 35, 1047-1051.
20. Ohkuma, T.; Ooka, H.; Hashiguchi, S.; Ikariya, T.; Noyori, R. *J. Am. Chem. Soc.* **1995**, 117, 2675. (b) Ohkuma, T.; Ooka, H.; Yamakawa, M.; Ikariya, T.; Noyori, R. *J. Org. Chem.*, **1996**, 61, 4872
21. (a) Hartwig, J. F. *Organotransition Metal Chemistry: From Bonding to Catalysis*, 1st ed., **2009**. (b) Crabtree, R. H. *The Organometallic Chemistry of the Transition Metals*, Wiley; 5th ed., **2009**.
22. (a) Jones, J.B. *Tetrahedron*, **1986**, 42, 3351-3403. (b) Schoffers, E.; Goleblowski, A.; Johnson, C.R. *Tetrahedron*, **1996**, 52, 3769-3826.
23. (a) M. T. Reetz, X. Li, *J. Am. Chem. Soc.* **2006**, 128, 1044-1045. (b) R. Kadyrov, T. H. Riermeier, U. Dingerdissen, V. Tararov, A. Borner, *J. Org. Chem.* **2003**, 68, 4067-4070. (c) Tripathi, R. P.; Verma, S. S.; Pandey, J.; Tiwari, V. K. *Curr. Org. Chem.* **2008**, 12, 1093-1115. (d) Zhou, S.; Fleischer, S.; Junge, K., Das, S.; Addis, D.; Beller, M. *Angew. Chem. Int. Ed.* **2010**, 49, 8121–8125. (e) Nguyen, T. B.; Bousserouel, H.; Wang, Q.; Guéritte, F. *Org. Lett.*, **2010**, 12, 4705-4707.
24. (a) N. J. A. Martin, L. Ozores, B. List, *J. Am. Chem. Soc.* **2007**, 129, 8976-8977. (b) D. Xue, Y.-C. Chen, X. Cui, Q.-W. Wang, J. Zhu, J.G. Deng, *J. Org. Chem.* **2005**, 70, 3584-3591; (c) N. J. A.

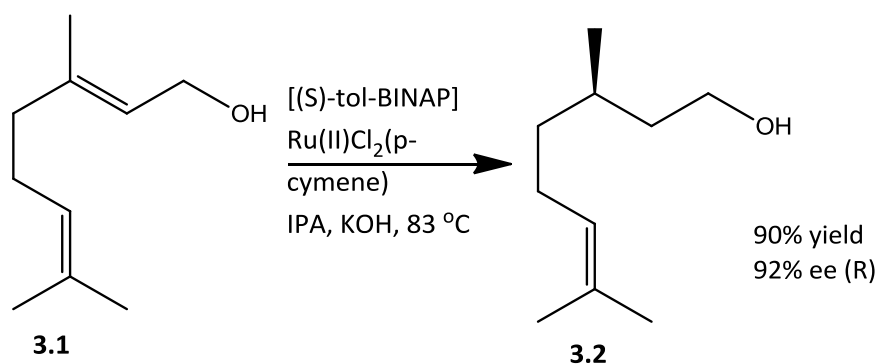
Martin, B. List, *J. Am. Chem. Soc.* **2006**, *128*, 13368-13369 (d) Yang, J. W.; Fonseca, M. T. H.; Vignola, N.; List, B. *Angew. Chem. Int. Ed.*, **2005**, *44*, 108–110.

25. Gordon, E. M.; Gaba, D. C.; Jebber, K. A.; Zacharias, D. M. *Organometallics*, **1993**, *12*, 5020-5022.

Chapter Three: Development and Optimization of the ATH Reaction of Secondary Allylic Alcohols

3.1: Development of the ATH reaction of secondary allylic alcohols

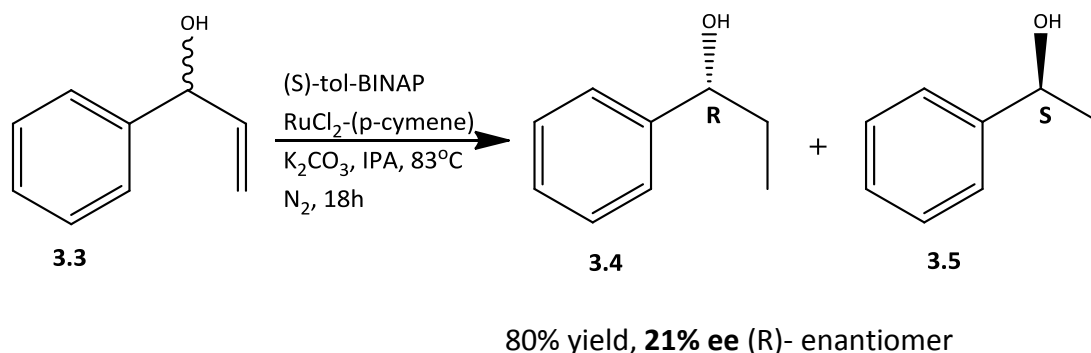
The investigation into the isomerization and ATH reaction of secondary allylic alcohols was initiated by adapting the reaction conditions optimized in the case of the primary allylic alcohol; geraniol, (Scheme 3.1).¹ These reaction conditions included (S)-tol-BINAP and ruthenium (II) *p*-cymene dissolved together in a mixture of IPA and the base KOH, and heated at 83 °C for 18 h.



Scheme 3.1. Optimized reaction conditions for the primary allylic alcohol, geraniol, **3.1**.¹

In my approach, a slight modification in the addition sequence of the reacting components was accomplished. In this manner, a stepwise addition of the reagents as opposed to a cocktail approach was adopted in order to generate the active catalyst first. Additionally, the base was changed from KOH to K₂CO₃, on the assumption that the OH group from KOH may lead to the generation of water which may poison catalyst reactivity. Thus, the initial reaction commenced with the degassing of the solvent and reducing agent (IPA) from room temperature

to 83 °C, followed by addition of the pre-catalyst, *di-μ-chlorobis[(p-cymene)chlororuthenium(II)]* **3.9**, (Figure 3.2) and the ligand, (S)-tol-BINAP, and then the substrate, - α-vinyl benzyl alcohol and K₂CO₃ as the base dissolved in isopropyl alcohol, respectively. The substrate/pre-catalyst /ligand /base mole ratio was 10:1:1:2. The reaction proceeded for 18 h and cleanly afforded good product conversion (>80%) and the product was isolated in yield of 75% via silica gel column chromatography (Scheme 3.2). However, low enantioselectivity (21% ee) for the R-enantiomer, **3.4**, was observed upon analysis by reverse phase chiral HPLC, using a Daicel Chiralcel OD-RH HPLC column and a 50/50 (v/v) mixture of methanol/water as mobile phase at 20 °C with 220 nm UV detection. The % ee was determined by peak area integration, and enantiomers were identified by retention times, as validated by reverse phase chiral HPLC analysis of the commercially available racemic mixture of the desired product; (±)-1-phenyl-1-propanol, under similar conditions.¹ (Figure 3.1). Nonetheless, these results were promising, because under similar conditions when the reacting components were added at the same time, the cocktail approach, no enantioselectivity was observed.



Scheme 3.2. First attempted ATH reaction of secondary allylic alcohols.

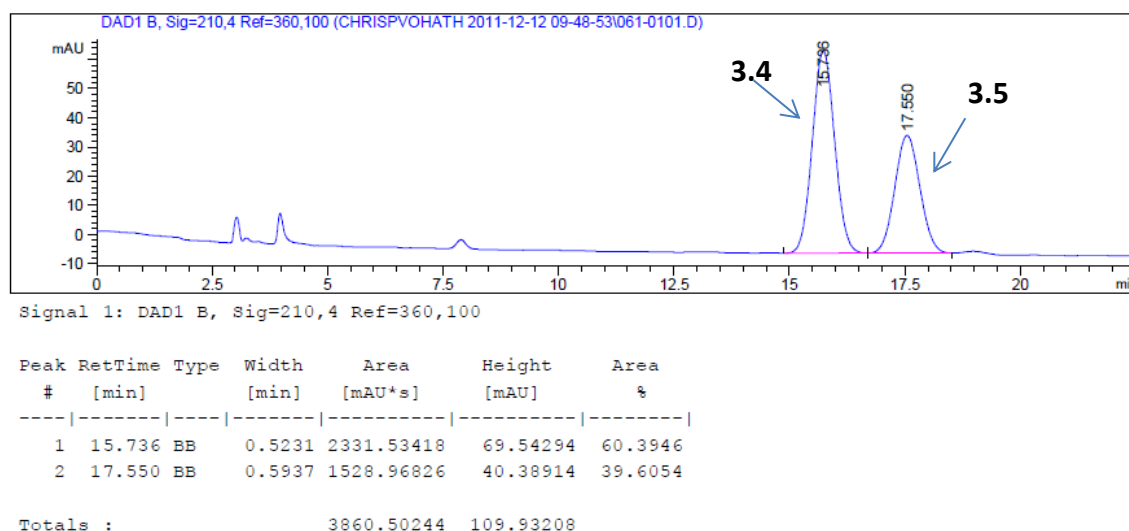
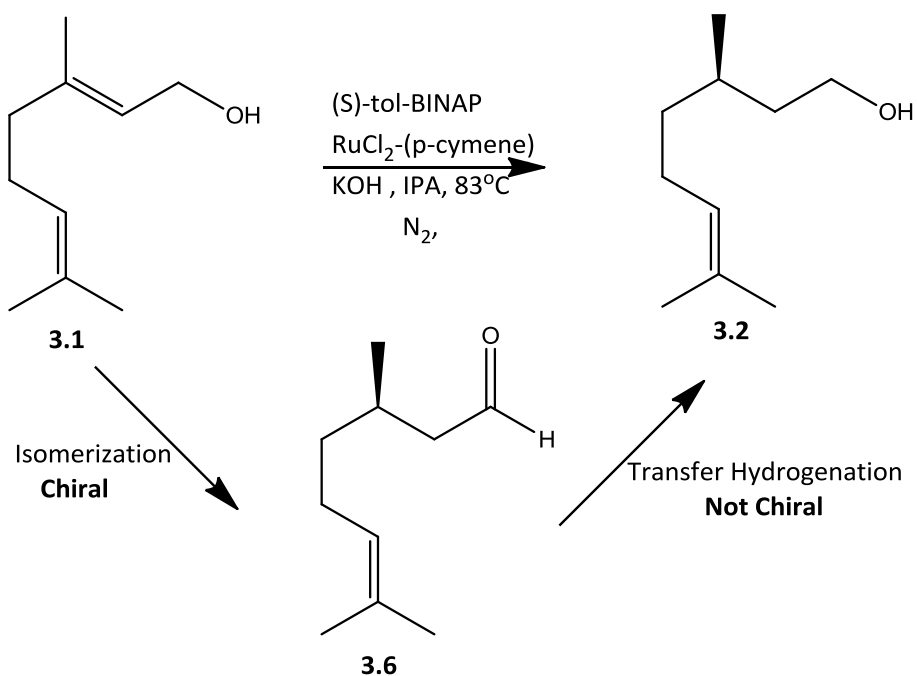


Figure 3.1. Chiral separation of the first attempted ATH reaction of secondary allylic alcohol.

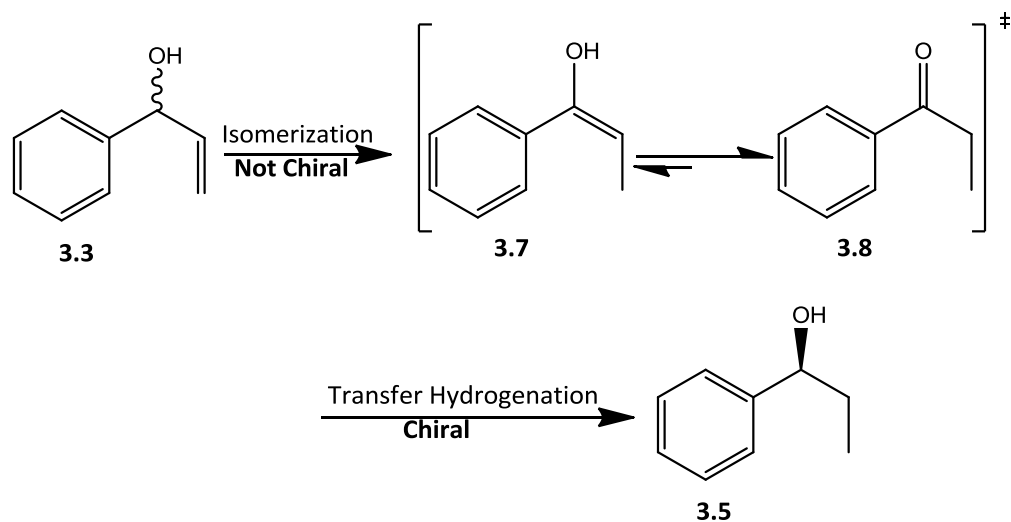
In an attempt to improve the enantioselectivity of the reaction, a review of the proposed reaction mechanism for the primary allylic alcohol under these conditions revealed that asymmetric induction occurred during the isomerization step, and also, the transfer hydrogenation step was achiral (Scheme 3.3). However, in the case of the secondary allylic alcohols, the isomerization step is considered to be achiral, whereas, the transfer hydrogenation step produces chirality (Scheme 3.4). The proposed reaction mechanisms are based on those published by our laboratory for the primary allylic alcohol, geraniol¹ and the isomerization reactions of allylic alcohols.²

This observation became an important point to consider in the subsequent optimization studies.



Scheme 3.3. Enantioselective isomerization/transfer hydrogenation mechanism of geraniol,

3.1.¹



Scheme 3.4. Isomerization/ATH of secondary allylic alcohol, α -vinyl benzyl alcohol, 3.3.²

Given that the tautomerization step following the isomerization of the secondary allylic alcohol produces a ketone intermediate, it was envisaged that a catalyst system known for

effective transfer hydrogenation of ketones might be able to form the isomer of the allylic alcohol substrate and also reduce the ketone intermediate to the corresponding alcohol.³ This has shown to be the case in the following examples, the reduction of acetophenone and unsymmetrically substituted 1,2-diketones to their corresponding optically active secondary alcohols.^{3a}

Based on the literature conditions for effective transfer hydrogenations of ketones, the following factors were explored in an attempt to optimize the enantioselectivity of the ATH reaction of secondary allylic alcohols.

- A. Ligand effect
- B. Metal - ligand mole ratio
- D. Change in reaction temperature
- E. Solvent and base effects

Consultation of the literature on the ATH reactions of ketones and imines led to the choice of the diamine ligand; (S,S)-TsDPEN, which showed enhanced selectivity in the screening reactions.^{3a, 4} The combination of this diamine ligand, (S,S)-*para*-toluene sulfonyldiphenyl ethylenediamine [(S,S)-TsDPEN] **3.10**, proved to be the most efficient with % ee ranging from 68-83% (Table 3.1, entries 1-2). A series of screening reactions were conducted with other ligands in combination with the pre-catalyst **3.9**.⁴ These screening reactions afforded significant

conversions of the substrate in over 80% yields, but the selectivity was poor in each case, with less than 40% ee (Table 3.1, entries 3-7).

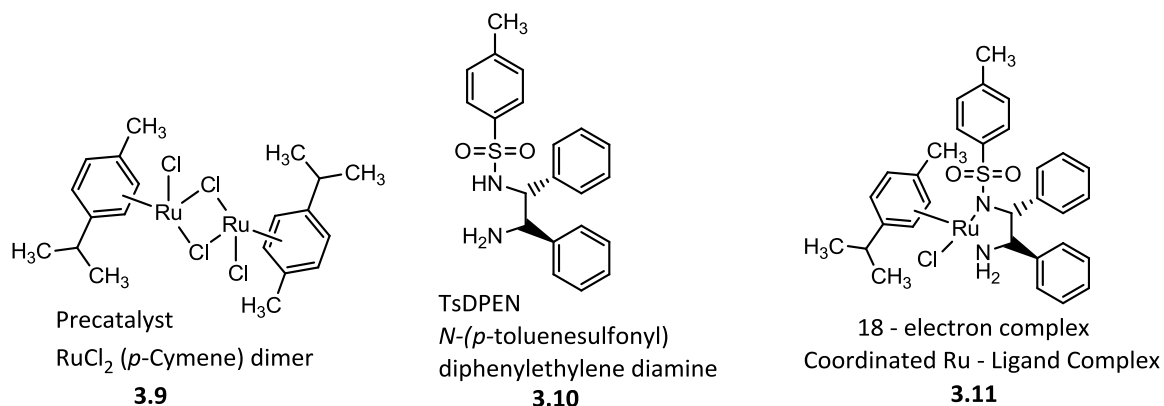


Figure 3.2. Structures of pre-catalyst, ligand, and presumed metal-ligand catalyst complex.

It is not so surprising that the combination of the Ru-pre-catalyst and TsDPEN; presumably forming the *Ru-TsDPEN complex 3.11*, led to higher %ee values (Table 3.1, entries 1-2). This combination is the well-known Noyori-Ikariya catalyst, which has afforded excellent enantioselectivities and product yields in the ATH of prochiral ketones and imines.⁵ Nonetheless, the efficiency of this catalyst system to effect the transposition of the double bond at low temperature (rt) was concerning, because it was noted during the screening experiments that isomerization of secondary allylic alcohol is enhanced at temperatures higher than 40 °C. Thus, a temperature dependent study was developed. This was achieved by initially mixing the pre-catalyst and the ligand at 80 °C for half-hour; and then lowering the temperature to around 50 – 60 °C, and adding the solutions of the base and the substrate, respectively. The reaction mixture was allowed to stir for about 2 h, and finally the temperature was lowered to 25 °C the reaction allowed to stir for 16 h. An appreciable increase in the % ee

(from 68 to 83 %) was achieved through this approach, which was further optimized for the ATH reaction of secondary allylic alcohols.

Variation of metal-ligand mole ratios from 1:1 to 1:2 was attempted during the screening experiments, but no significant difference was observed in the reaction outcome.

The ATH reaction was also attempted under microwave conditions (MW, 120 °C, 20 bar, 25 min.). Furthermore, a 40/60 percentage of water/IPA mixture as solvent and source of hydrogen atom was also attempted. In both cases, no enantioselectivity was observed.

Table 3.1. Study of catalytic activity and selectivity.

Entry	Pre-Catalyst ^a	Ligand ^b	Base ^c	ee (%) ^d
1	di-μ-chlorobis[(<i>p</i> -cymene)chlororuthenium(II)]	(S, S)-TsDPEN	K ₂ CO ₃	83
2	di-μ-chlorobis[(<i>p</i> -cymene)chlororuthenium(II)]	(S, S)-TsDPEN	K ₂ CO ₃	68
3	di-μ-chlorobis[(<i>p</i> -cymene)chlororuthenium(II)]	(S)-PHANEPHOS	K ₂ CO ₃	36
4	di-μ-chlorobis[(<i>p</i> -cymene)chlororuthenium(II)]	(S,S)-i-Pr-DUPHOS	K ₂ CO ₃	30
5	di-μ-chlorobis[(<i>p</i> -cymene)chlororuthenium(II)]	(S)-Tol-BINAP	K ₂ CO ₃	21
6	di-μ-chlorobis[(<i>p</i> -cymene)chlororuthenium(II)]	(R)-Tol-BINAP	K ₂ CO ₃	11
^e 7	di-μ-chlorobis[(<i>p</i> -cymene)chlororuthenium(II)]	(S)-PHANEPHOS	K ₂ CO ₃	<1

^a Pre-catalyst/ligand mixed in IPA at 80 °C for 20 min., substrate/base added at 60 °C. Reaction held at different temperatures between 60 and 25 °C. ^e Microwave conditions (MW, 120 °C, 20 bar, 25 min.)

3.2: Optimization of the ATH reaction of secondary allylic alcohols

Following the preliminary results obtained from the combination of **3.9** and **3.10** (Figure 3.1), it became desirable to further optimize the reaction conditions for improving the enantioselectivity of the ATH reaction. Based on the chosen metal-ligand catalyst complex (Table 3.1, entry 1), the ATH reaction of secondary allylic alcohols was studied over a temperature range (15 – 80 °C) in order to examine the influence of temperature on enantioselectivity. In asymmetric catalysis, the diastereomeric energy difference ($\Delta\Delta G^\ddagger$) of possible transition states of the substrate-catalyst adduct can seriously impact enantioselectivity. In fact, about 2 kcal/mol of diastereomeric transition states energy difference is known to cause 95% ee (equation 3.1 and 3.2).⁶

Therefore, the selectivity of the ATH reaction recorded at each temperature was then correlated to the difference in energy of the diastereomeric transition states of the substrate-catalyst adduct of the reaction using the following equations:

$$\text{Enantiomeric ratio} = \frac{\text{Major enantiomer}}{\text{Minor enantiomer}} = e^{-(\Delta\Delta G^\ddagger/RT)} \dots\dots\dots 3.1$$

$$-\Delta\Delta G^\ddagger = \ln \left(\frac{\text{Major enantiomer}}{\text{Minor enantiomer}} \right) RT \dots\dots\dots 3.2$$

where $-\Delta\Delta G^\ddagger$ is the diastereomeric energy difference, R is the gas constant and T is the temperature.

In my investigation, an average of 90% ee was obtained in several attempted reactions at 25 °C. According to experimentally obtained data shown in Figure 3.3, this translates to an average diastereomeric energy difference of 1.24 kcal/mol, as deduced from the plot of

enantioselectivity versus diastereomeric transition states energy difference obtained over the range of temperatures. This value is consistent with literature reports and advanced publications in the field of asymmetric catalysis.⁶

Plot of Enantioselectivity vs Difference in Energy of Diastereomeric Transition States

Reaction Temperature (°C)	ee (%)	$\Delta\Delta G^{++}$ (kcal/mol)
0		
15	92	1.39
25	89	1.24
35	83	0.97
45	68	0.48

$\Delta\Delta G^{++}$ was calculated from the following equation

$$\text{Enantiomeric ratio} = \text{major enantiomer/minor enantiomer} = e^{-(\Delta\Delta G^{++}/RT)}$$

$$-\Delta\Delta G^{++} = \ln(\text{major enantiomer/minor enantiomer}) RT$$

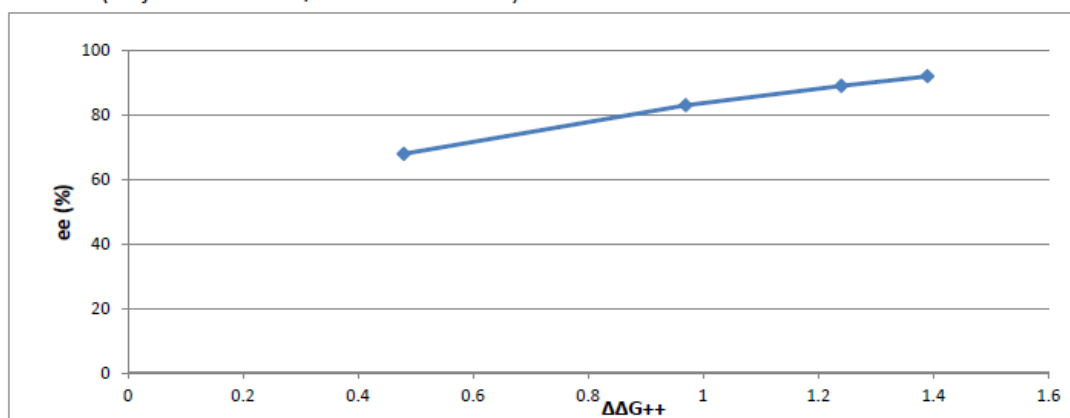
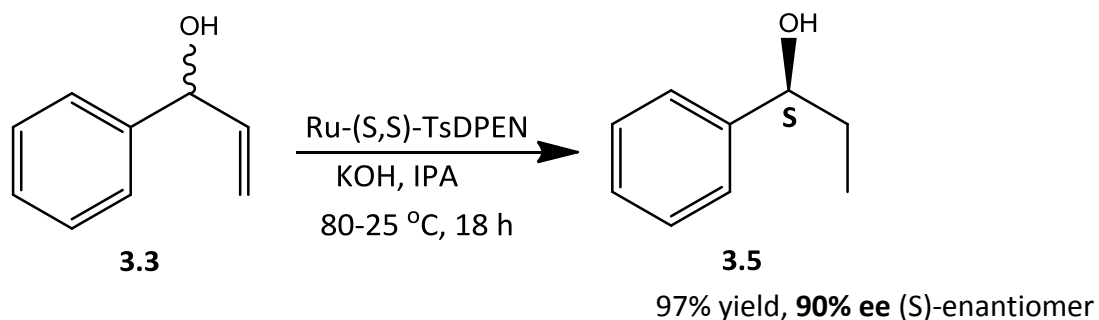


Figure 3.3. Plot of enantioselectivity vs. energy difference of the diastereomeric transition states.

The choice of potassium hydroxide (KOH) in the optimized conditions was selected because of its solubility in IPA. A stoichiometric ratio of (1-2:1, ligand:pre-catalyst) was used in the reaction.

With these conditions, a solution of IPA was degassed from rt to 80 °C, with nitrogen. At 80 °C the pre-catalyst and ligand were added and allowed to mix for 25 minutes to generate the active catalyst complex, **3.11**, *in situ*. The reaction temperature was then lowered to 55 °C, at which point a solution of KOH in IPA was added. The substrate, α -vinyl benzyl alcohol, was dissolved in IPA and was then added to initiate the reaction. The mixture was stirred for about 2 h, after which the reaction temperature was further lowered to 25 °C, and allowed to stir for an additional 16 h. The reaction mixture was sampled for % ee analysis by reverse phase chiral HPLC. Purification and isolation of the product via flash chromatography on silica gel afforded (S)-1-phenyl-1-propanol in 90% ee and 97% yield (Scheme 3.5).⁷ The product was characterized by FT-IR, NMR and GC/MS.



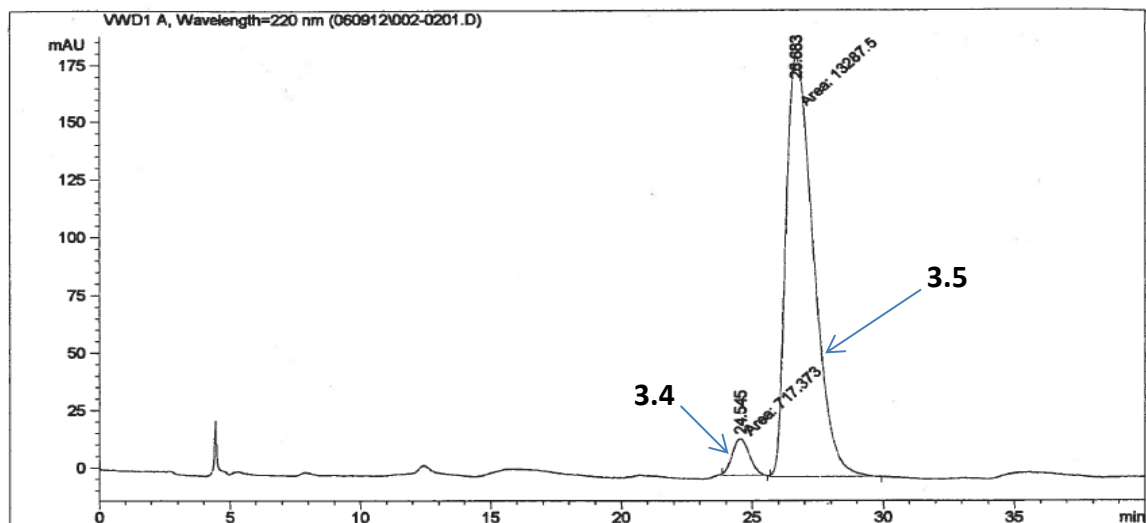
Scheme 3.5. Optimized conditions for isomerization/ATH reaction of secondary allylic alcohol, **3.3**.

The preference for the formation of the S-enantiomer observed with the chiral TsDPEN ligand can be rationalized by the ligand participation in the reduction step. In this case, the substrate-catalyst adduct is a transient *planar bicyclic* species **3.19** (Scheme 3.6) in which rotation of the substrate is impossible, whereas with the tol-BINAP ligand the substrate-catalyst adduct is formed through a direct coordination between the substrate and the metal center; an

arrangement that permits rotation of the substrate in order to overcome possible steric hindrance around the metal center.

Data File C:\HPCHEM\1\DATA\060912\002-0201.D

Sample Name: 1X11 060912



Area Percent Report

Sorted By : Signal
Multiplier : 1.0000
Dilution : 1.0000

Signal 1: VWD1 A, Wavelength=220 nm

Peak #	RetTime [min]	Type	Width [min]	Area [mAU*s]	Height [mAU]	Area %
1	24.545	MM	0.7556	717.37329	15.82323	5.1223
2	26.683	MM	1.2144	1.32875e4	182.35742	94.8777

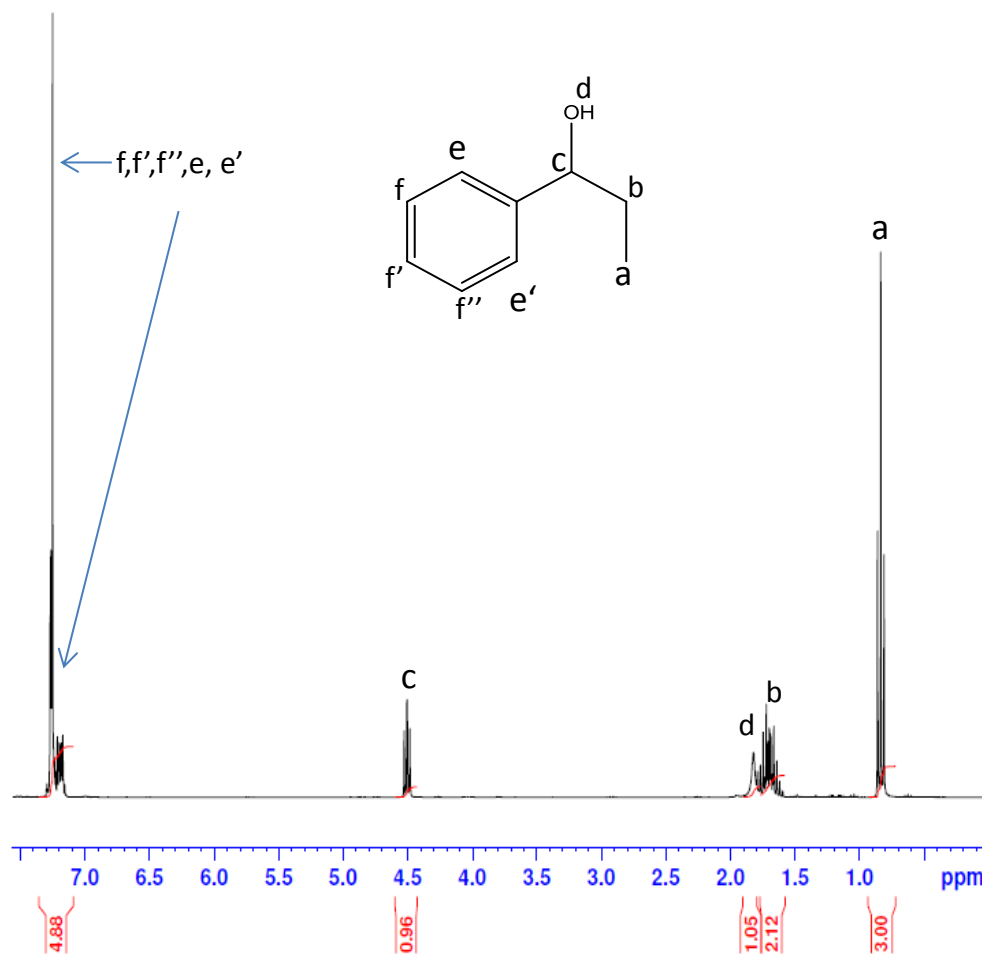
Totals : 1.40049e4 198.18066

Results obtained with enhanced integrator!

*** End of Report ***

Figure 3.4. Chiral separation of products of isomerization/ATH reaction of secondary allylic alcohol.

¹H NMR CS510



Current Data Parameters
NAME Mar24-2014-NJACSHOOLA
EXPNO 1
PROCNO 1

F2 - Acquisition Parameters
Date_ 20140324
Time_ 10.11
INSTRUM spect
PROBHD 5 mm PABBO BB-
PULPROG zg30
TD 65536
SOLVENT CDCl3
NS 128
DS 2
SWH 6009.615 Hz
FIDRES 0.091699 Hz
AQ 5.4525952 sec
RG 114
DW 83.200 usec
DE 6.50 usec
TE 300.0 K
D1 1.00000000 sec
TD0 1

----- CHANNEL f1 -----
SF01 300.1318534 MHz
NUC1 1H
P1 15.00 usec
PLW1 8.02000046 W

F2 - Processing parameters
SI 32768
SF 300.1300329 MHz
WDW EM
SSB 0
LB 0.30 Hz
GB 0
PC 1.00

Figure 3.5. ¹H NMR spectrum of 1-phenyl-1-propanol,3.5.

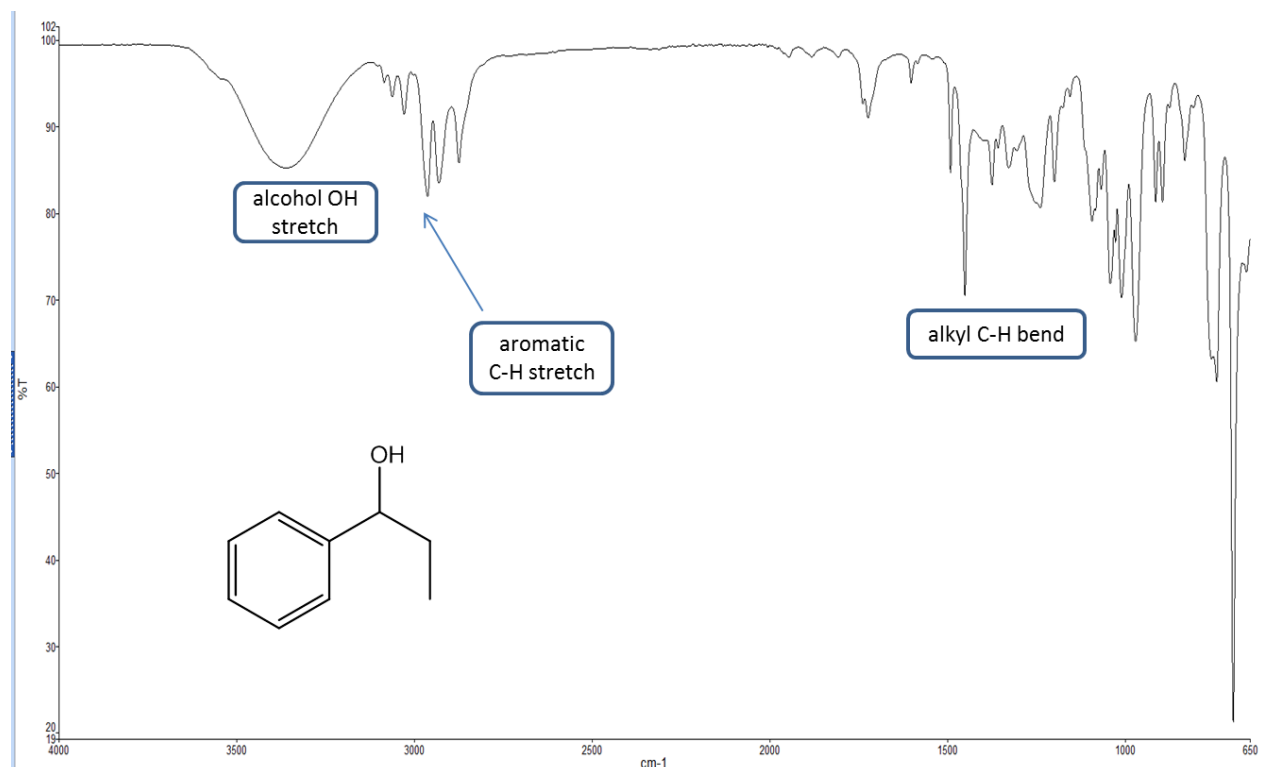


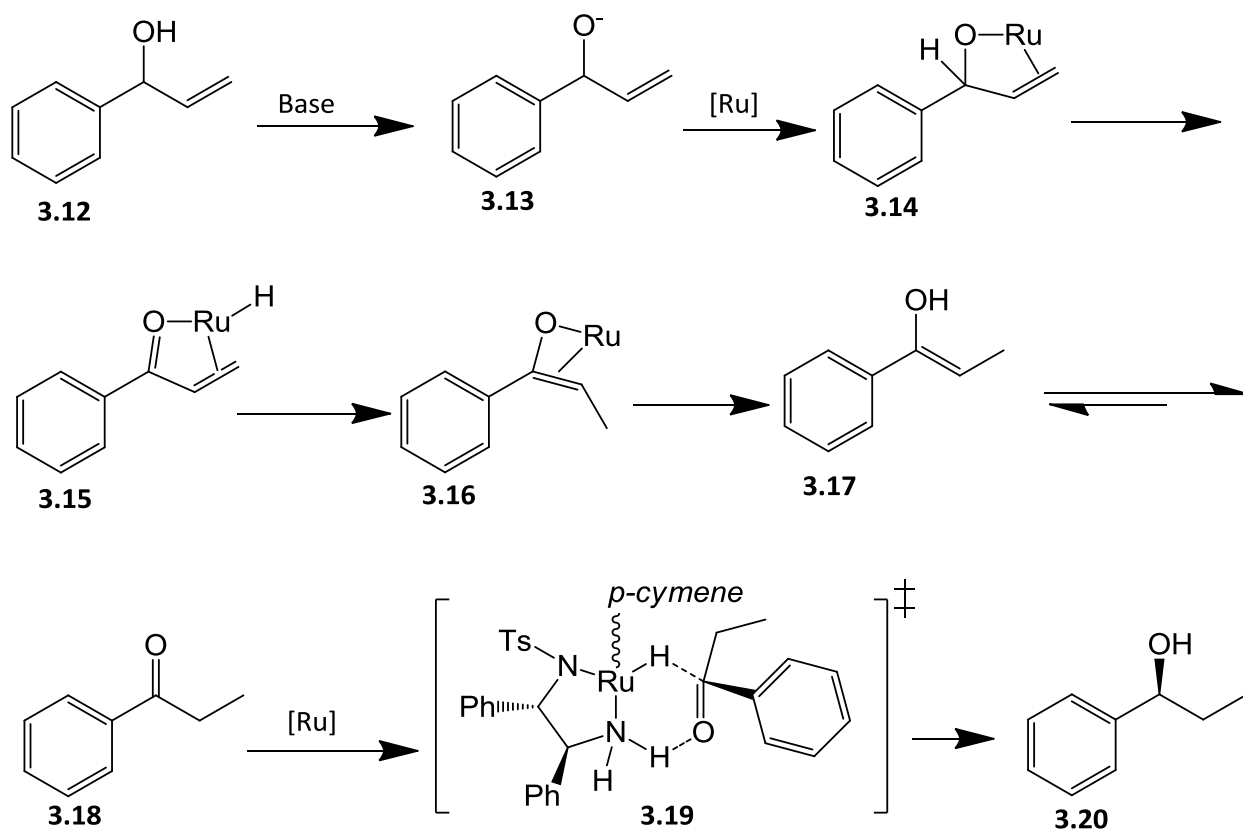
Figure 3.6. FT-IR spectrum of 1-phenyl-1-propanol, **3.5**.

3.3: Postulated mechanism of ATH reaction of secondary allylic alcohols

The previous work of our laboratory in deducing the mechanism for enantioselective isomerization and transfer hydrogenation reaction of geraniol,¹ and the excellent work of Noyori and Ikariya, on the mechanism of metal-ligand bifunctional catalysis,^{8, 9} provided the rationale for the suggested mechanism of the ATH reaction of the secondary allylic alcohol; α -vinyl benzyl alcohol. This mechanism may be described as a synergy of the inner-sphere and

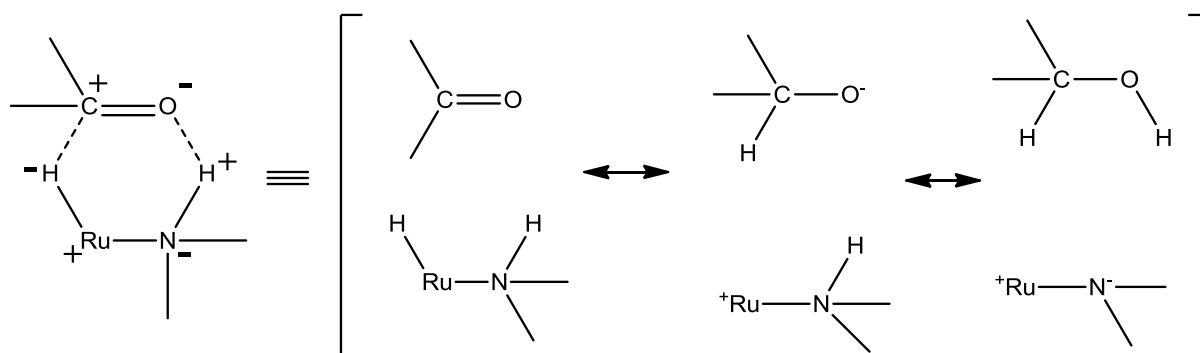
outer-sphere pathways. In this manner, the inner-sphere pathway involves initial direct interaction of the substrate with the metal center up to the formation of the ketone intermediate. This ketone intermediate then reacts through bifunctional metal-ligand catalysis in an outer-sphere pathway to afford the corresponding chiral alcohol.

The proposed mechanism begins with the base deprotonation of the allylic alcohol **3.12**, to generate the allylic alkoxide **3.13**, which quickly coordinates to the chiral [Ru]-complex. A 1,3-hydride shift from the benzylic position in **3.14** via the metal hydride complex **3.15**, onto terminal vinyl carbon generates the metal oxy-allyl species **3.16**. Upon dissociation of the metal the enol intermediate **3.17** tautomerizes to the ketone intermediate **3.18**.



Scheme 3.6. Proposed mechanism for isomerization/ATH reaction of secondary allylic alcohol.

This ketone intermediate then reacts further with the active chiral Ru-catalyst in an outer-sphere metal-ligand bifunctional mechanism which dictates chiral induction. The formation of the six-membered ring transition state, **3.19**, with alternate charge distribution⁸ via hydrogen bonding (Scheme 3.7), affords the optically active alcohol product, **3.20**. The chirality leading to **3.20** originates from the existing five-membered ring structure of the catalyst system which was dictated by the amino end group of the chiral ligand and the metal center. This ring structure locks the catalyst system in a planar position thereby forcing the ketone intermediate to orient its large group away from the catalyst system. This favors transfer of hydrogen on the *si*-face of the prochiral ketone intermediate.

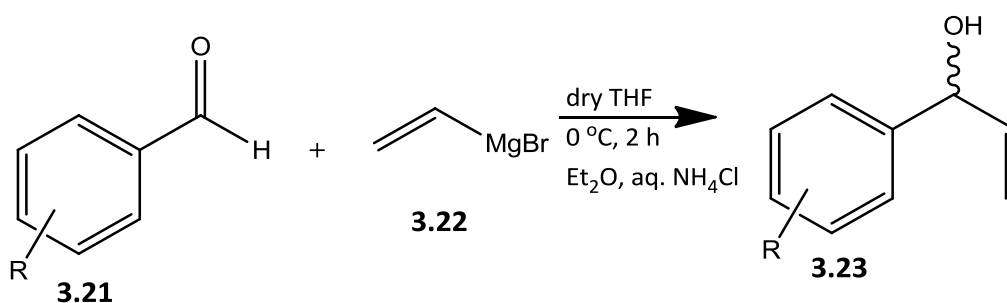


Scheme 3.7. Charge distribution in the transition state via H-bonding.⁸

3.4: ATH reaction of derivatives of α -vinyl benzyl alcohol

Derivatives of the model substrate α -vinyl benzyl alcohol were not commercially available. They were therefore synthesized in the laboratory from their corresponding benzaldehydes via the Grignard reaction, using the modified method of Wagner and co-workers¹⁰ (Scheme 3.8). Reactions were conducted in dry THF at 0 °C, with solutions of the

corresponding aldehyde and slow addition of vinyl magnesium bromide. The mixture was stirred for two hours, and quenched with diethyl ether and aqueous ammonium chloride, after a TLC check showed no presence of the aldehyde. Products were purified and isolated via flash chromatography on silica gel giving an average isolated yield of over 80%. The secondary α -vinyl benzyl alcohols were characterized by FT-IR, NMR and GC/MS techniques (Table 3.2)

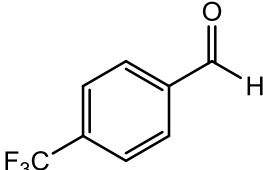
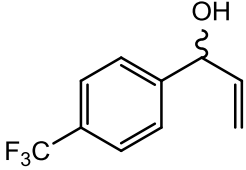
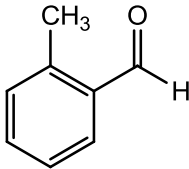
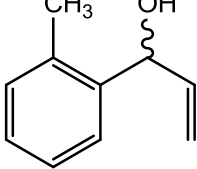


$\text{R} = p\text{-CH}_3$ - **3.24** $o\text{-CH}_3$ - **3.25** $p\text{-OCH}_3$ - **3.26** $p\text{-CF}_3$ - **3.27**

Scheme 3.8. Synthesis of derivatives 3.15-3.18 of α -vinyl benzyl alcohol.¹⁰

Table 3.2. Derivatives of α -vinyl benzyl alcohols.

Entry	Substrate	Product	%Yield ^a
1.			85
2.			87

3.			82
4.			80

^a isolated yield

The compound *trans*-1,3-diphenyl-2-propen-1-ol was purchased from Sigma-Aldrich and used without further purification (Figure 3.5).

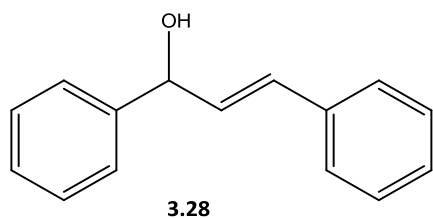
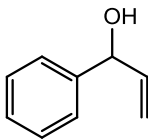
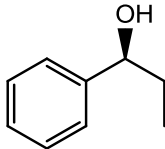
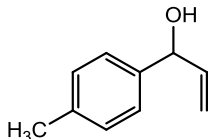
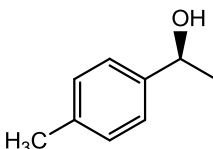
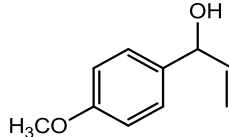
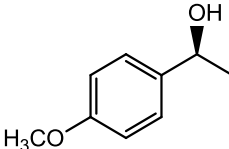
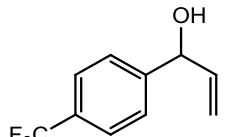
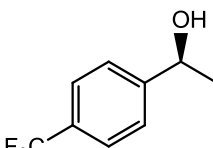
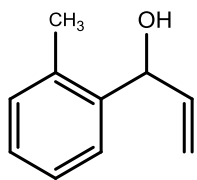
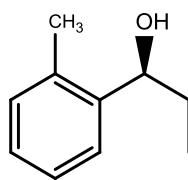
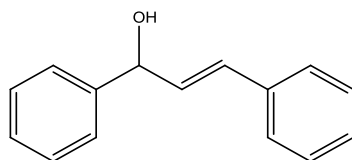
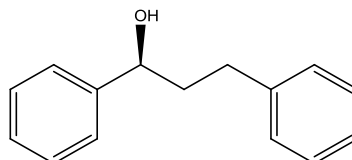


Figure 3.7. *trans*-1,3-diphenyl-2-propen-1-ol.

The isomerization and ATH reactions of these secondary allylic alcohols were conducted using the optimized conditions for the model substrate, **3.3**. Under these conditions, overall yields ranged from 77-92%, and 30-93% ee (Table 3.3). The anisole derivative (entry 3) gave the best % ee, 93%. The lowest enantioselectivity was obtained with the sterically hindered *o*-tolyl substrate (entry 5, 30%) and the α,β -unsaturated *trans*-1,3-diphenyl-2-propen-1-ol derivative (entry 6, 40%).

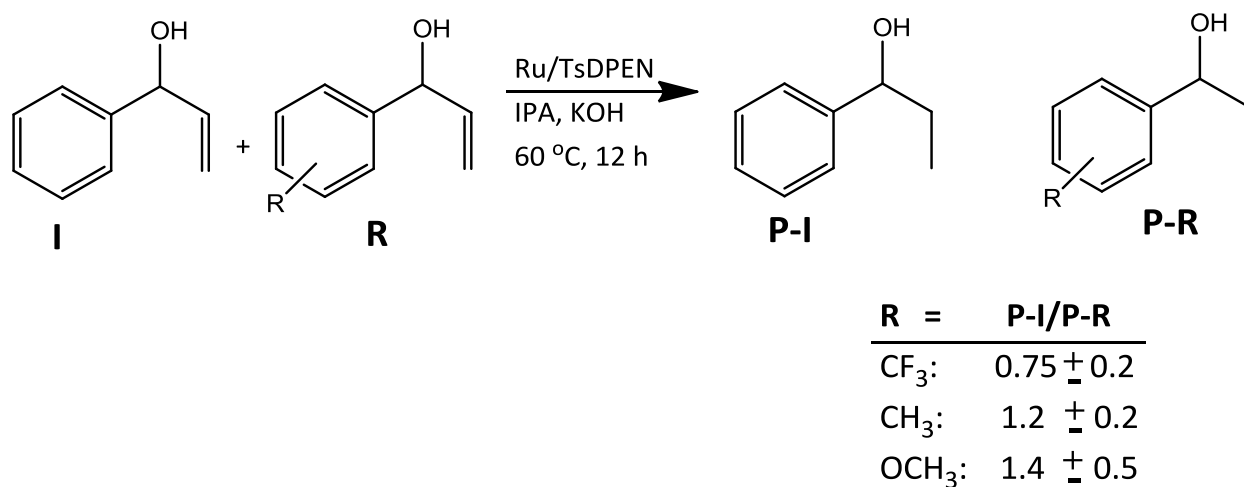
Table 3.3. Isomerization/ATH of substrates under the optimized conditions.

Entry	Racemic compound	Product	Yield% ^a	%ee ^b
1			97	90
2			86	71
3			82	93
4			92	69
5			86	30
6			77	40

^a. Determined by GC-MS analysis (Column: ZB5-MS , 60 m, 0.25 mm ID, 0.25 μ m, Flow rate: 1.2mL/min., FID @ 280 $^{\circ}$ C). ^b. Determined by chiral HPLC analysis (Chiralpak AS-3R column- 100 x 4.6 mm, 3 μ with 35/65% acetonitrile/water, Flow rate, 1 mL/min. λ_{max} 220 nm)

3.5: Evaluation of the Electronic Effects

It has been experimentally established in physical organic chemistry that the presence of a substituent on an aromatic ring system can result in the polarization of electron density around the ring through the π system in both the reactant and the product.¹¹ This also affects the position of equilibrium and the relative rates of reaction in the reactants and the transition states. One way to study this is through resonance, charge distribution and bond dipoles effects with electron withdrawing groups (EWG) and electron donating groups (EDG). Thus, a series of competition experiments between the model substrate (**I**) and its derivatives (**R**) were conducted (Scheme 3.9).



Scheme 3.9. Evaluation of electronic effects using competition experiments.

Each reaction in Scheme 3.9 was run in triplicate, the relative product ratio of **I** vs. the substituted derivative **R** was determined by GC-MS with relative rate expressed as [P-I]/[P-R].

The trend indicated that the reaction favors P-R, when R is the EWG substituent CF₃. As noted in previous work from our laboratory, the isomerization step is likely the rate

determining step in this type of ATH reaction. The electronic effects observed in this reaction can be rationalized by the field effects of the $-\text{CF}_3$ group, which favors hydride abstraction (Scheme 3.6, steps 4-5) to form the enolate intermediate. Conversely, electron donating resonance ($-\text{OCH}_3$) and inductive ($-\text{CH}_3$) effects destabilize the enolate intermediate, thus slowing its formation. Therefore, on the average, and within experimental error, the trend shows the relative rate of reactivity as, **3.3** > **3.24** and **3.26**, but < **3.27** (Figure 3.5).

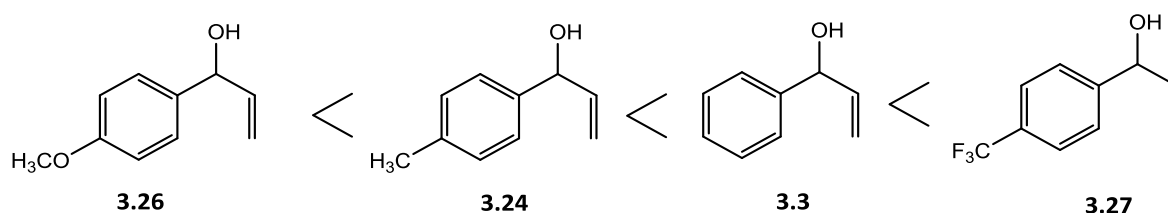


Figure 3.7. Comparative trend of relative rates of ATH reaction of secondary allylic alcohols, **3.3**, **3.24**, **3.26**, **3.27**.

3.6: Conclusions

In this thesis a new methodology for the transformation of racemic secondary allylic alcohols was developed and optimized for α -vinyl benzyl alcohol and a small set of its derivatives. This process featured a ruthenium catalyzed isomerization and asymmetric transfer hydrogenation reaction. The reaction method was optimized via a substrate/catalyst/ligand /base mole ratio of 10/1/1/2 and a temperature programmed strategy to improve selectivity. Evaluation of electronic effects revealed the sensitivity of the reaction method to both EWG and EDG, as demonstrated by the competition experiments.

3.7: Experimental Section

3.7.1: General Information

Reactions were conducted using oven-dried glassware, and under nitrogen atmosphere for all ATH reaction procedures. The catalyst system was generated *in situ* using Noyori's method. Derivatives of the model allylic alcohol substrate, α -vinyl benzyl alcohol, were synthesized using modified method of Wagner and co-workers.¹⁰

Reagents were purchased from commercial vendors and used as such. The FT-IR spectra were measured with Perkin-Elmer Spectrum 100 FT-IR spectrometer. The NMR spectra were obtained with Bruker 300MHz. Chemical shifts (δ) are reported in ppm, using the residual undeuterated protio-solvent peak (CDCl_3 : δH 7.26 and δC 77.16) as internal standard and TMS (δH 0.00 and δC 0.00) as reference peak. Coupling constants (J) are given in Hz.

Enantiomeric excess was determined with Agilent HP1090 HPLC, using chiral column OD RH, with 50/50 methanol/water as mobile phase. The flow rate was 0.5 mL/min. Or, a Chiralpak AS-3R column with 35/65% acetonitrile/water, 1 mL/min. λ_{max} 220 nm

GC/MS Parameters^a

Column Phenomenex ZB5-MS , 60 m, 0.25 mm ID, 0.25 μm

Injection

Injection Volume	1 μ L split (150:1)
Liner	4 mm ID straight inlet liner S/SL w/wool
Injection Temperature	250 $^{\circ}$ C
Split Vent Flow Rate	178.5 mL/min
Oven	
Oven Temperature	100 $^{\circ}$ C (hold 7 min) to 300 $^{\circ}$ C at 10 $^{\circ}$ C/min (hold 15 min)
Carrier Gas	He, constant flow
Flow Rate	1.2 mL/min
Detector	FID @ 280 $^{\circ}$ C
Make-Up Gas Flow Rate	45.0 mL/min
Make-Up Gas Type	He
Data Rate	20 Hz
Detector	MS
Mode	Scan
Transfer Line Temperature	280 $^{\circ}$ C
Analyzer Type	Quadrupole
Source Temperature	230 $^{\circ}$ C

Electron Energy	70 eV
Solvent Delay Time	0.55 min.
Tune Type	PFTBA
Ionization Mode	Electron Impact (EI)
Scan Range	35-400 amu
Scan Rate	3.89 scans/sec
Instrument	Agilent 5973 Inert Mass Selective Detector (MSD)

^aProvided by Tom Del Mastro

3.7.2: Procedure for Isomerization/Asymmetric Transfer Hydrogenation of Model Substrate

To a degassed solution of IPA (40 mL) in a three-neck round bottomed flask, was added the pre-catalyst $[\text{RuCl}_2(\eta^6\text{-}p\text{-cymene})]_2$ (61 mg, 0.1 mmol) and (1*S*,2*S*)-*N*-(*p*-toluenesulfonyl)-1,2-diphenylethylenediamine [(*S,S*)-TsDPEN] ligand (36 mg, 0.1 mmol), (Ru atom: TsDPEN mole ratio = 1:1), under an inert atmosphere, and stirred for 25 min at 80 °C, to give an orange solution, which was then cooled to 45 °C. A pre-mixed solution of the base KOH (11 mg, 0.2 mmol) and substrate- α -vinyl benzyl alcohol (134 mg, 1.0 mmol) in IPA was added, and allowed to mix for 2 h. The reaction mixture was then cooled to 25 °C, and stirred for 16 h. The yield was determined by GC-MS and the ee % value was determined by HPLC with a Daicel chiral OJ-RH

column with 50/50 (v/v) methanol/water as mobile phase at 20 °C at 220 nm. The product was characterized by GC-MS, NMR, FT-IR and chiral HPLC techniques and was isolated by evaporation of the solvent under vacuum and purification by chromatography on silica gel with hexane/ethyl acetate as the eluent.

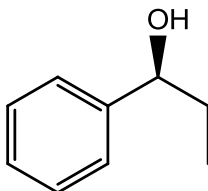
3.7.3: Procedure for Synthesis of Allylic Alcohol Derivatives

Corresponding aldehyde *p*-tolualdehyde (1.80 g, 14.99 mmol) was dissolved in a solution of THF (60 mL) contained in a 100 mL two-neck round bottomed flask fitted with a drying tube and an addition funnel, at 0 °C and stirred for 5 min. Then 18 mL of vinyl magnesium bromide (1.0 M in THF) was added slowly to the mixture and stirred at 0 °C for an additional 2 hours. The TLC was checked after this period and indicated no presence of the aldehyde. The reaction mixture was diluted with diethyl ether (10 mL), quenched with ammonium chloride (10 mL) and allowed to warm up to room temperature. The reaction mixture was transferred into a separatory funnel and extracted with diethyl ether three times. The combined organic layer was washed with brine, dried over MgSO₄, and concentrated under vacuum. The crude product was purified and isolated by column chromatography using silica gel with dichloromethane/ethyl acetate (10/1) as eluent.

3.8: Experimental Data

3.8.1: ATH Product of Model Substrate – α -vinylbenzyl alcohol

(S)-1-phenyl-1-propanol (**3.5**)¹²



Compound **3.5** was prepared according to the procedure described in section 3.7.2. and afforded a pale yellow oil as the product in 97% yield and 90% ee.

¹H NMR (300 Hz, CDCl₃): δ = 7.17-7.02 (m, 5H), 4.74-4.48 (t, 1H, J = 6.65 Hz), 1.79–1.55 (m, 2H), 0.65–0.60 (t, 3H, J = 7.35 Hz), 1.92-1.75 (brs, 1H)

¹³C NMR (300Hz, CDCl₃): δ = 144.65, 128.40, 127.71, 127.49, 125.98, 76.02, 31.89, 10.13.

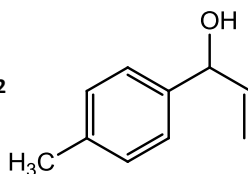
IR (neat, ν_{max} /cm⁻¹): 3357, 3029, 1452, 1375.

Enantiomeric excess was determined by chiral HPLC analysis (Daicel chiral OJ-RH column with 50/50 (v/v) methanol/water, 0.5 mL/min. λ_{max} 220 nm). R_t = 24.545 min (R)-enantiomer, R_t = 26.683 min (S)-enantiomer, 90% ee.

GC/MS - m/z = 136.1

3.8.2: Synthesis of Intermediates – Derivatives of the model substrate

1-(4-methylphenyl)-2-propen-1-ol (**3.24**)¹²



p-Tolualdehyde (1.80 g 14.99 mmol) was dissolved in a solution of THF (60 mL), to synthesize compound **3.24** in accordance with the procedure described in section 3.7.3. A yellow oil was obtained as the product in 85% yield, and was characterized with NMR, IR and GC/MS.

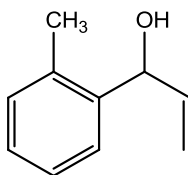
¹H NMR (300 MHz, CDCl₃): δ = 7.35-7.15 (m, 4H), 6.23-5.93 (m, 1H), 5.48-5.33 (m, 1H), 5.25-5.10 (m, 2H), 2.4 (s, 3H), 2.15-1.95 (brs, 1H).

¹³C NMR (75 MHz, CDCl₃): δ = 140.41, 139.77, 129.58, 127.11, 126.57, 114.82, 75.16, 60.42, 21.11, 14.19.

IR (neat, ν_{max} /cm⁻¹): 3365, 2922, 1512, 1420.

GC/MS – m/z = 148.1

1-(2-methylphenyl)-2-propen-1-ol (**3.25**)



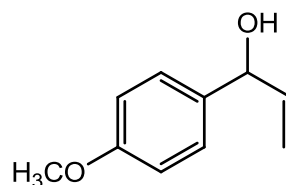
o-Tolualdehyde (2.25 g, 18.72 mmol) was dissolved in a solution of THF (50mL), to synthesize compound **3.25** in accordance with the procedure described in section 3.7.3. A yellow oil was obtained as the product in 80% yield, and was characterized with NMR, IR and GC/MS.

^1H NMR (300 MHz, CDCl_3): δ = 7.55-7.10 (m, 4H), 6.0-5.75 (m, 1H), 5.80-5.65 (m, 1H), 5.30-5.00 (m, 2H), 2.25 (s, 3H), 2.0-1.85 (brs, 1H).

IR (neat, $\nu_{\text{max}}/\text{cm}^{-1}$): 3364, 2977, 1694, 1487.

GC/MS – m/z = 148.1

1-(4-methoxyphenyl)-2-propen-1-ol (3.26)¹²



p-Methoxybenzaldehyde (2.37g, 17.43 mmol) was dissolved in a solution of THF (50 mL), to synthesize compound **3.26** in accordance with the procedure described in section 3.7.3. A yellow oil was obtained as product in 95% yield, and was characterized with NMR, IR and GC/MS.

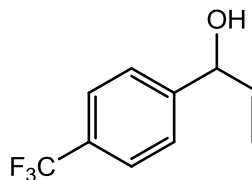
^1H NMR (300 MHz, CDCl_3) : δ = 7.40-7.25 (m, 2H), 6.95-6.85 (m, 2H), 6.15-5.95 (m, 1H), 5.45-5.30 (m, 1H), 5.22-5.08 (m, 2H), 3.84 (s, 3H), 2.32- 2.15 (brs, 1H).

^{13}C NMR (75 MHz, CDCl_3) : δ = 159.20, 140.41, 134.90, 127.68, 126.88, 114.73, 113.95, 71.19, 67.93, 55.29, 25.58.

IR (neat, $\nu_{\text{max}}/\text{cm}^{-1}$): 3410, 2836, 1608, 1509.

GC/MS – m/z = 164.1

1-(4-trifluoromethylphenyl)-2-propen-1-ol (3.27)



p-Trifluoromethylbenzaldehyde (2.25g, 13.10 mmol) was dissolved in a solution of THF (50 mL), to synthesize compound **3.27** in accordance with the procedure described in section 3.7.3. An orange oil was obtained as the product in 80% yield, and was characterized with NMR, IR and GC/MS.

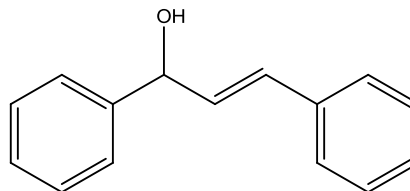
^1H NMR (300 MHz, CDCl_3) : δ = 7.65-7.55 (m, 2H), 7.45-7.30 (m, 2H), 6.10-5.60 (m, 1H), 5.38-5.30 (m, 1H), 5.25-5.10 (m, 2H), 2.25-1.59 (brs, 1H).

^{13}C NMR (75 MHz, CDCl_3) : δ = 146.5, 139.6, 128.9, 126.2, 116.7, 77.5, 76.4, 74.9.

IR (neat, $\nu_{\text{max}}/\text{cm}^{-1}$): 3347, 1619, 1417, 1322.

GC/MS – m/z = 202.1

***trans*-1,3-diphenyl-2-propen-1-ol (3.28)**



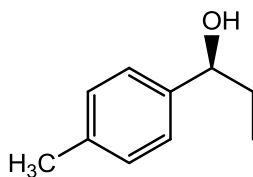
Purchased from Sigma-Aldrich and used without further purification.

3.8.3: Isomerization/Asymmetric Transfer Hydrogenation Products

Derivatives of the model substrate – α -vinyl benzyl alcohol were subjected to the optimized conditions for isomerization/ATH reaction to afford saturated optically active alcohol

products, ranging between 77 - 86% in yield and 30 – 93% ee. Each product was characterized by NMR, IR and GC/MS and chiral HPLC techniques.

(S)- 1-(4-methylphenyl)propan-1-ol (3.29)¹²



In accordance with the procedure described in section 3.7.2. The Isomerization/ATH reaction of **3.24** afforded **3.29** as yellow oil in 86% yield and 71% ee.

¹H NMR (300 MHz, CDCl₃): δ = 7.25-6.59 (m, 4H), 4.55-4.40 (t, 1H, *J* = 6.63 Hz), 2.25 (s, 3H), 1.75-1.53 (m, 2H), 1.80 (brs, 1H), 0.90-0.70 (t, 3H, *J* = 7.61)

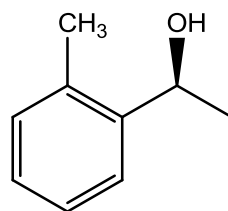
¹³C NMR (75 MHz, CDCl₃): δ = 141.67, 137.13, 129.08, 125.94, 75.89, 31.94, 29.67, 22.70, 14.12, 10.18.

IR (neat, ν_{max}/cm⁻¹): 3389, 2927, 1513, 1455.

Chiral HPLC : (Chiralpak AS-3R column- 100 x 4.6 mm, 3μm with 35/65% acetonitrile/water, 1 mL/min. λ_{max} 220 nm). R_t = 4.43 min (R)-enantiomer, R_t = 4.92 min (S)-enantiomer, 71% ee.

GC/MS - *m/z* = 150.10

(S)-1-(2-methylphenyl)-2-propen-1-ol (3.30)



In accordance with the procedure described in section 3.7.2. The isomerization/ATH reaction of **3.25** afforded **3.30** as yellow oil in 86% yield and 30% ee.

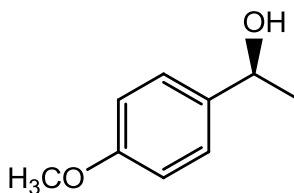
^1H NMR (300 MHz, CDCl_3): δ = 7.40-7.0 (m, 4H), 4.85-4.70 (t, 1H, J = 6.70 Hz), 2.35 (s, 3H), 1.75-1.65 (m, 2H), 1.55 (brs, 1H), 0.95-0.80 (t, 3H, J = 7.55)

IR (neat, $\nu_{\text{max}}/\text{cm}^{-1}$): 3408, 2928, 1688, 1572.

Chiral HPLC : (Chiralpak AS-3R column- 100 x 4.6 mm, 3μ with 35% acetonitrile/65% water, 1 mL/min. λ_{max} 220 nm). R_t = 5.64 min (R)-enantiomer, R_t = 5.99 min (S)-enantiomer, 30% ee.

GC/MS - m/z = 150.10

(S)-1-(4-methoxyphenyl)propan-1-ol (3.31)¹²



In accordance with the procedure described in section 3.7.2. The isomerization/ATH reaction of **3.26** afforded **3.31** as yellow oil in 82% yield and 93% ee.

^1H NMR (300 MHz, CDCl_3): δ = 7.30-7.15 (m, 2H), 6.95-6.80 (m, 2H), 4.60-4.40 (t, 1H J = 6.73 Hz), 3.75 (s, 3H), 1.85-1.60 (m, 2H), 1.30-1.20 (brs, 1H) 0.90-0.75 (t, 3H J = 7.45 Hz).

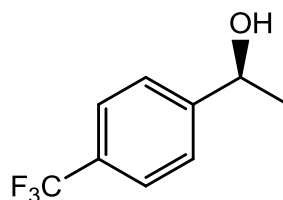
^{13}C NMR (75 MHz, CDCl_3): δ = 159.02, 136.77, 127.20, 113.79, 75.66, 64.43, 55.27, 31.78, 10.19.

IR (neat, $\nu_{\text{max}}/\text{cm}^{-1}$): 3410, 2836, 1445, 1350.

Chiral HPLC : (Chiralpak AS-3R column- 100 x 4.6 mm, 3 μ with 35/65% acetonitrile/water, 1 mL/min. λ_{max} 220 nm). R_t = 5.31 min (R)-enantiomer, R_t = 5.61 min (S)-enantiomer, 93% ee.

GC/MS - m/z = 166.10

(S)-1-(4-trifluoromethyl)propan-1-ol (3.32)



In accordance with the procedure described in section 3.7.2. The isomerization/ATH reaction of **3.27** afforded **3.32** as yellow oil in 92% yield and 69% ee.

^1H NMR (300 MHz, CDCl_3): δ = 7.65-7.30 (m, 4H), 4.70-4.55 (t, 1H, J = 5.86 Hz), 2.0-1.85 (brs, 1H), 1.80-1.55 (m, 2H), 0.94-0.82 (t, 3H, J = 7.62 Hz).

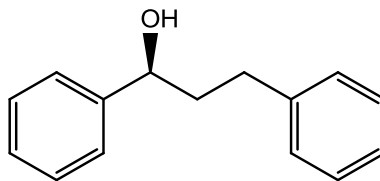
^{13}C NMR (75 MHz, CDCl_3): δ = 142.5, 136.8, 129.8, 126.5, 76.1, 32.5, 29.8, 21.0, 14.2, 10.0.

IR (neat, ν_{max} /cm $^{-1}$): 3395, 2959, 1464, 1376.

Chiral HPLC : (Chiralpak AS-3R column- 100 x 4.6 mm, 3 μ with 35% acetonitrile with 0.1% formic acid/ 65% water with 0.1% formic acid, 1 mL/min. λ_{max} 220 nm). R_t = 6.15 min (R)-enantiomer, R_t = 6.56 min (S)-enantiomer, 69% ee.

GC/MS - m/z = 204.08

(S)-1,3-diphenylpropan-1-ol (3.33)¹³



Racemic 1,3-diphenyl-2-propen-1-ol (**3.28**) the precursor to compound **3.33** was purchased from Sigma-Aldrich and used without further purification. Thus, in accordance with the procedure described in section 3.7.2. The isomerization/ATH reaction of this precursor afforded **3.33** as yellow oil in 77% yield and 40% ee.

¹H NMR (300 MHz, CDCl₃): δ = 7.45-7.15 (m, 10H), 4.75-4.60 (t, 1H, J = 6.11 Hz), 2.85-2.55 (m, 2H), 2.25-2.00 (m, 2H), 1.95-1.85 (brs, 1H).

¹³C NMR (75 MHz, CDCl₃): δ = 144.58, 141.78, 128.97, 128.51, 128.44, 128.38, 128.05, 127.63, 125.92, 125.85, 73.88, 60.40, 40.46, 32.05, 31.79, 29.66, 21.02, 14.19.

IR (neat, ν_{max} /cm⁻¹): 3395, 2859, 1602, 1494.

Chiral HPLC : (Chiralpak AS-3R column- 100 x 4.6 mm, 3 μ with 35% acetonitrile with 0.1% formic acid/ 65% water with 0.1% formic acid, 1 mL/min. λ_{max} 220 nm). R_t = 8.28 min (R)-enantiomer, R_t = 8.61 min (S)-enantiomer, 40% ee.

GC/MS - m/z = 212.10

References

1. Wu, R.; Beauchamps, M. G.; Laquidara, J. M.; Sowa, Jr. J. R. *Angew. Chem. Int. Ed.*, **2012**, *51*, 1-6.
2. (a) van der Drift, R. C.; Bouwman, E. and Drent, E. *J. of Organomet. Chem.*, **2002**, *650*, 1-24. (b) Uma, R.; Crevisy, C. and Gree, R. *Chem. Rev.* **2003**, *103*, 27-51.
- 3.(a) Noyori, R.; Hashiguchi, S. *Acc. Chem. Res.* **1997**, *30*, 97-102. (b) Noyori, R. *Asymmetric Catalysis in Organic Synthesis*, John Wiley, NewYork, 1994. (c) Noyori, R. *Angew. Chem. Int. Ed.* **2002**, *41*, 2008 -2022.
4. Palmer, M. J. and Wills, M. *Tetrahedron: Asymmetry*, **1999**, *10*, 2045–2061.
5. (a) Hashiguchi, S.; Fujii, A.; Takehara, J.; Ikariya, T.; Noyori, R. *J. Am. Chem. Soc.* **1995**, *117*, 7562-7563. (b) Noyori, R.; Hashiguchi, S. *Acc. Chem. Res.* **1997**, *30*, 97-102.
6. (a) Knowles, W. S.; *Acc. Chem. Res.*, **1983**, *16*, 106-112. (b) Gawley, R. E. *J. Org. Chem.* **2006**, *71*, 2411-2416. (c) Hartwig, J. F. *Organotransition Metal Chemistry: From Bonding to Catalysis*, 1st ed., **2009** (d) Walsh, P. J.; Kozlowski, M. C. *Fundamentals of Asymmetric Catalysis*, University Science Books, **2009** (e) Gawley, R. E.; Aube, J. *Tetrahedron Org. Chem. Series, Vol. 14: Principles of Asymmetric Synthesis*, **2006**.
7. Shoola, C. O.; DelMastro, T.; Wu, R. and Sowa, Jr., J. R. *Eur. J. Org. Chem.*, **2015**, 1670-1673.
8. (a) Yamakawa, M.; Ito, H.; and Noyori, R. *J. Am. Chem. Soc.* **2000**, *122*, 1466-1478. (b) Ikariya, T. and Blacker, A. J. *Acc. Chem. Res.* **2007**, *40*, 1300–1308.
9. Noyori, R.; Yamakawa, M.; Hashiguchi, S. *J. Org. Chem.*, **2001**, *66*, 7931-7944.
10. Briot, A.; Baeher, C.; Brouillard, R.; Wagner, A.; Mioskowski, C. *J. Org. Chem.*, **2004**, *69*, 1374-1377.
11. (a) Hammett, L. P. *Some Relations Between Reaction Rates and Equilibrium Constants*, **1935**. Hammett, L. P. *The Effect of Structure upon the Reactions of Organic Compounds. Benzene Derivatives*, **1937**. (C) Carey, F. A. and Sundberg, R. J. *Advanced Organic Chemistry, Part A, Second Edition*, Plenum Press ISBN 0-306-41198-9. (d) Anslyn, E. V. and Dougherty, D. A. *Modern Physical Organic Chemistry*, University Science Books ISBN 1-891389-31-9.
12. T. Slagbrand, H. Lundberg, H. Adolfsson, *Chem. Eur. J.* **2014**, *20*, 16102–16106.
13. C. Qin, H. Wu, J. Cheng, X. a. Chen, M. Liu, W. Zhang, W. Su and J. Ding, *J. Org. Chem.*, 2007, **72**, 4102-4107

Chapter Four: Conclusions and Future Work

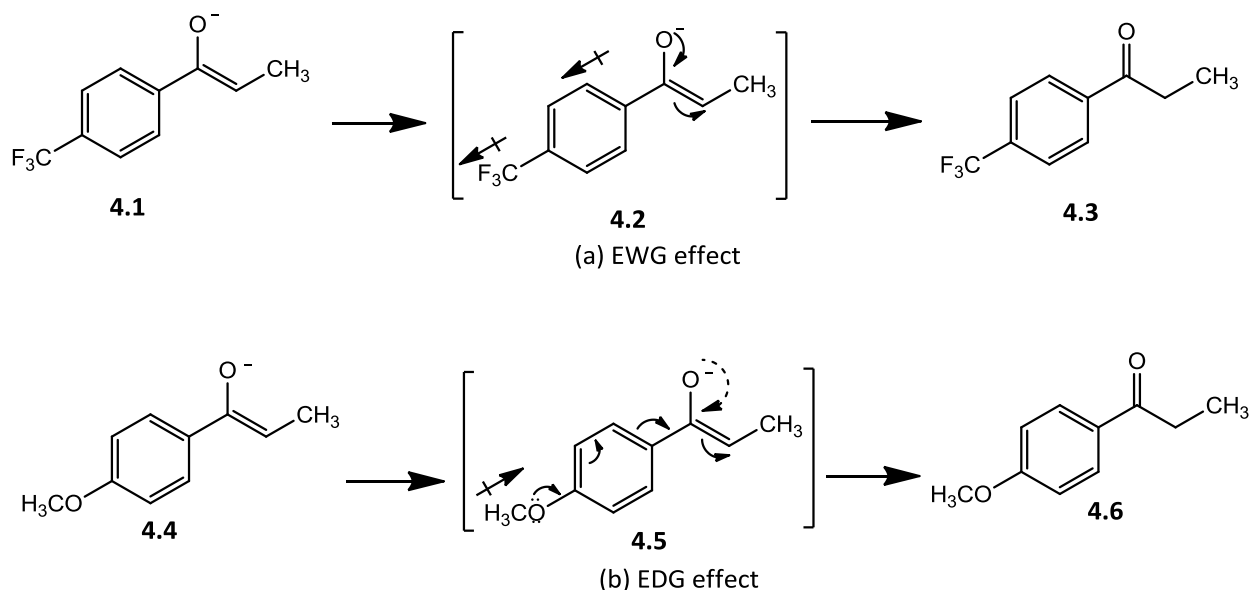
4.1: General Conclusion

Isomerization and asymmetric transfer hydrogenation reactions of secondary allylic alcohols were carefully studied and developed in our laboratory. This was accomplished following the success with the enantioselective isomerization and transfer hydrogenation reactions of the primary allylic alcohol, geraniol.

In this thesis work, the isomerization and ATH reaction technique has been validated and optimized as a new methodology for the transformation of racemic secondary allylic alcohols into optically active secondary alcohols. This efficient reaction method is catalyzed by a combination of a ruthenium metal complex with TsDPEN as chiral ligand, which is believed to form the active catalyst that effectively reduces both the carbon-to-carbon double bond and the carbonyl group in a one pot process.

The reaction is clean and environmentally friendly, simple to operate and gives good to excellent (70-97%) yields, with high (90-93%) enantioselectivity for a small set of substituted α -vinyl benzyl alcohols. The reaction rate was found to be sensitive to EWG and EDG; the EWG is postulated to remove electron density from the benzylic carbon via field effects and speeds the rate of reaction through enhanced rate of tautomerization (Scheme 4.1a). Meanwhile the EDG is hypothesized to push electron density towards the reactive site via resonance and inductive effects (Scheme 4.1b). This slows down the rate of tautomerization and the overall reaction rate. The selectivity of the reaction is comparatively consistent with literature reports on the

isomerization/ATH of secondary allylic alcohols using protected amino acid hydroxyamide chiral ligand.¹ It appears to be much more affected by sterics in the ortho-substituted derivatives and the disubstituted olefin substrates. However, a more carefully optimized procedure targeted at overcoming steric hindrance may enhance the reactivity and selectivity in these difficult substrates.



Scheme 4.1. Substituent (a) EWG and (b) EDG effects on the rate of reaction for the ATH of substituted α -vinyl benzyl alcohols.

4.2: Mechanistic Rationale

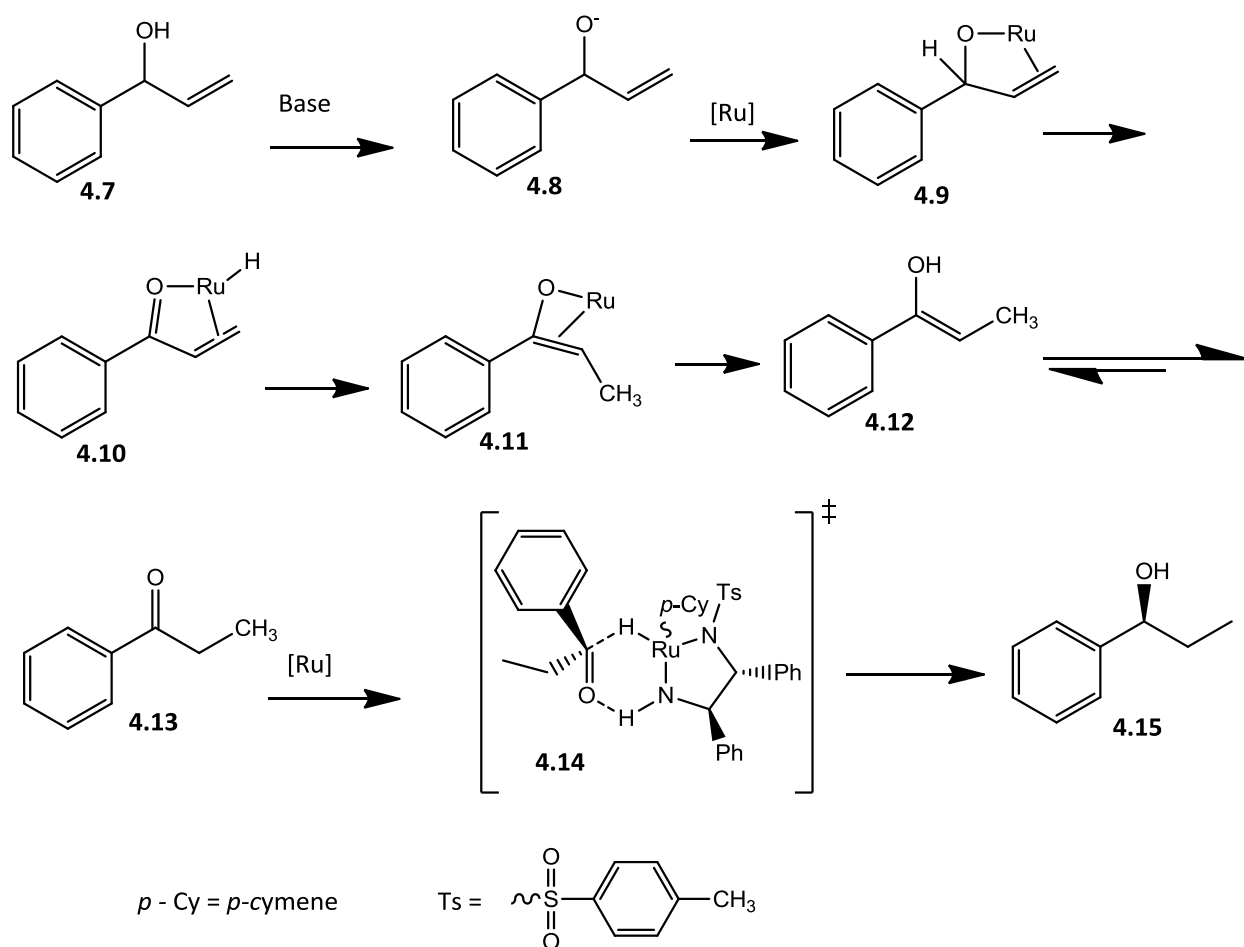
The proposed mechanism of this reaction is believed to follow in part; the published mechanism of the ATH reaction for the primary allylic alcohol, geraniol.² The mechanistic steps outlined in the proposed mechanism (Scheme 4.2) are in agreement with the established

mechanisms of the isomerization of primary allylic alcohol leading to the formation of a carbonyl compound, in this case a ketone intermediate.

The ketone intermediate **4.13** generated from the transposition of the secondary allylic alcohol olefinic moiety **4.7** is believed to undergo reduction through an outer-sphere enantiofacial transfer of the hydrogen atom via a six-membered ring transition state **4.14**. This is stabilized and activated towards the reduction step by hydrogen – bonding promoted alternate charge distribution.

This mechanistic reasoning has been demonstrated by extensive experimental studies on the ATH reactions of prochiral ketones conducted by Noyori and co-workers, and established that the reduction of the ketone substrate occurred through a metal-ligand bifunctional mechanism. In this case, the ligand participated in tandem with the metal to effect hydrogen transfer and formation of the optically active alcohol.³

Similarly, the enantiofacial discrimination in the reduction of the ketone intermediate **4.13** from the secondary allylic alcohol **4.7** is facilitated by the participation the amino end group of the ligand TsDPEN, which formed a five membered ring structure with the ruthenium metal center and locks the catalyst system in a planar orientation. This promotes hydrogen transfer more favorably on one face of the prochiral ketone intermediate **4.13**. In this way, the ketone intermediate is oriented in a position that places the larger group away from the catalyst system, thereby favoring the S-enantiomer chiral alcohol product **4.15**.



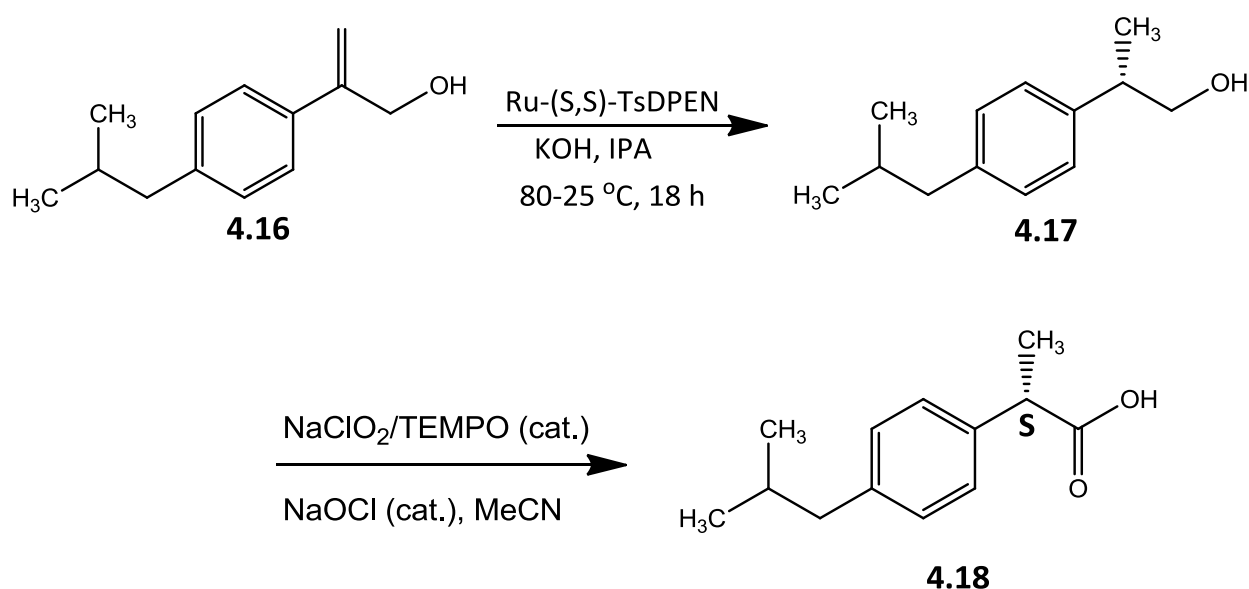
Scheme 4.2. Proposed mechanism of the chiral ATH of α -vinyl benzyl alcohols.

4.3: Future Work

The synthetic applications of the ATH reaction are proposed in the synthetic designs of two bioactive compounds: ibuprofen and the LTD₄ antagonist; Singulair.

Ibuprofen is a common over the counter non-steroidal anti-inflammatory drug (NSAID),⁴ currently synthesized in a four step process both in the industry and academia.⁵ Employing the isomerization/ATH reaction, its synthesis can be conveniently accomplished in two reaction

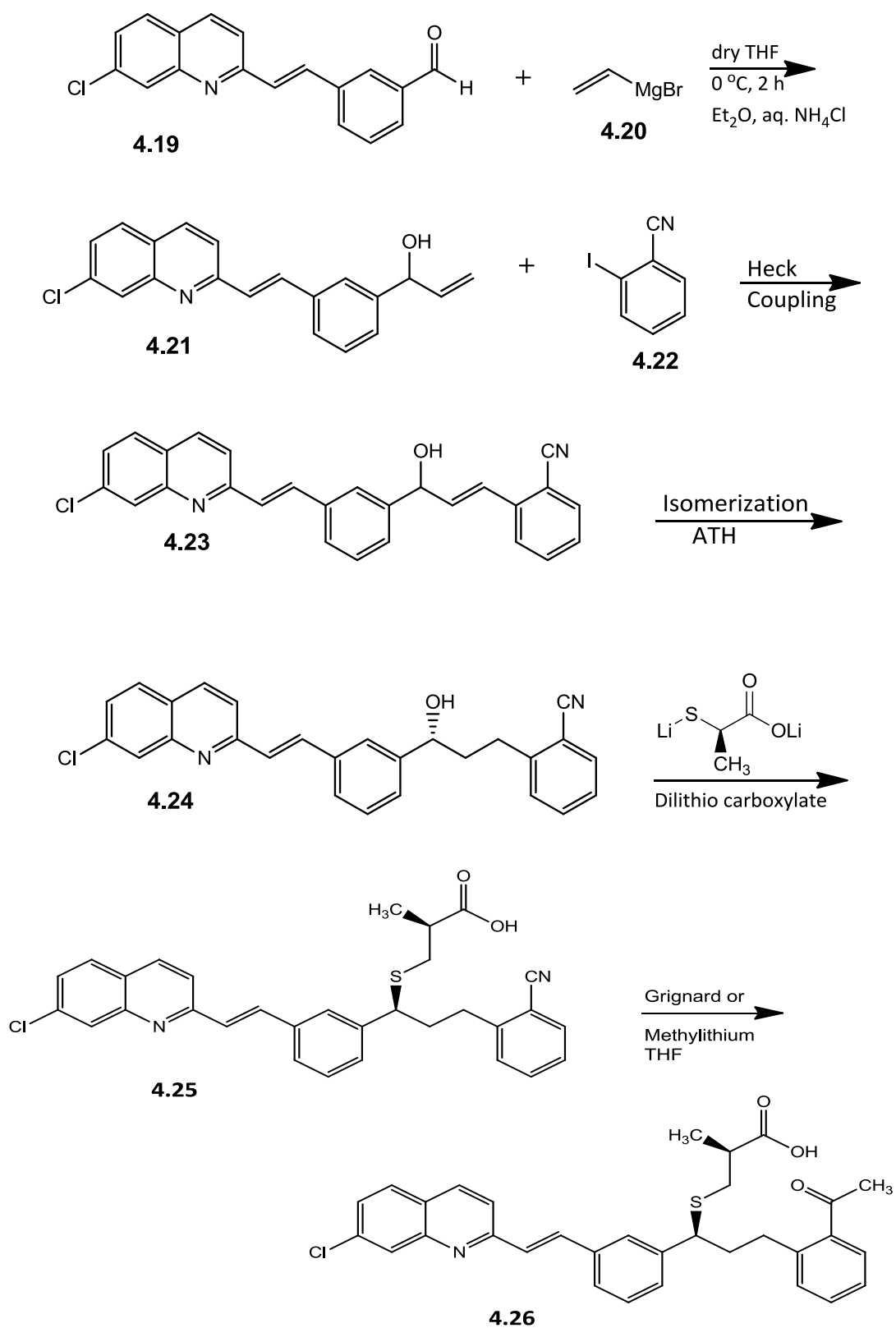
steps starting from the commercially available 2-(4-isobutylphenyl)-propen-1-ol (Scheme 4.1). The first step features the optimized conditions for the isomerization/ATH reaction to generate the important precursor **4.17**, to ibuprofen, followed by TEMPO oxidation to afford the biologically active S-enantiomer product **4.18**. The final product may be characterized using traditional analytical techniques such as, NMR, GC-MS, FT-IR and chiral HPLC. Additionally, biological studies may be conducted to validate the pharmacological activity of the product.⁶



Scheme 4.3. Proposed synthesis of ibuprofen.

Also, LTD_4 is an endogenous agonist, which causes contractions of smooth muscle lining the trachea, leading to inflammation in asthma and allergic rhinitis.⁷ The LTD_4 antagonist currently marketed as SingulairTM is synthesized in about eight reaction steps including a non-environmentally friendly key step.⁸ This key step utilizes the organoboron reduction chemistry, involving β -chlorodiisopinocampheylborane; a compound known for its sensitivity to air and moisture, as well as its high toxicity and explosive tendencies.⁹ This antagonist compound has a

single chiral center which can originate from a secondary allylic alcohol. The key step in the de novo total synthesis of Singulair™ will be to synthesize intermediate **4.23**, a core component of the antagonist, by the optimized ATH reaction shown in Scheme 4.4. If this step can be optimized in high yield and % ee, then this synthetic design may prove to be an excellent alternative to the current synthesis. Additionally, the proposed synthesis strategy features an initial formation of the allylic alcohol **4.21** through vinylation of the commercially available aldehyde **4.19**. The Heck reaction features coupling of **4.21** with 2-iodobenzonitrile **4.22** and is expected to generate the core component of the antagonist; intermediate **4.23**. This will be reduced to the chiral alcohol **4.24** through the optimized conditions of the isomerization/ATH reaction developed in this thesis work. Further reaction of **4.24** with dilithio carboxylate and transformation of the nitrile functionality to ketone, will produce the antagonist compound **4.26**. This synthetic approach presents two key catalytic steps (the Heck coupling and the isomerization/ATH reaction) that will not only reduce the cost of the synthetic process but are also atom economic. In fact, the current stereoselective step in this synthesis involves a stoichiometric organoborane reduction, which is not as atom economical as the proposed ATH reaction methodology.⁸



Scheme 4.4. Stereoselective synthesis step for the LTD4 antagonist.

The reaction steps in these synthetic targets as highlighted in both Schemes 4.3 and 4.4 are based on reactions that are known to function reliably well with high-yielding product outcomes.^{2, 8, 10, 11, 12} A careful retrosynthetic analyses will lead to the target components to which isomerization/ATH reaction can be effectively applied.

A careful optimization of this reaction method with the target components could provide a better alternative route to the current syntheses of these bioactive compounds. Moreover, the total synthesis of SingulairTM (LTD₄ antagonist) and IbuprofenTM, is proposed to occur through better atom economy, shortened reaction steps, and environmentally benign processes.

4.4: Publication and Presentations

This work has been published as a communication in the European Journal of Organic Chemistry, under the digital object identifier DOI: 10.1002/ejoc.201500075.¹³ This contribution to knowledge has not only expanded the scope of this important reaction but will also lead to new technological developments within the organic, inorganic and organometallic communities.

Additional work that may be published from this thesis work include detailed mechanistic studies of the proposed mechanisms for the ATH reaction of secondary allylic alcohols. The Hammett study of the rates of reaction to quantitatively validate the observed effects of the EWG and EDG groups. This can be used to gain a better understanding of the low selectivity recorded with the *ortho*-substituted derivatives and *di*-substituted olefin substrates.

This work has also been presented as seminal project at a symposium organized by the Catalysis Society of Metropolitan New York, held at Princeton University, Princeton, NJ, in 2013.¹⁴ It has also been featured at the Petersheim Science Exhibitions in 2013 and 2014, organized by the department of Chemistry and Biochemistry, Seton Hall University, South Orange, NJ.

Reference

1. T. Slagbrand, H. Lundberg, H. Adolfsson, *Chem. Eur. J.* **2014**, *20*, 16102–16106.
2. Wu, R.; Beauchamps, M. G.; Laquidara, J. M.; Sowa, Jr. J. R. *Angew. Chem. Int. Ed.*, **2012**, *51*, 1-6.
3. (a) Noyori, R. ; Yamakawa, M. ; Hashiguchi, S. *J. Org. Chem.*, **2001**, *66*, 7931 – 7944. (b) Yamakawa, M. ; Ito, H.; Noyori, R. *J. Am. Chem. Soc.* **2000**, *122*, 1466-1478.
4. Van Esch, A.; Van Steensel-Moll, H. A.; Steyerberg, E. W.; Offringa, M.; Habbema, J. D.; Derksen-Lubsen, G. *Archives of Pediatrics & Adolescent Medicine*, **1995**, *149*, 632–637.
5. Kjonaas, R. A.; Williams, P. E.; Counce, D. A.; Crawley, L. R. *J. Chem. Educ.* **2011**, *88*, 825–828.
6. (a) Geisslinger, G., Dietzel, K., Loew, D., Schuster, O., Rau, G., Lachmann, G., Brune, K. *J. Chrom. B: Biomedical Sciences and Applications*, **1989**, *491*, 139–149 . (b) Reddy, R. Chandiran, S., Jayaveera, K., Koteswara, R. *Arch. Apl. Sci. Res.*, **2010**, *2* (3): 101-111.
7. Lipkowitz, Myron A. and Navarra, Tova (**2001**) *The Encyclopedia of Allergies* (2nd ed.) Facts on File, New York, p. 178.
8. (a) King, A.O.; Corley, E. G.; Anderson, R. K.; Larsen, R. D.; Verhoeven, T. R.; Reider, P. J. *J. Org. Chem.* **1993**, *58*, 3731-3735. (b) Shinkai, I.; King, A. O.; Larsen, R. D. *Pure & Appl. Chem.*, **1994**, *66*, 1551-1556. (c) Srebnik, M.; Ramachandran, P. V.; Brown, H. C. *J. Org. Chem.*, **1988**, *53*, 2916-2920.

9. Review of MSDS from various manufacturers and suppliers

10. Zhao, M. M.; Li, J.; Mano, E.; Song, Z. J.; Tschaen, D. M. *Org. Synth.* **2005**, *81*, 195

11. Briot, A.; Baeher, C.; Brouillard, R.; Wagner, A.; Mioskowski, C. *J. Org. Chem.*, **2004**, *69*, 1374-1377.

12. (a) Heck, R. F. *J. Am. Chem. Soc.* **1969**, *91* (24), 6707. (b) Heck, R. F. *Org. React.*, **1982**, *27* 345–390. (c) Beletskaya, I. P.; Cheprakov, A. V. *Chem. Rev.* **2000**, *100* (8): 3009–3066.

13. Shoola, C. O.; DelMastro, T.; Wu, R. and Sowa, Jr., J. R. *Eur. J. Org. Chem.*, **2015**, 1670-1673.

14. *The Catalysis Society of Metropolitan New York*, **2013 Spring Symposium**

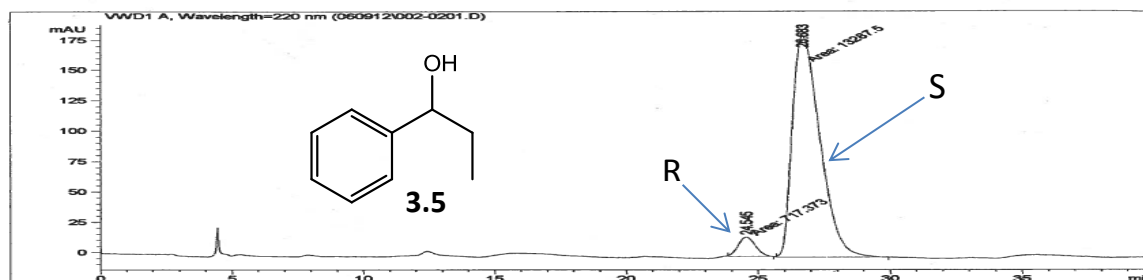
Appendix

Table of Contents

Figure A1. The chiral HPLC chromatogram of compound 3.5	116
Figure A2. The ^1H NMR spectrum of compound 3.5	117
Figure A3. The ^{13}C NMR spectrum of compound 3.5	118
Figure A4. The FT-IR spectrum of compound 3.5	119
Figure A5. The mass spectrum of compound 3.5	120
Figure A6. The ^1H NMR spectrum of compound 3.24	121
Figure A7. The ^{13}C NMR spectrum of compound 3.24	122
Figure A8. The ^1H NMR spectrum of compound 3.25	123
Figure A9. The ^1H NMR spectrum of compound 3.26	124
Figure A10. The ^{13}C NMR spectrum of compound 3.26	125
Figure A11. The ^1H NMR spectrum of compound 3.27	126
Figure A12. The ^{13}C NMR spectrum of compound 3.27	127
Figure A13. The chiral HPLC chromatogram of compound 3.29	128
Figure A14. The ^1H NMR spectrum of compound 3.29	129

Figure A15. The ^{13}C NMR spectrum of compound 3.29	130
Figure A16. The FT-IR spectrum of compound 3.29	131
Figure A17. The mass spectrum of compound 3.29	132
Figure A18. The chiral HPLC chromatogram of compound 3.30	133
Figure A19. The ^1H NMR spectrum of compound 3.30	134
Figure A20. The FT-IR spectrum of compound 3.30	135
Figure A21. The chiral HPLC chromatogram of compound 3.31	136
Figure A22. The ^1H NMR spectrum of compound 3.31	137
Figure A23. The ^{13}C NMR spectrum of compound 3.31	138
Figure A24. The FT-IR spectrum of compound 3.31	139
Figure A25. The mass spectrum of compound 3.31	140
Figure A26. The chiral HPLC chromatogram of compound 3.32	141
Figure A27. The ^1H NMR spectrum of compound 3.32	142
Figure A28. The FT-IR spectrum of compound 3.32	143
Figure A29. The mass spectrum of compound 3.32	144
Figure A30. The chiral HPLC chromatogram of compound 3.33	145
Figure A31. The ^1H NMR spectrum of compound 3.33	146

Figure A32. The ^{13}C NMR spectrum of compound 3.33	147
Figure A33. The mass spectrum of compound 3.33	148



Area Percent Report

Sorted By : Signal
Multiplier : 1.0000
Dilution : 1.0000

Signal 1: VWD1 A, Wavelength=220 nm

Peak #	RetTime [min]	Type	Width [min]	Area [mAU*s]	Height [mAU]	Area %
1	24.545	MM	0.7556	717.37329	15.82323	5.1223
2	26.683	MM	1.2144	1.32873e4	182.35742	94.8777

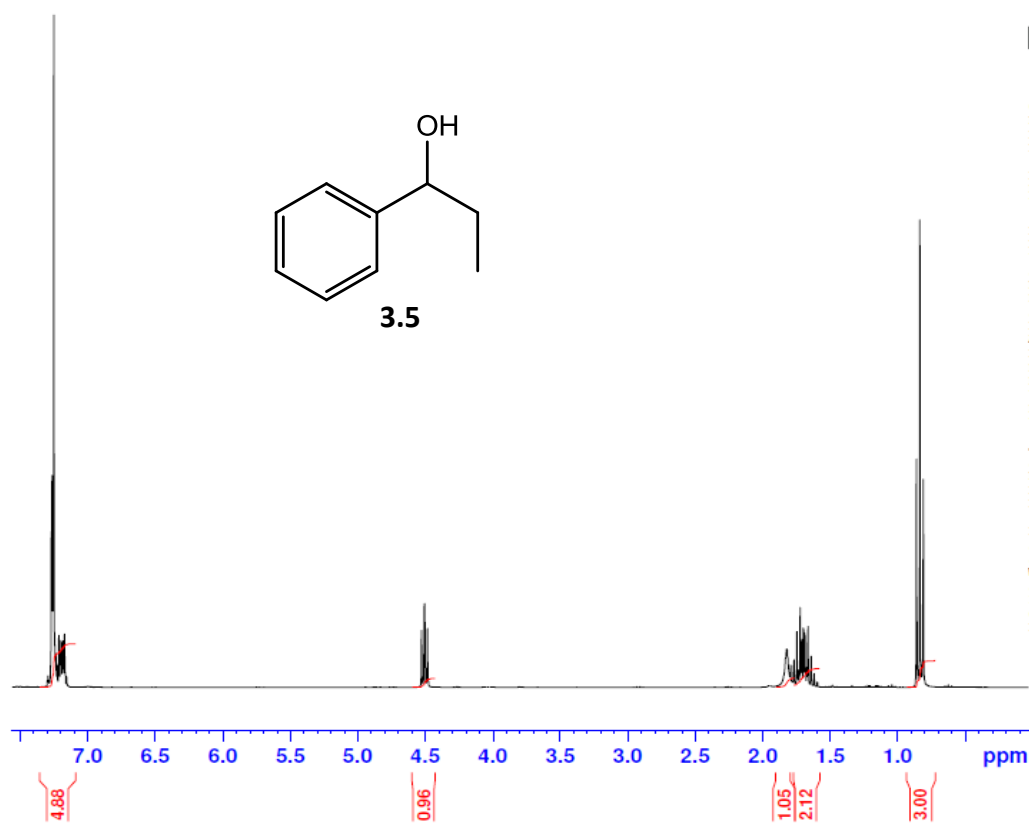
Totals : 1.40049e4 198.18066

Results obtained with enhanced integrator!

*** End of Report ***

Figure A1. The chiral HPLC chromatogram of compound **3.5**

¹H NMR CS510



Current Data Parameters
NAME Mar24-2014-NJACSHOOLA
EXPNO 1
PROCNO 1

F2 - Acquisition Parameters
Date_ 20140324
Time 10.11
INSTRUM spect
PROBHD 5 mm PABBO BB-
PULPROG zg30
TD 65536
SOLVENT CDCl₃
NS 128
DS 2
SWH 6009.615 Hz
FIDRES 0.091699 Hz
AQ 5.4525952 sec
RG 114
DW 83.200 usec
DE 6.50 usec
TE 300.0 K
D1 1.00000000 sec
TD0 1

----- CHANNEL f1 -----
SF01 300.1318534 MHz
NUC1 1H
P1 15.00 usec
PLW1 8.02000046 W

F2 - Processing parameters
SI 32768
SF 300.1300329 MHz
WDW EM
SSB 0
LB 0.30 Hz
GB 0
PC 1.00

Figure A2. The ¹H NMR spectrum of compound 3.5

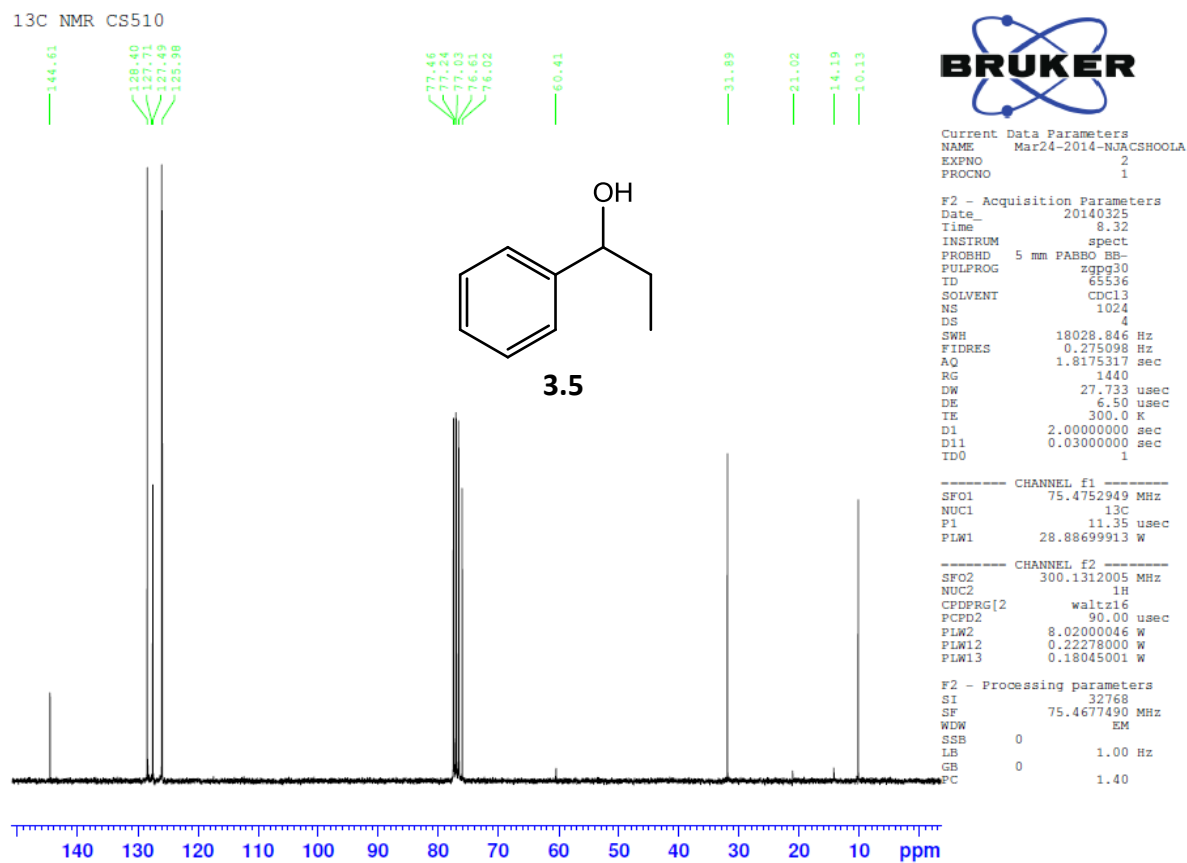


Figure A3. The ^{13}C NMR spectrum of compound 3.5

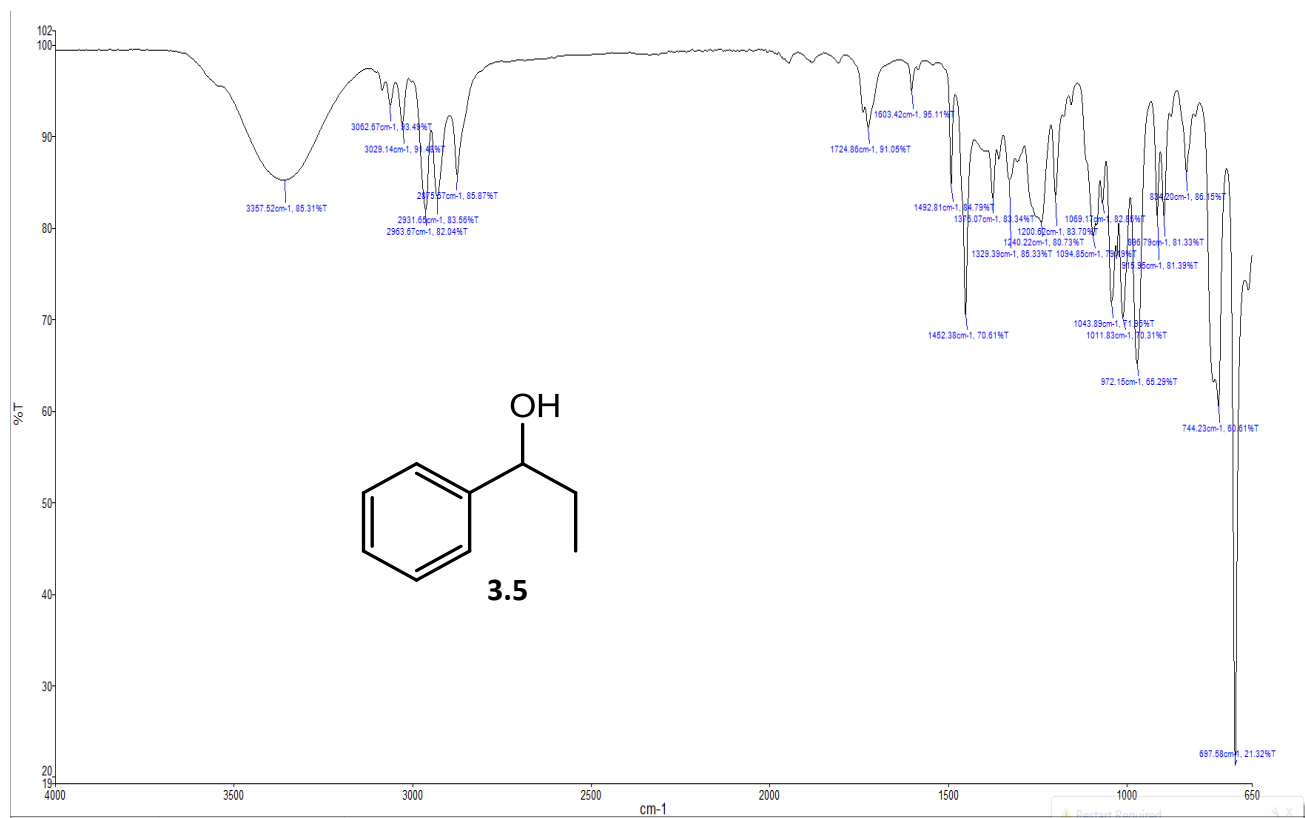


Figure A4. The FT-IR spectrum of compound **3.5**

File : C:\DATA\1404\EXP001.D
Operator : TOM
Acquired : 7 Apr 2014 9:07 using AcqMethod ZB100ND_F_MANUAL.M
Instrument : GCMS04
Sample Name: EXPERIMENT
Misc Info : ZB100ND_FMANUAL, SP150:1, NEAT,
Vial Number: 1

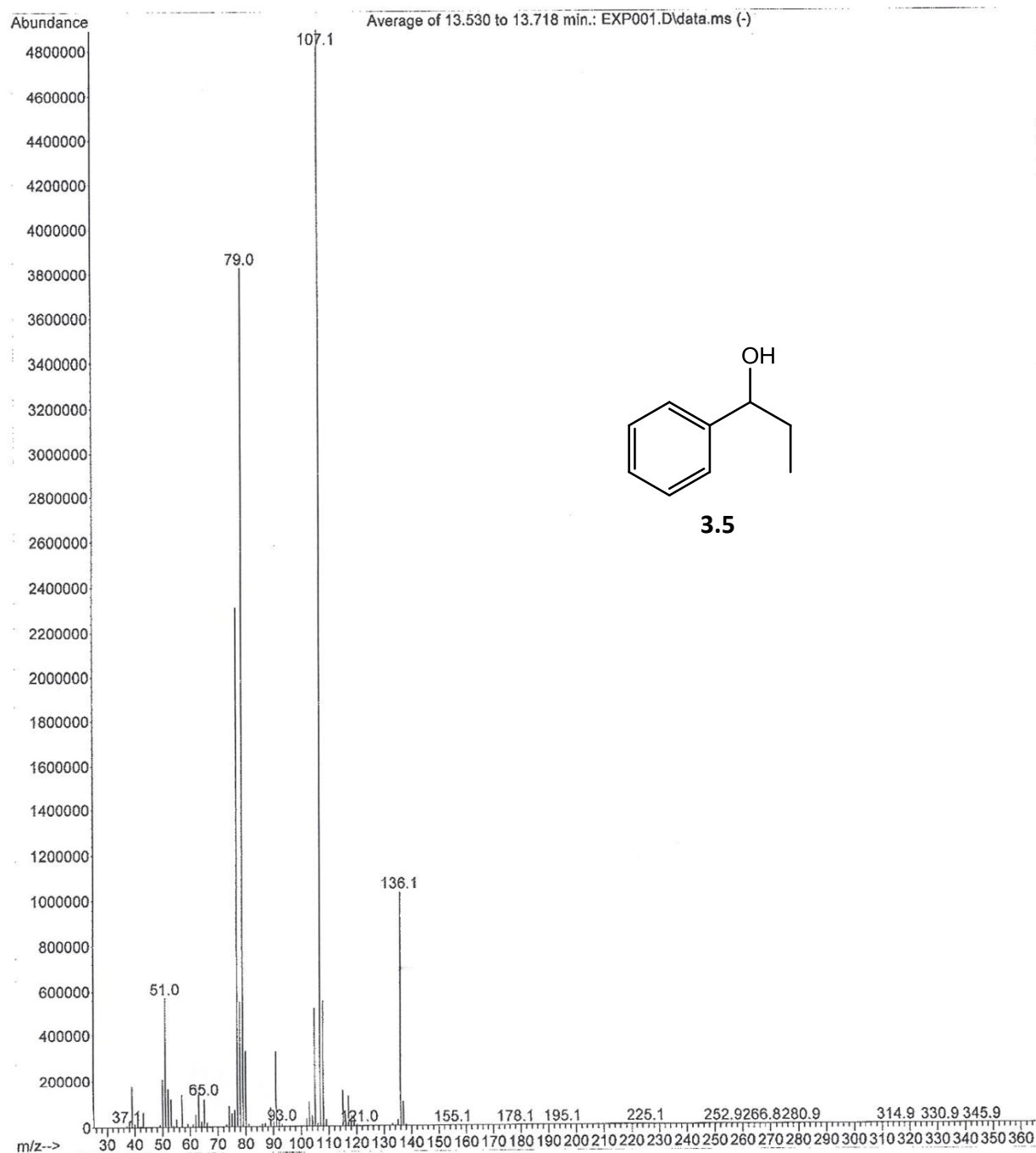


Figure A5. The mass spectrum of compound **3.5**

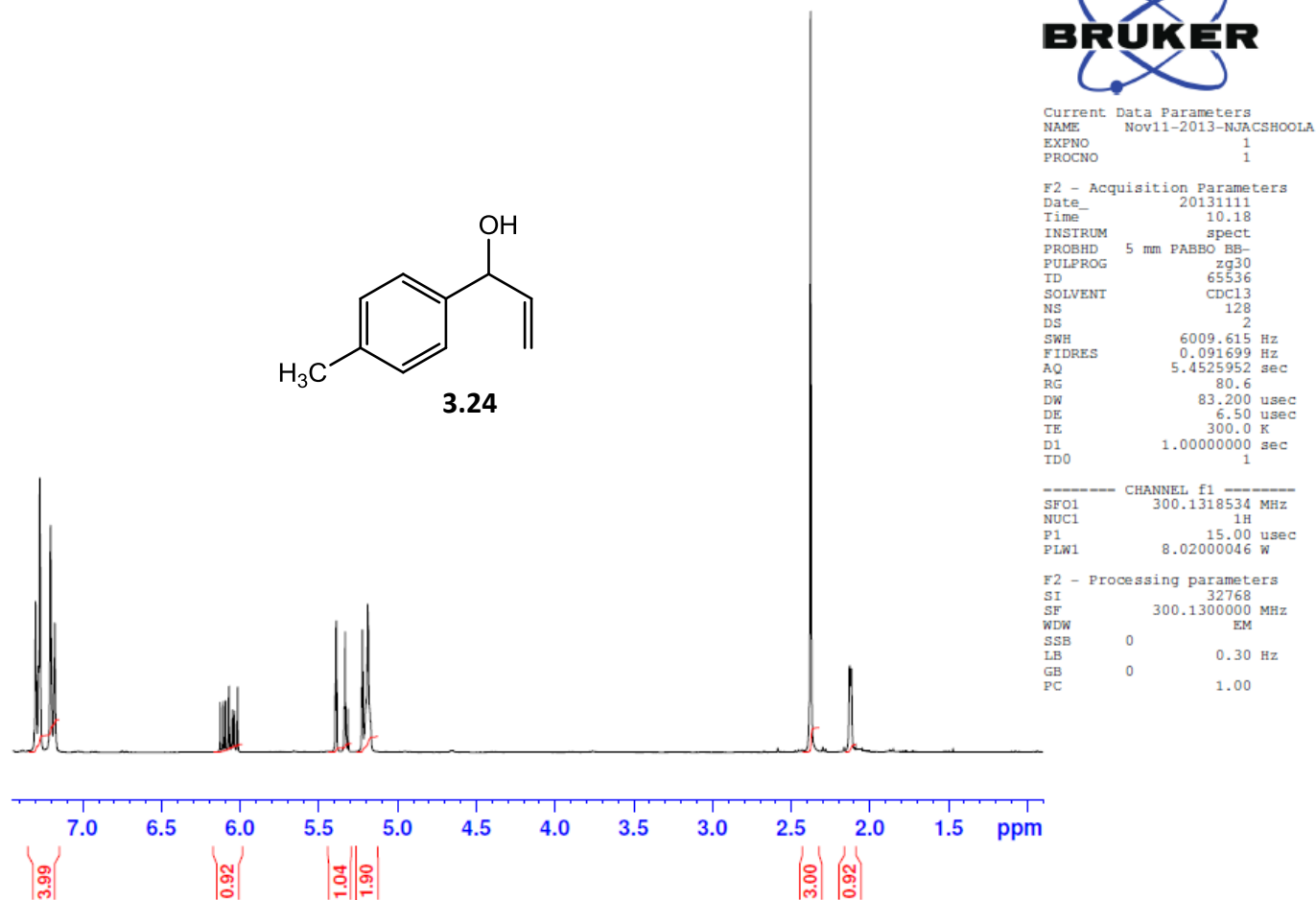
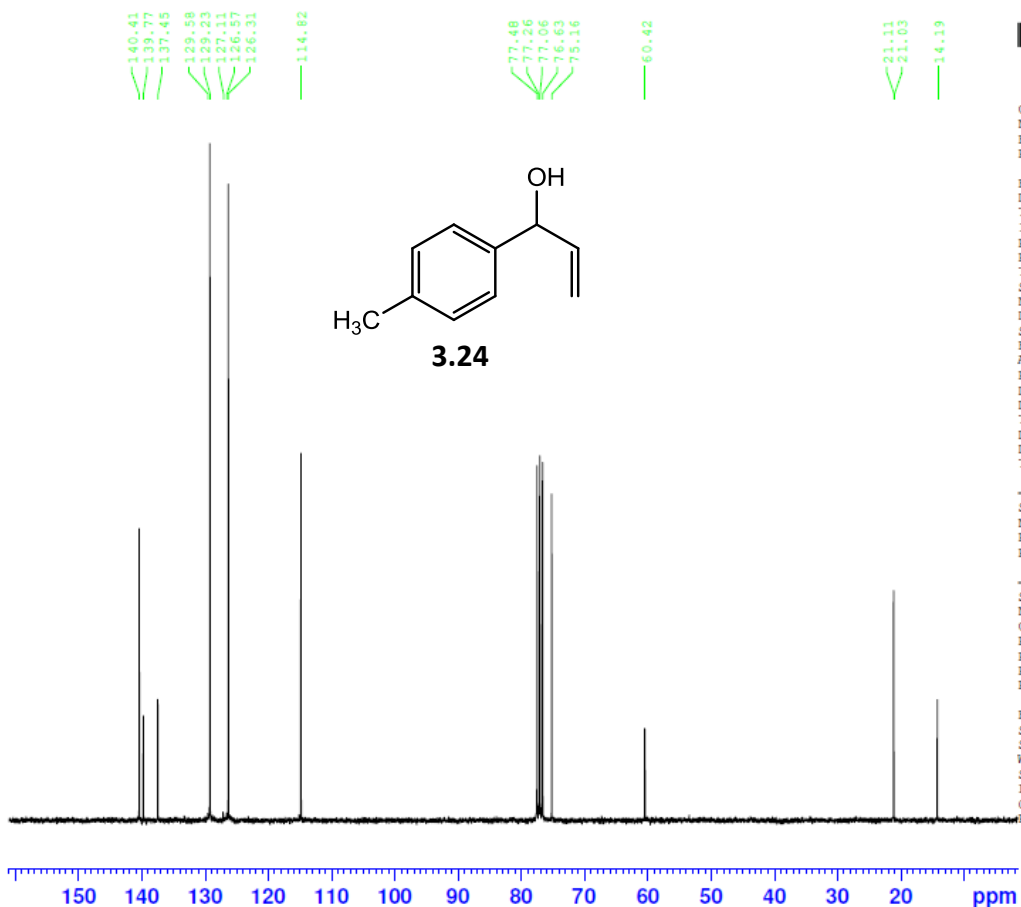


Figure A6. The ^1H NMR spectrum of compound **3.24**

CS 1110 - 13C



Current Data Parameters
NAME Nov11-2013-NJACSHOOLA
EXPNO 2
PROCNO 1

F2 - Acquisition Parameters
Date_ 20131111
Time 11.46
INSTRUM spect
PROBHD 5 mm PABBO BB-
PULPROG zgpg30
TD 65536
SOLVENT CDCl3
NS 1024
DS 4
SWH 18028.846 Hz
FIDRES 0.275098 Hz
AQ 1.8175317 sec
RG 1290
DW 27.733 usec
DE 6.50 usec
TE 300.0 K
D1 2.00000000 sec
D11 0.03000000 sec
TD0 1

----- CHANNEL f1 -----
SFO1 75.4752949 MHz
NUC1 13C
P1 11.35 usec
PLW1 28.88699913 W

----- CHANNEL f2 -----
SFO2 300.1312005 MHz
NUC2 1H
CPDPRG[2] waltz16
PCPD2 90.00 usec
PLW2 8.02000046 W
PLW12 0.22278000 W
PLW13 0.18045001 W

F2 - Processing parameters
SI 32768
SF 75.4677490 MHz
WDW EM
SSB 0
LB 1.00 Hz
GB 0
PC 1.40

Figure A7. The ¹³C NMR spectrum of compound **3.24**

CS719414

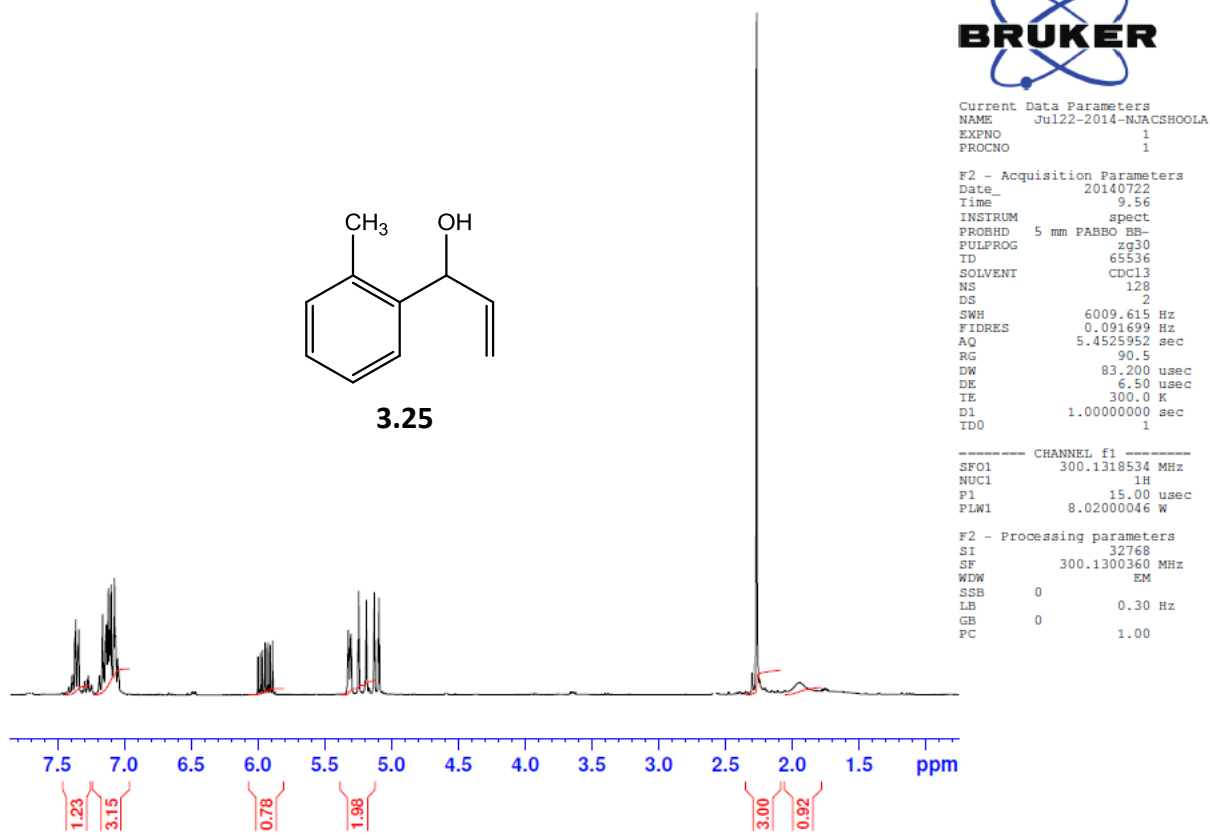


Figure A8. The ^1H NMR spectrum of compound **3.25**

CS742013 - 1H

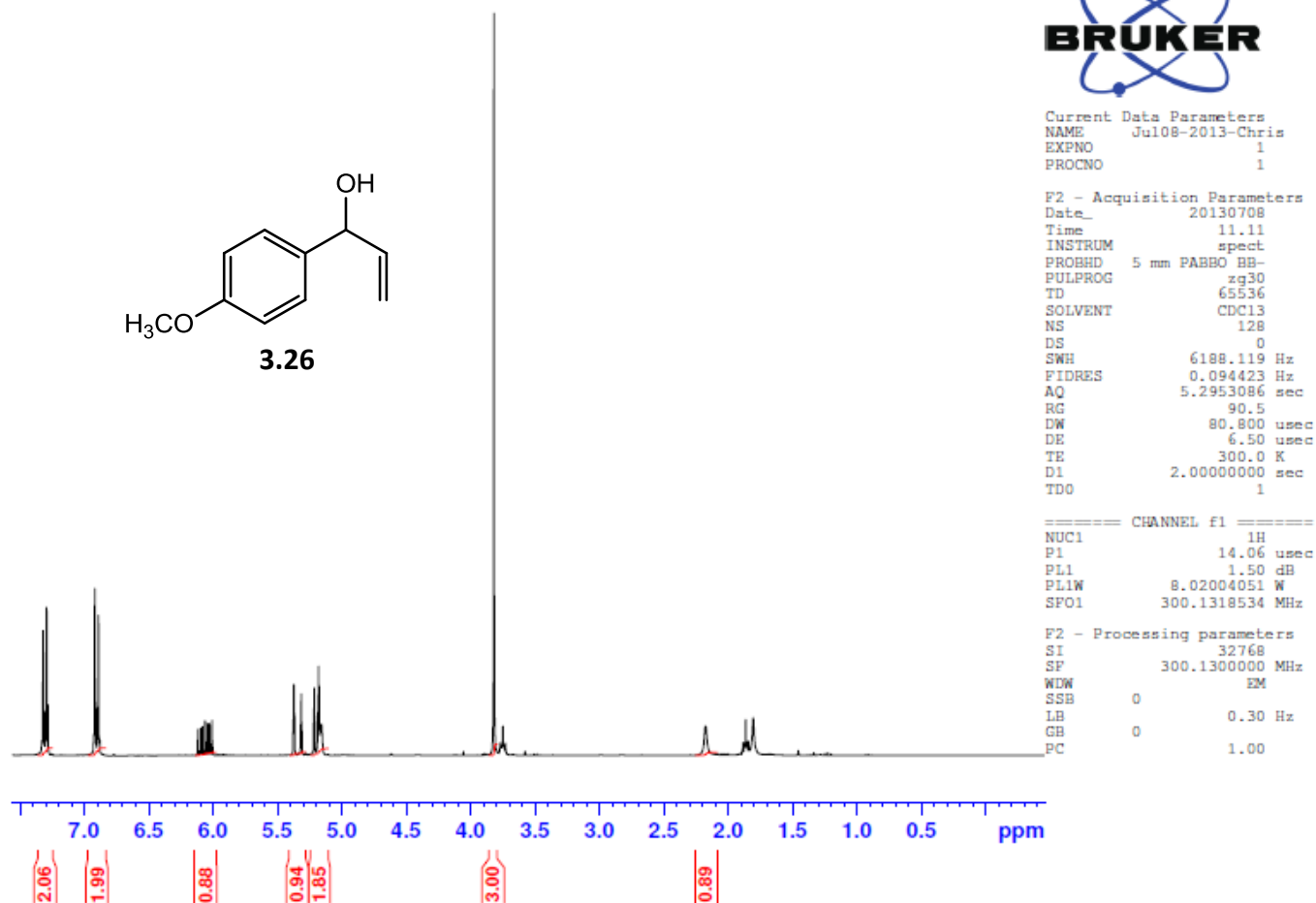


Figure A9. The ^1H NMR spectrum of compound **3.26**

CS742013 - 13C

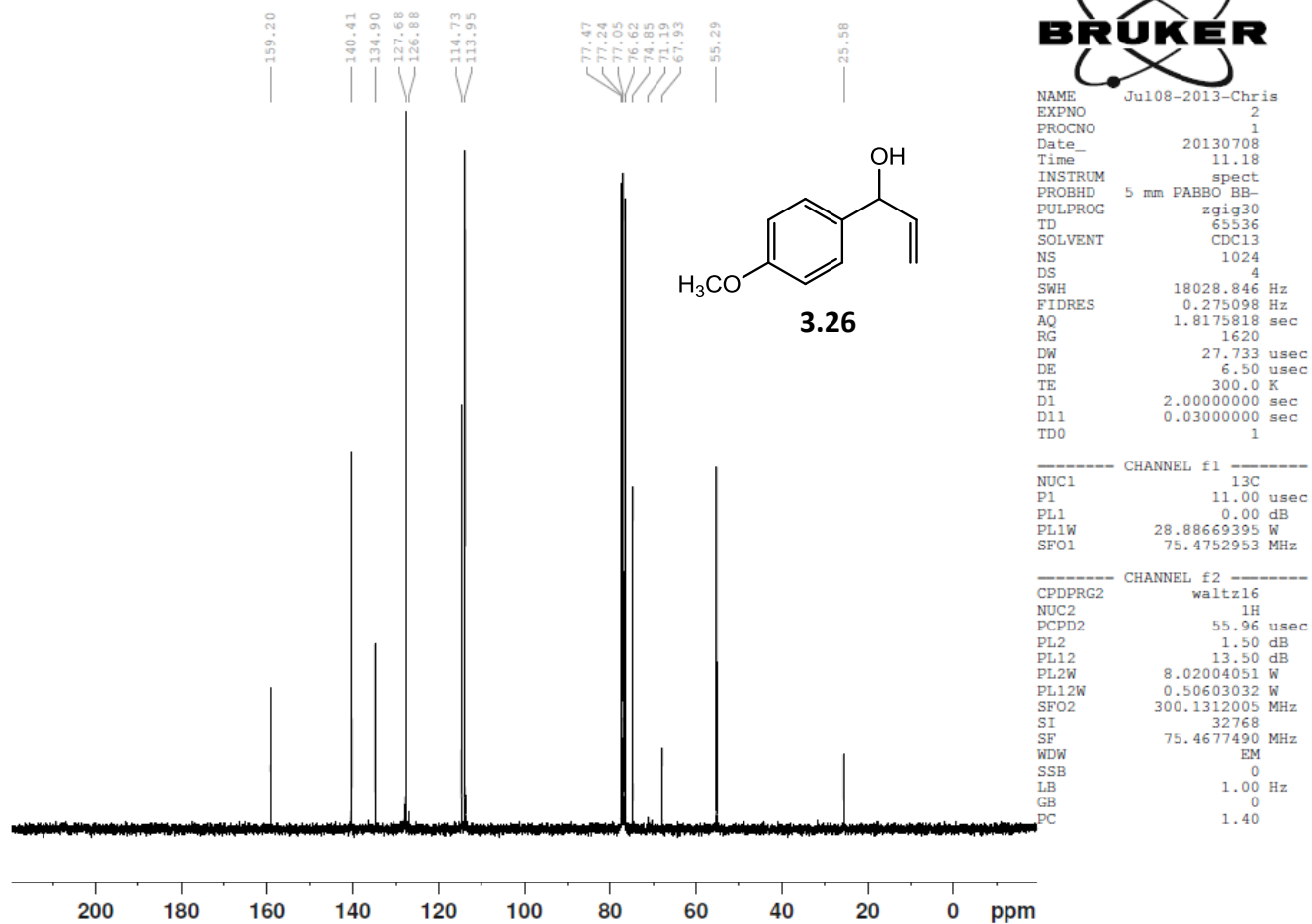


Figure A10. The ^{13}C NMR spectrum of compound **3.26**



Current Data Parameters
NAME Feb11-2014-NJACSHOOLA
EXPNO 3
PROCNO 1

F2 - Acquisition Parameters
Date_ 20140211
Time 11.18
INSTRUM spect
PROBHD 5 mm PABBO BB-
PULPROG zg30
TD 65536
SOLVENT CDCl3
NS 128
DS 2
SWH 6009.615 Hz
FIDRES 0.091699 Hz
AQ 5.4525952 sec
RG 161
DW 83.200 usec
DE 6.50 usec
TE 300.0 K
D1 1.00000000 sec
TD0 1

----- CHANNEL f1 -----
SFO1 300.1318534 MHz
NUC1 1H
P1 15.00 usec
PLW1 8.02000046 W

F2 - Processing parameters
SI 32768
SF 300.1300311 MHz
WDW EM
SSB 0
LB 0.30 Hz
GB 0
PC 1.00

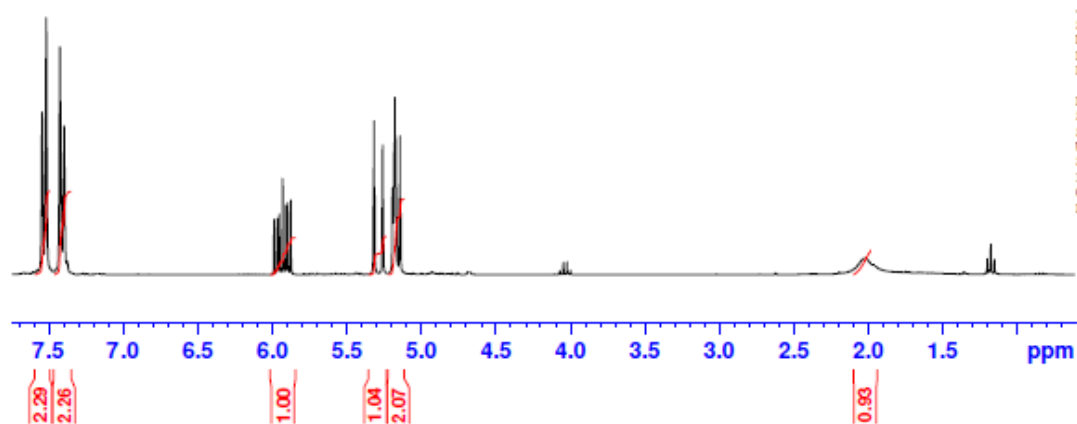
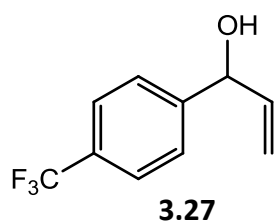
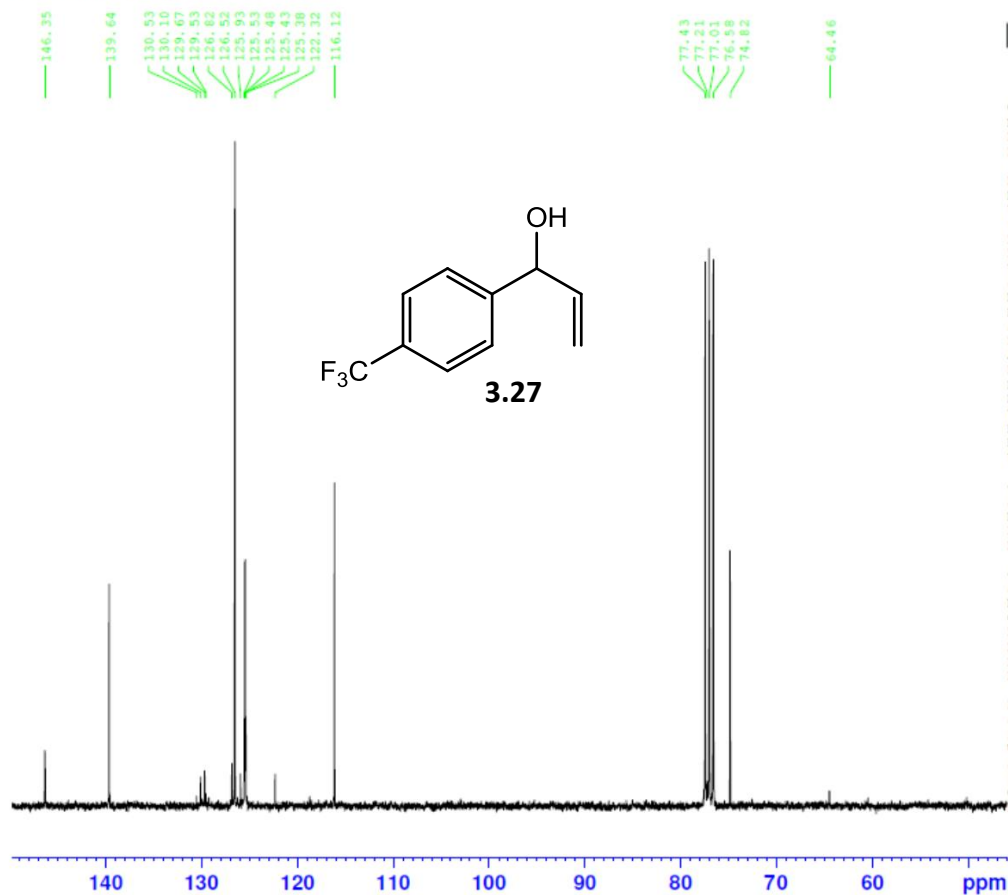


Figure A11. The ^1H NMR spectrum of compound **3.27**

CS102213 (SM for 21014)



Current Data Parameters
NAME Feb11-2014-NJACSHOOLA
EXPNO 4
PROCNO 1

F2 - Acquisition Parameters
Date_ 20140211
Time 18.24
INSTRUM spect
PROBHD 5 mm FABBO BB-
PULPROG zgpg30
TD 65536
SOLVENT CDCl3
NS 1024
DS 4
SWH 18028.846 Hz
FIDRES 0.275098 Hz
AQ 1.8175317 sec
RG 1290
DW 27.733 usec
DE 6.50 usec
TE 300.1 K
D1 2.00000000 sec
D11 0.03000000 sec
TD0 1

----- CHANNEL f1 -----
SFO1 75.4752949 MHz
NUC1 13C
P1 11.35 usec
PLW1 28.88699913 W

----- CHANNEL f2 -----
SFO2 300.1312005 MHz
NUC2 1H
CPDPRG[2] waltz16
PCPD2 90.00 usec
PLW2 8.02000046 W
PLW12 0.22278000 W
PLW13 0.18045001 W

F2 - Processing parameters
SI 32768
SF 75.4677490 MHz
WDW EM
SSB 0
LB 1.00 Hz
GB 0
PC 1.40

Figure A12. The ¹³C NMR spectrum of compound 3.27

Chemical Formula: C₁₀H₁₄O
 Exact Mass: 150.10
 Molecular Weight: 150.22
 m/z: 150.10 (100.0%), 151.11 (11.0%)

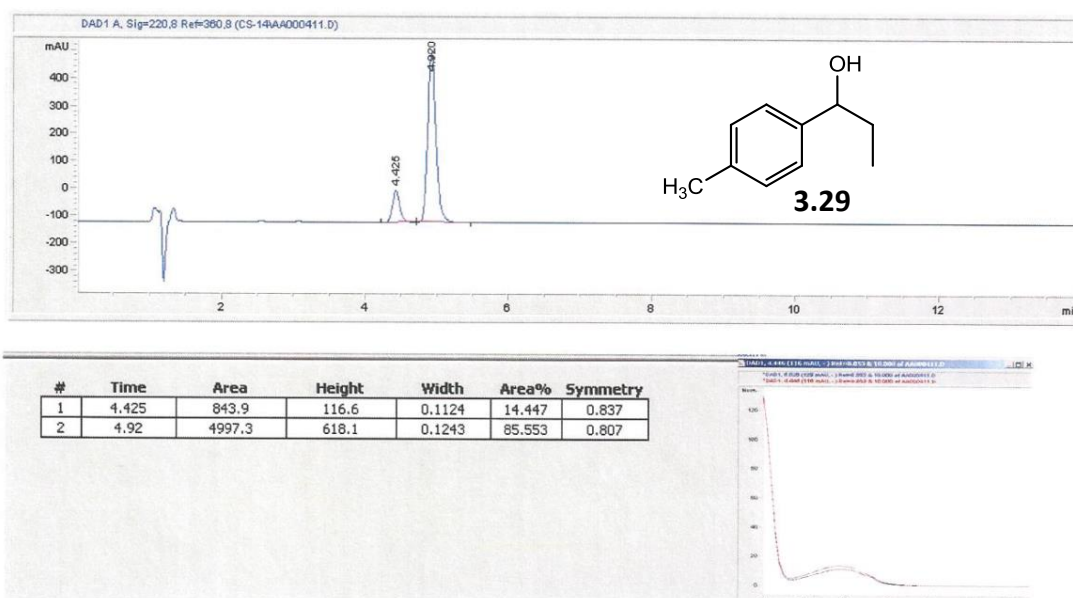


Figure A13. The chiral HPLC chromatogram of compound **3.29**

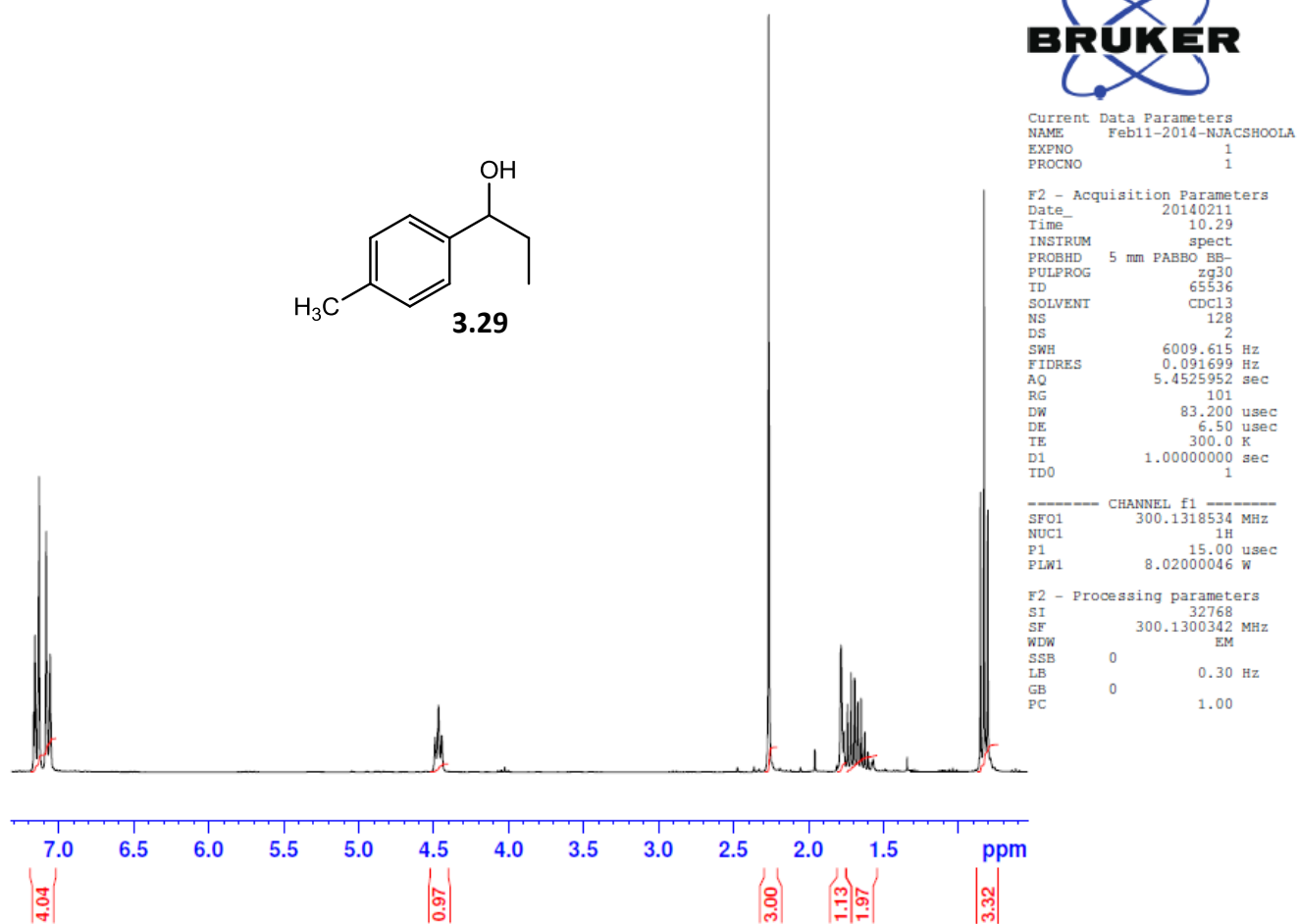


Figure A14. The ^1H NMR spectrum of compound **3.29**

CS12414 (1/31/2014) - 2

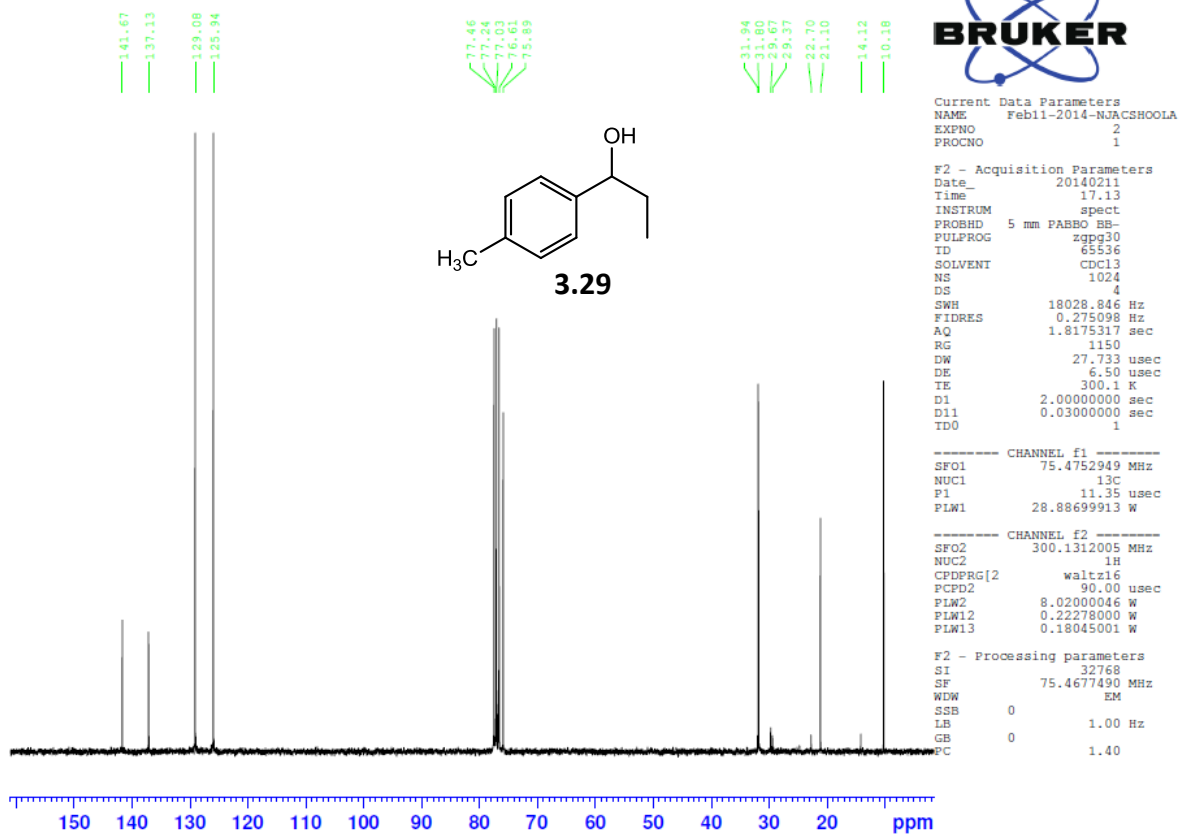


Figure A15. The ^{13}C NMR spectrum of compound 3.29

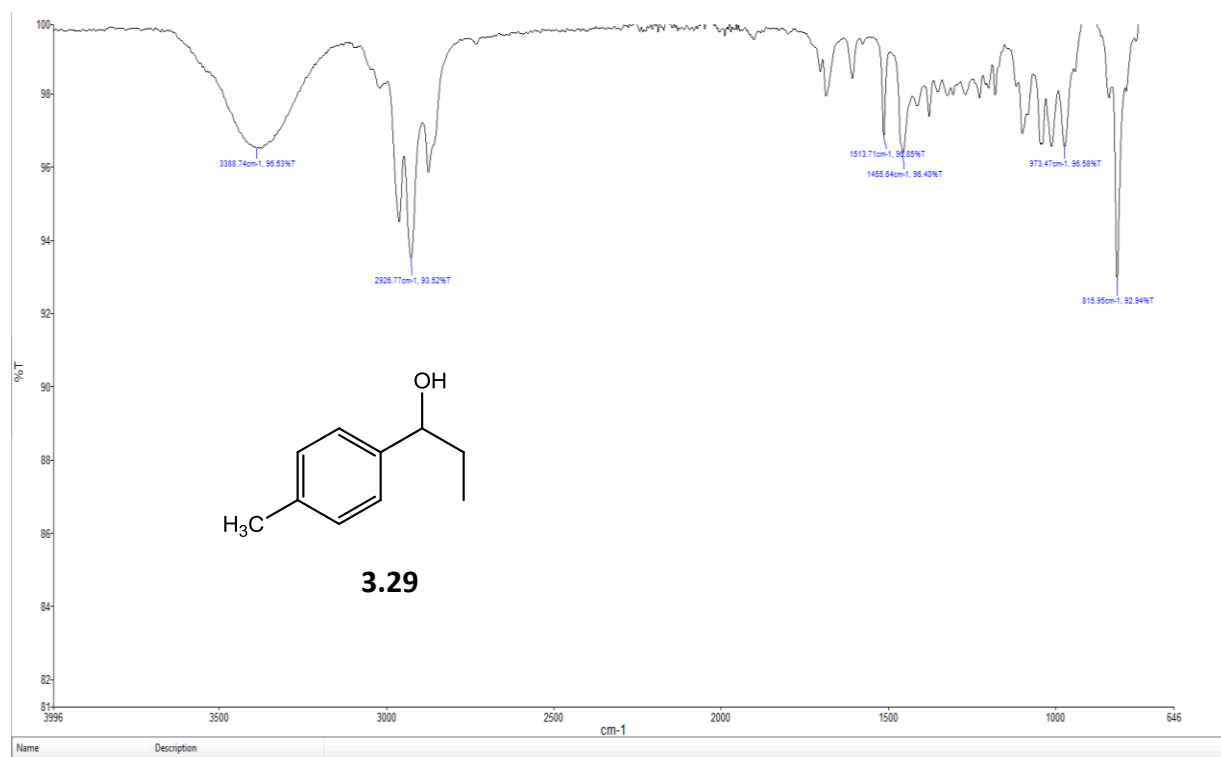


Figure A16. The FT-IR spectrum of compound **3.29**

File : C:\DATA\1401\RESEARCH001.D
Operator :
Acquired : 30 Jan 2014 8:47 using AcqMethod ZB100ND_F_MANUAL.M
Instrument : GCMS04
Sample Name: RESEARCH
Misc Info : ZB100ND_F, SP150:1, NEAT
Vial Number: 1

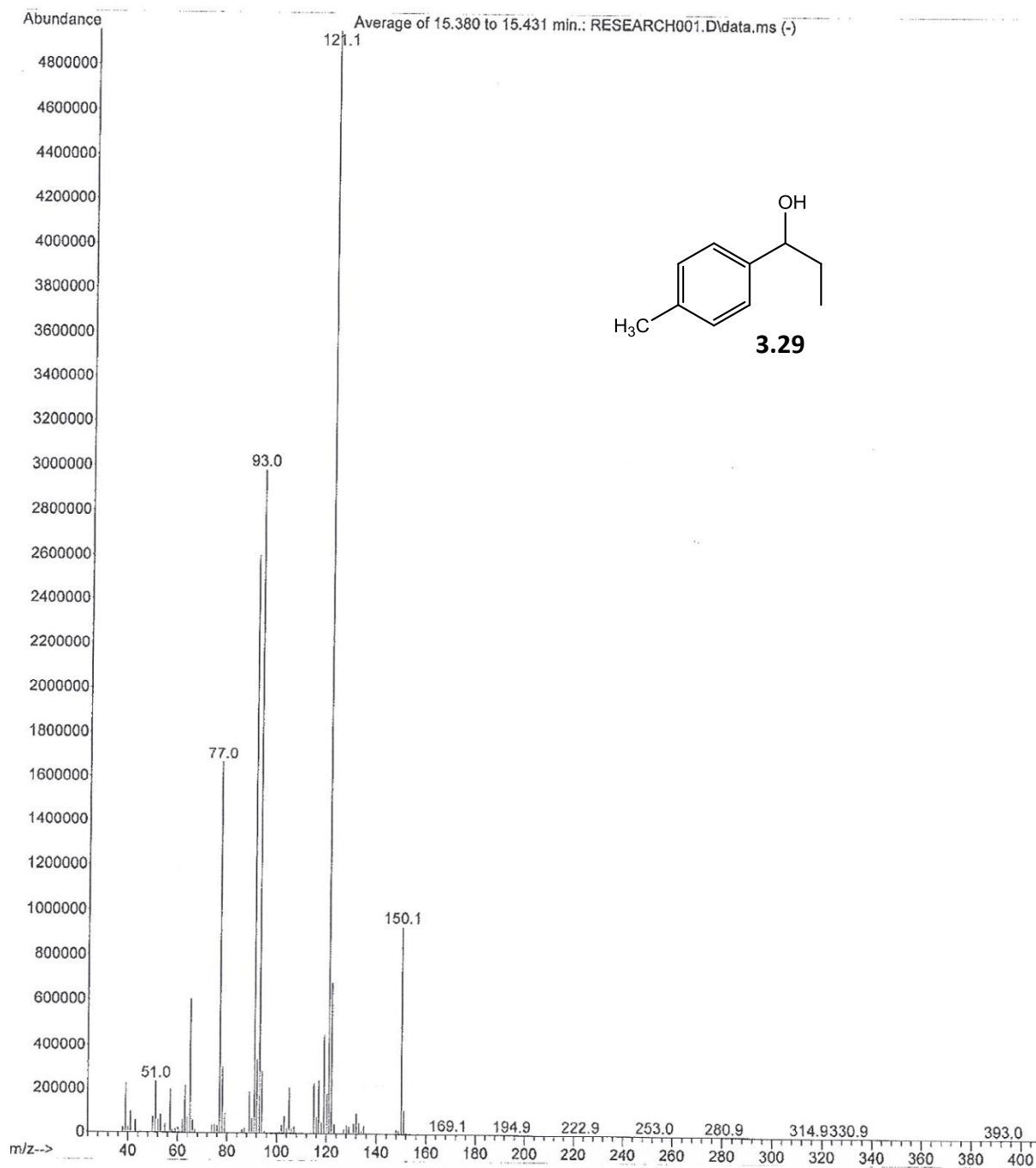


Figure A17. The mass spectrum of compound **3.29**

Chemical Formula: C ₁₀ H ₁₄ O	#	Time	Area	Height	Width	Area%	Symmetry
Exact Mass: 150.10	1	5.639	546.8	143.8	0.0604	34.817	0.974
Molecular Weight: 150.22	2	5.994	1023.6	254.4	0.0649	65.183	0.931
m/z: 150.10 (100.0%), 151.11 (11.0%)							

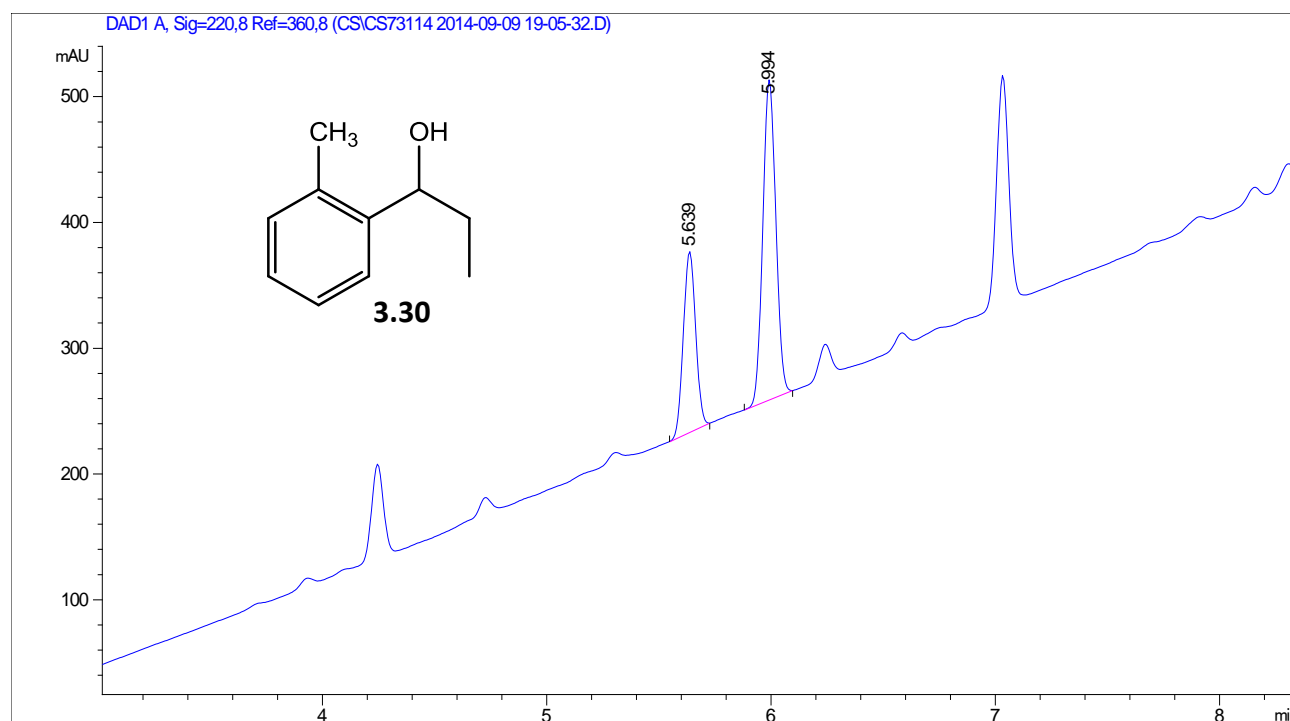


Figure A18. The chiral HPLC chromatogram of compound **3.30**

CS73114 - Proton

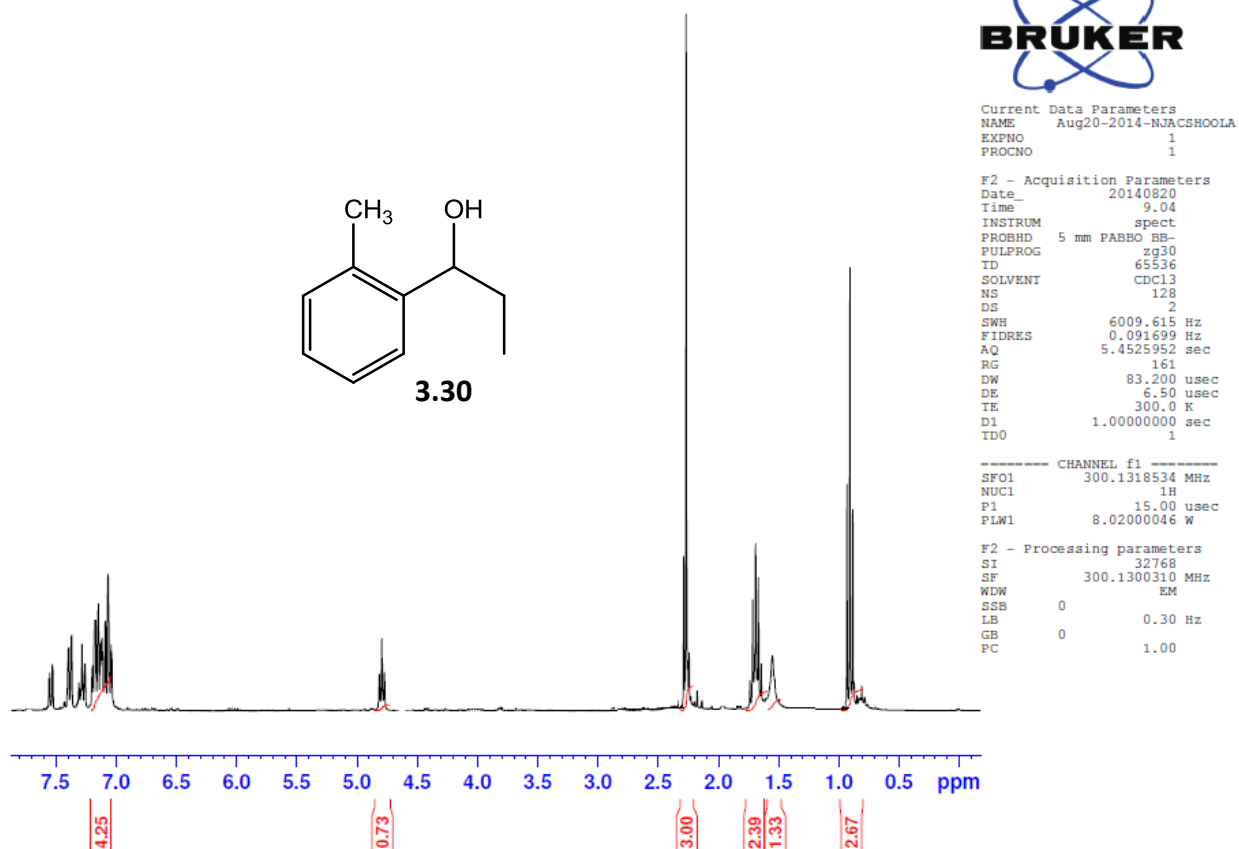


Figure A19. The ^1H NMR spectrum of compound **3.30**

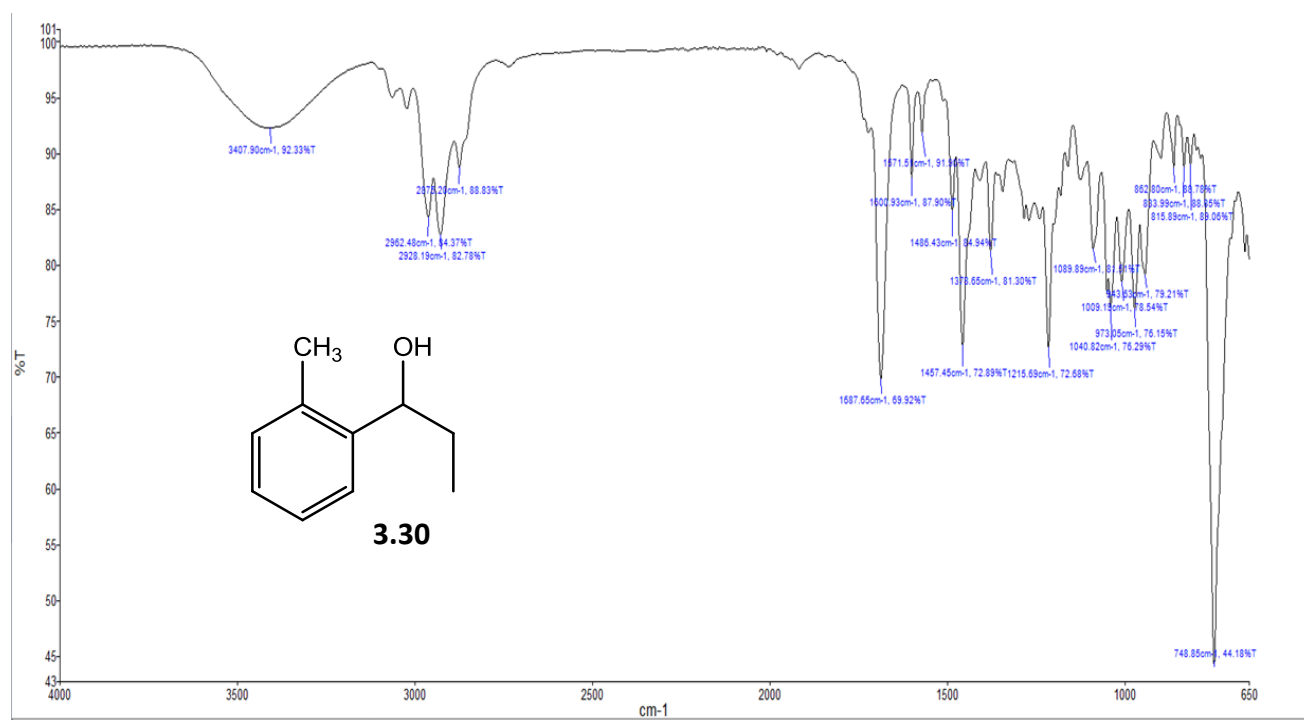


Figure A20. The FT-IR spectrum of compound **3.30**

Chemical Formula: C ₁₀ H ₁₄ O ₂	#	Time	Area	Height	Width	Area%	Symmetry
Exact Mass: 166.10	1	5.305	44.4	10.1	0.0694	3.492	1.548
Molecular Weight: 166.22							
m/z: 166.10 (100.0%), 167.10 (10.9%)	2	5.608	1228.5	308	0.0625	96.508	0.947

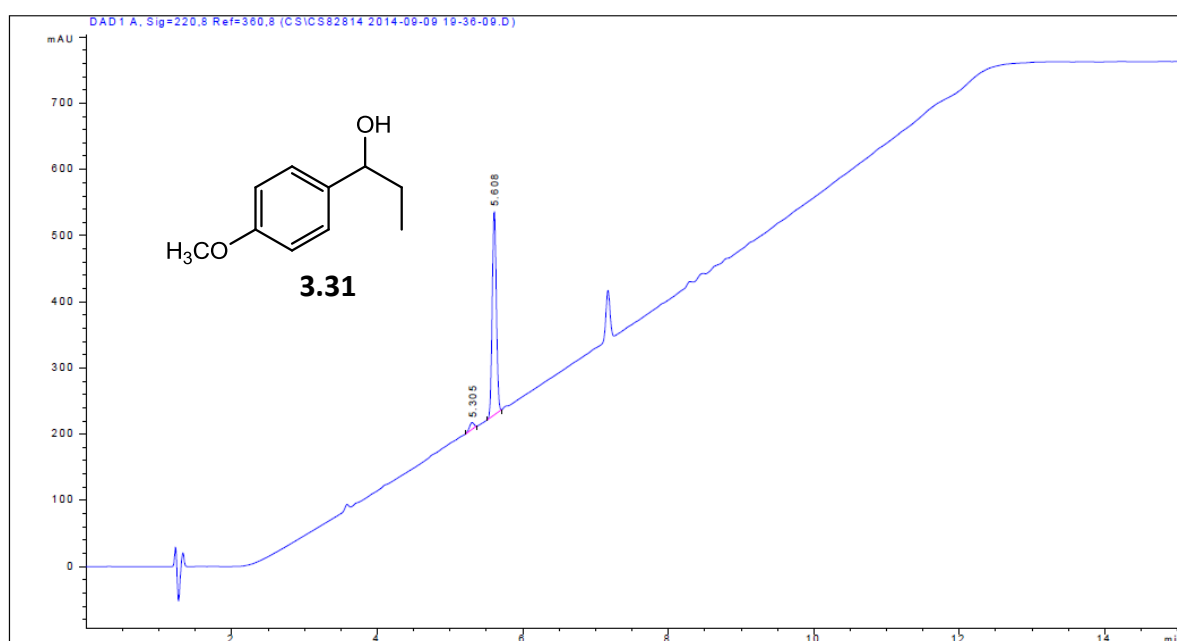


Figure A21. The chiral HPLC chromatogram of compound **3.31**

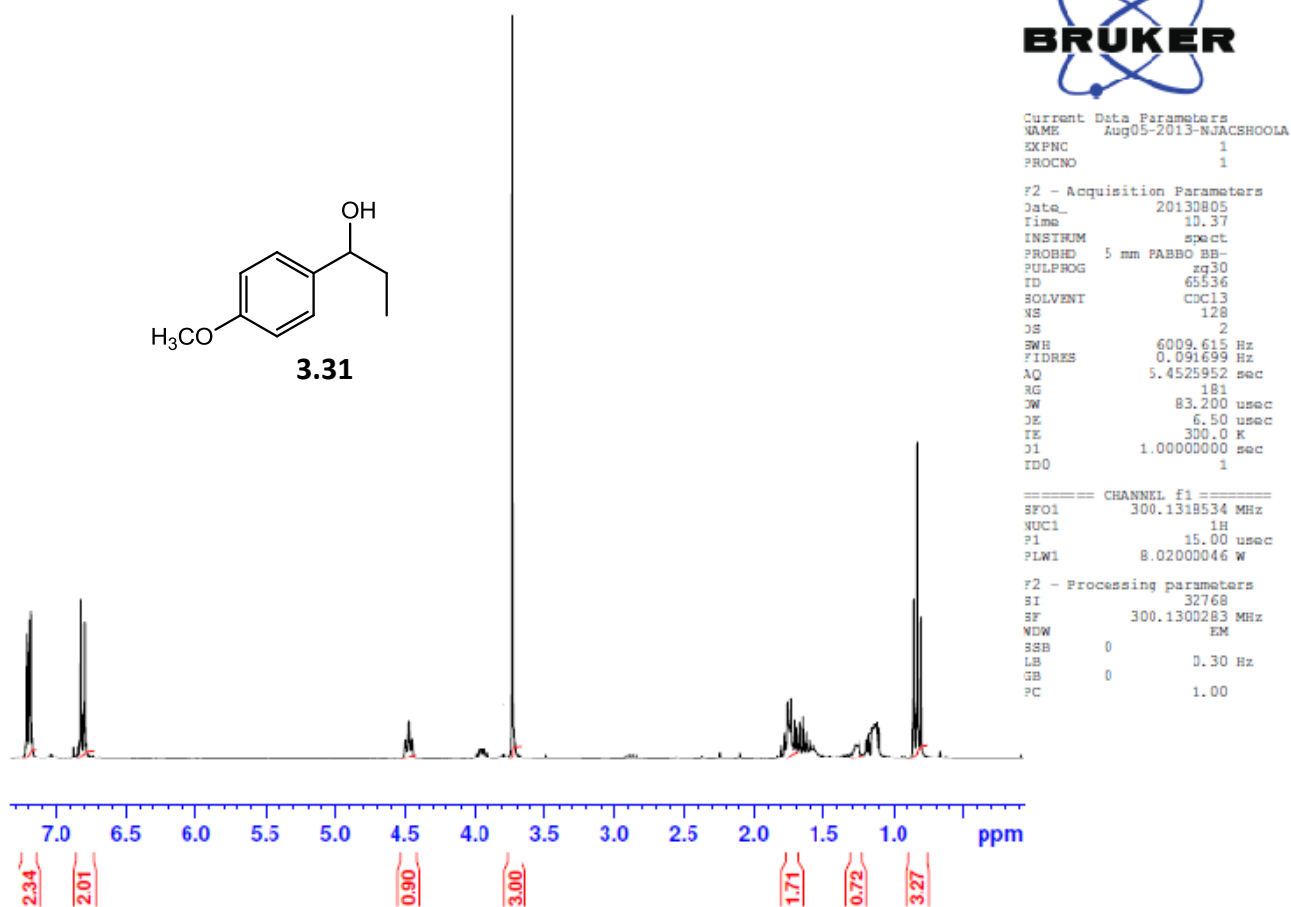
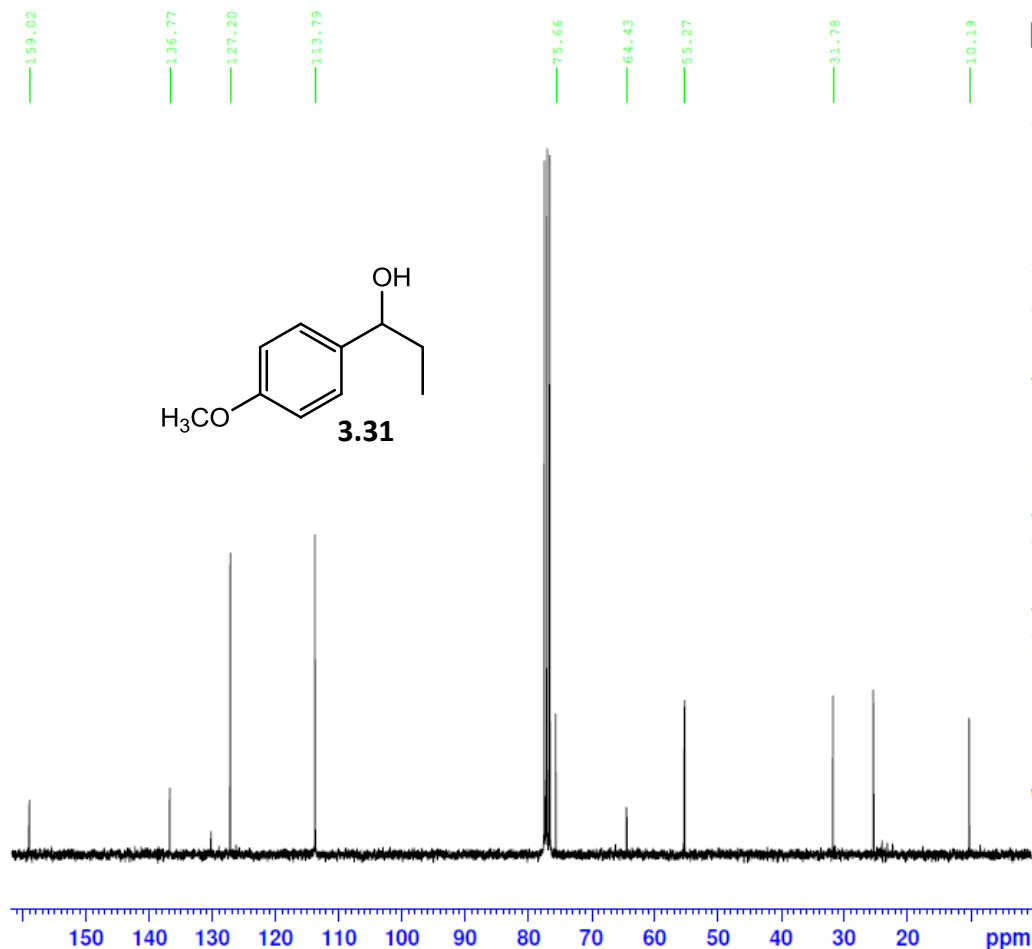


Figure A22. The ^1H NMR spectrum of compound **3.31**

CS812013 - 13C



Current Data Parameters
 NAME Aug05-2013-NJACSHOOLA
 EXPNO 2
 PROCNO 1

F2 - Acquisition Parameters
 Date_ 20130805
 Time 11.46
 INSTRUM spect
 PROBHD 5 mm PABBO BB-
 PULPROG zgpg30
 TD 65536
 SOLVENT CDCl3
 NS 1024
 DS 4
 SWH 18028.846 Hz
 FIDRES 0.275098 Hz
 AQ 1.8175317 sec
 RG 1440
 DW 27.733 usec
 DE 6.50 usec
 TE 300.0 K
 D1 2.00000000 sec
 D11 0.03000000 sec
 TD0 1

----- CHANNEL f1 -----
 SFO1 75.4752949 MHz
 NUC1 13C
 P1 11.35 usec
 PLW1 28.88699913 W

----- CHANNEL f2 -----
 SFO2 300.1312005 MHz
 NUC2 1H
 CPDPRG[2] waltz16
 PCPD2 90.00 usec
 PLW2 8.02000046 W
 PLW12 0.22278000 W
 PLW13 0.18045001 W

F2 - Processing parameters
 SI 32768
 SF 75.4677490 MHz
 WDW EM
 SSB 0
 LB 1.00 Hz
 GB 0
 PC 1.40

Figure A23. The ^{13}C NMR spectrum of compound **3.31**

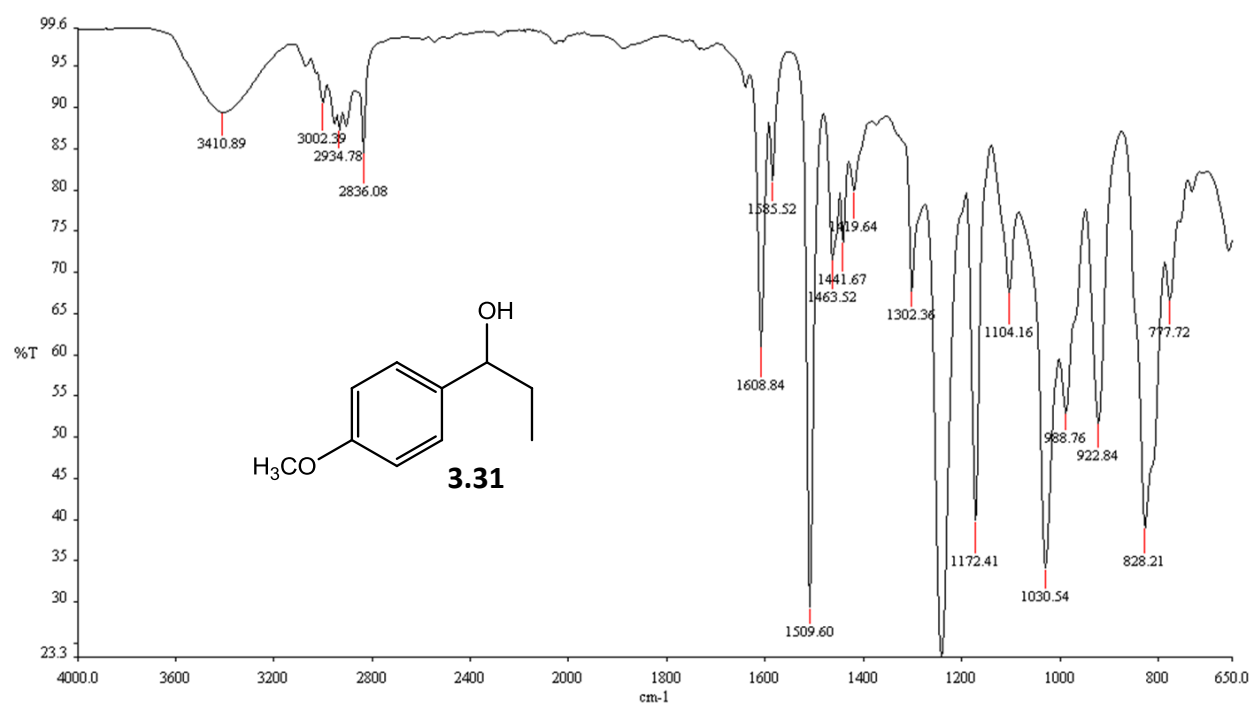


Figure A24. The FT-IR spectrum of compound **3.31**

File :C:\DATA\1308\EXP1.D
Operator :
Acquired : 14 Aug 2013 14:00 using AcqMethod ZB100ND_F_MANUAL.M
Instrument : GCMS04
Sample Name: EXPERMINET 7-26-2013
Misc Info :
Vial Number: 15

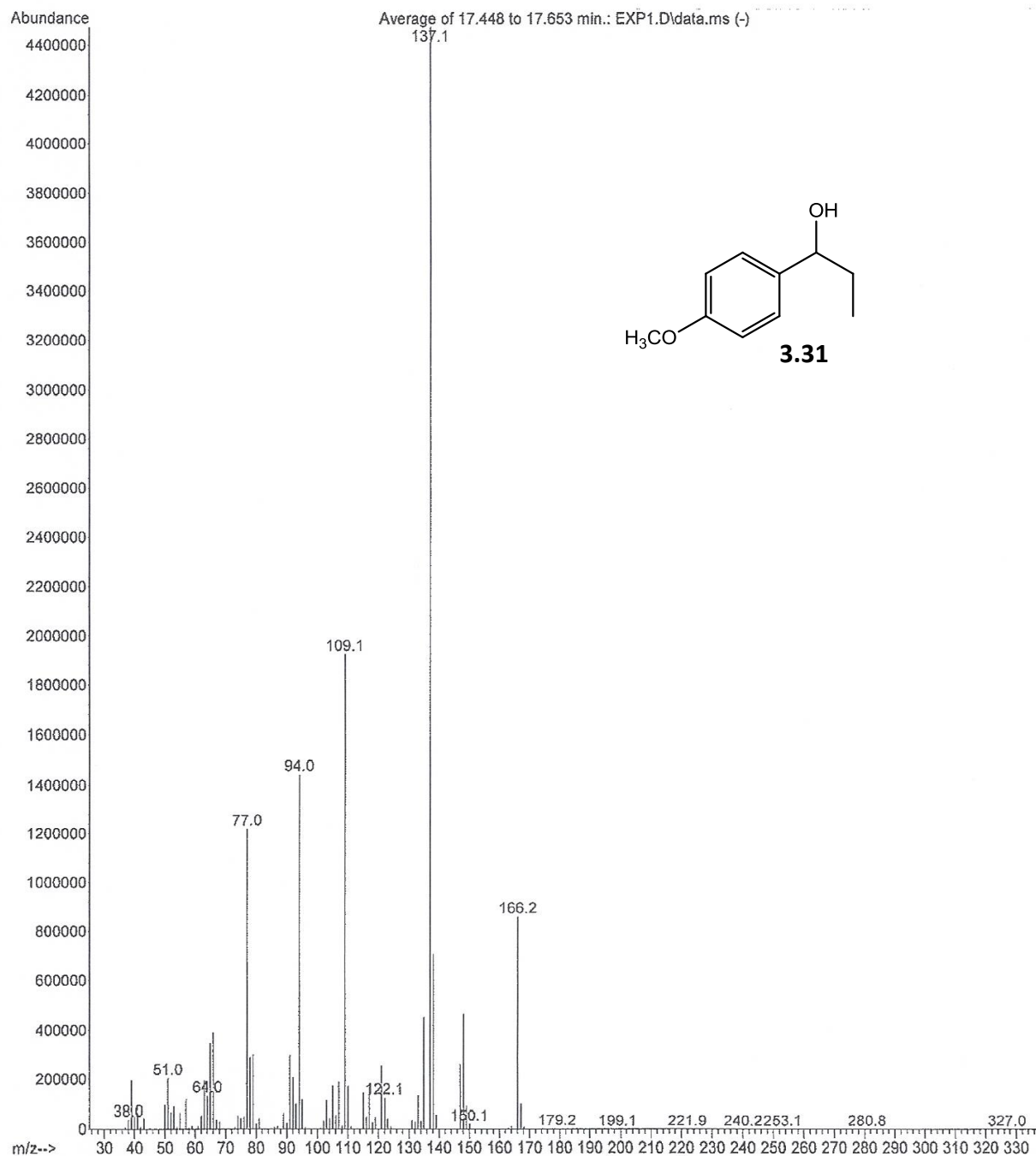


Figure A25. The mass spectrum of compound **3.31**

Chemical Formula: C₁₀H₁₁F₃O
 Exact Mass: 204.08
 Molecular Weight: 204.19
 m/z: 204.08 (100.0%), 205.08 (11.0%)

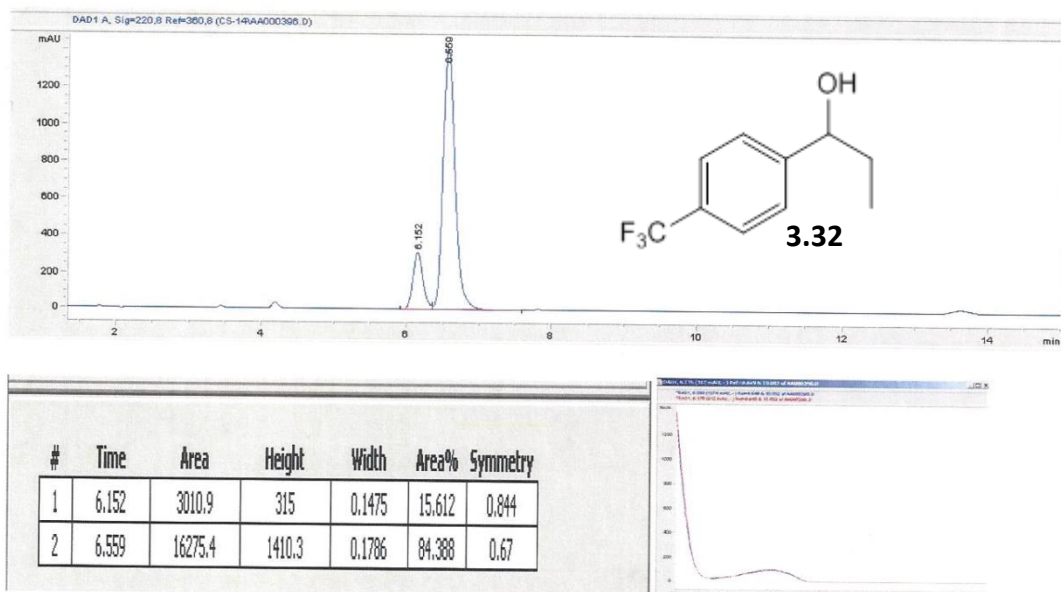


Figure A26. The chiral HPLC chromatogram of compound **3.32**

CS21214 - 1H

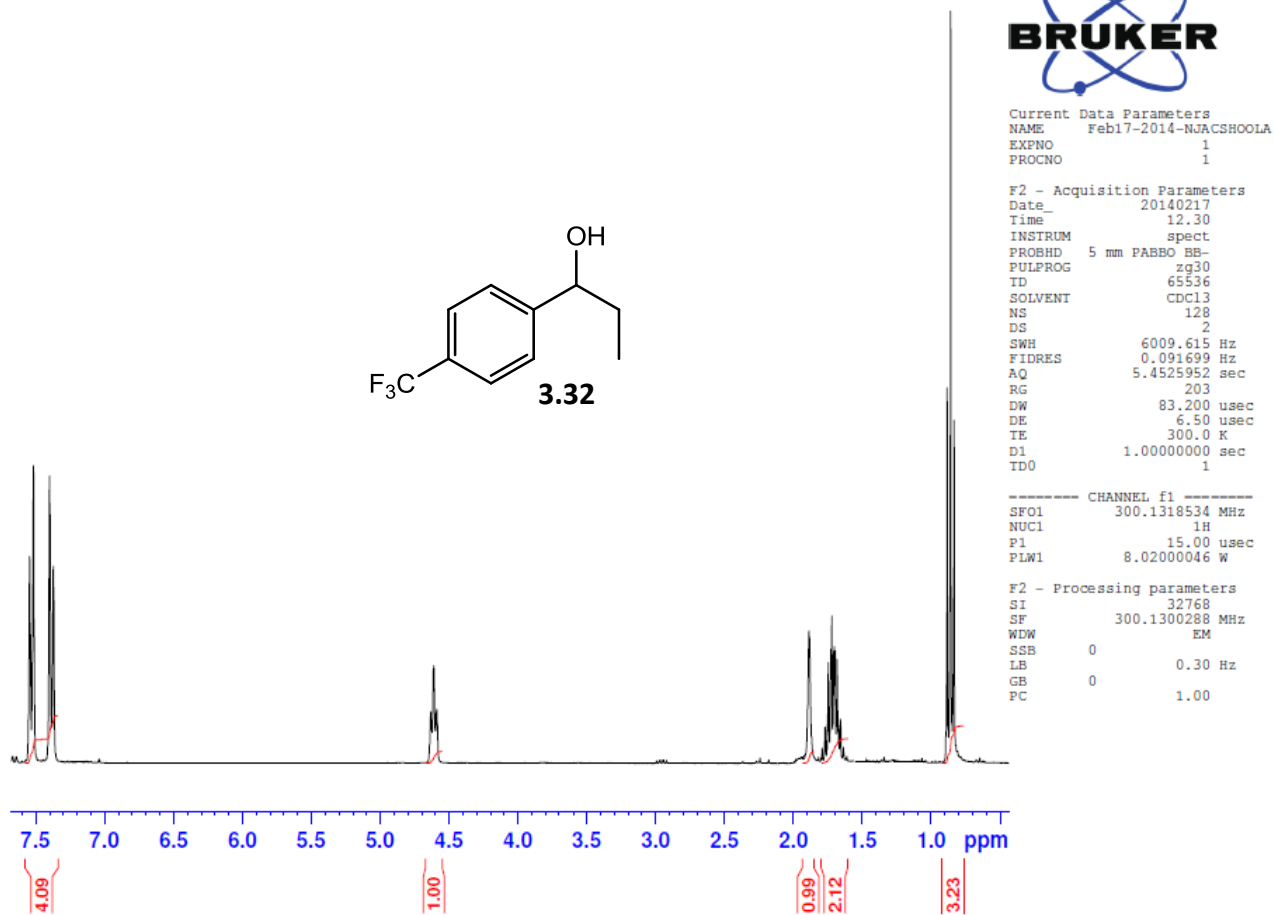


Figure A27. The ^1H NMR spectrum of compound **3.32**

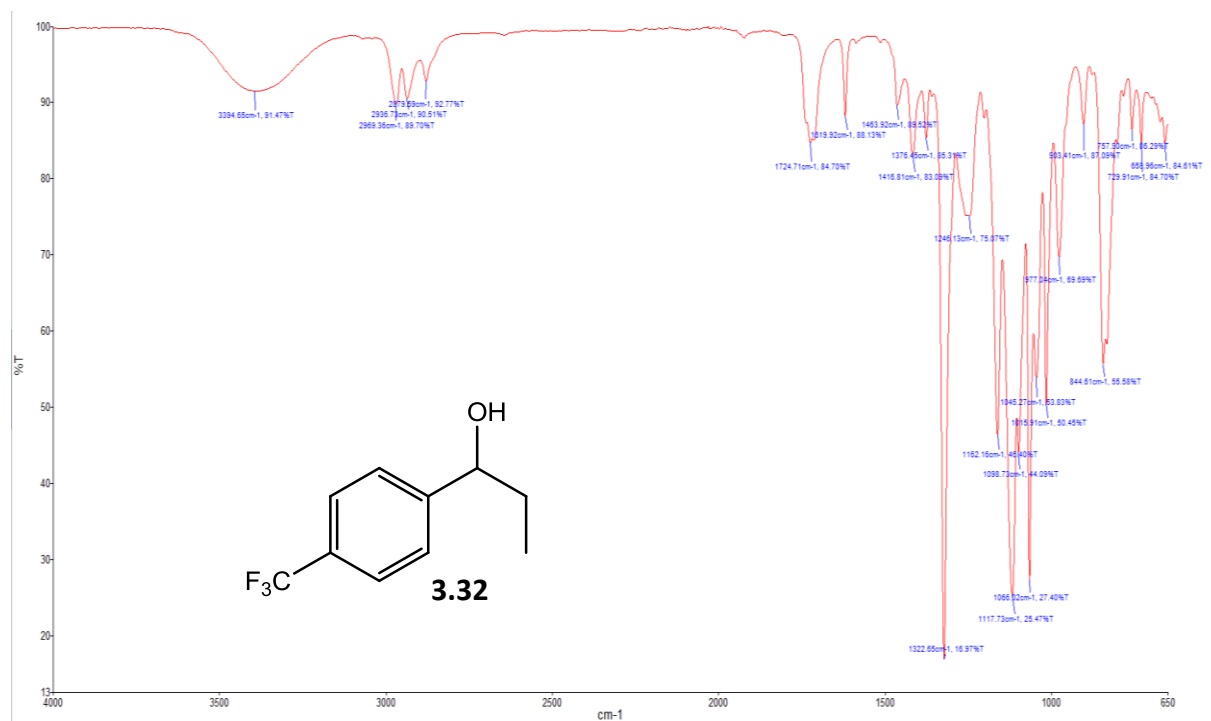


Figure A28. The FT-IR spectrum of compound **3.32**

File :C:\DATA\1403\EXPER002.D
Operator :
Acquired : 3 Mar 2014 10:10 using AcqMethod ZB100ND_F_MANUAL.M
Instrument : GCMS04
Sample Name: EXPERIMENT
Misc Info : ZB100ND_FMANUAL, SP150:1, NEAT,
Vial Number: 14

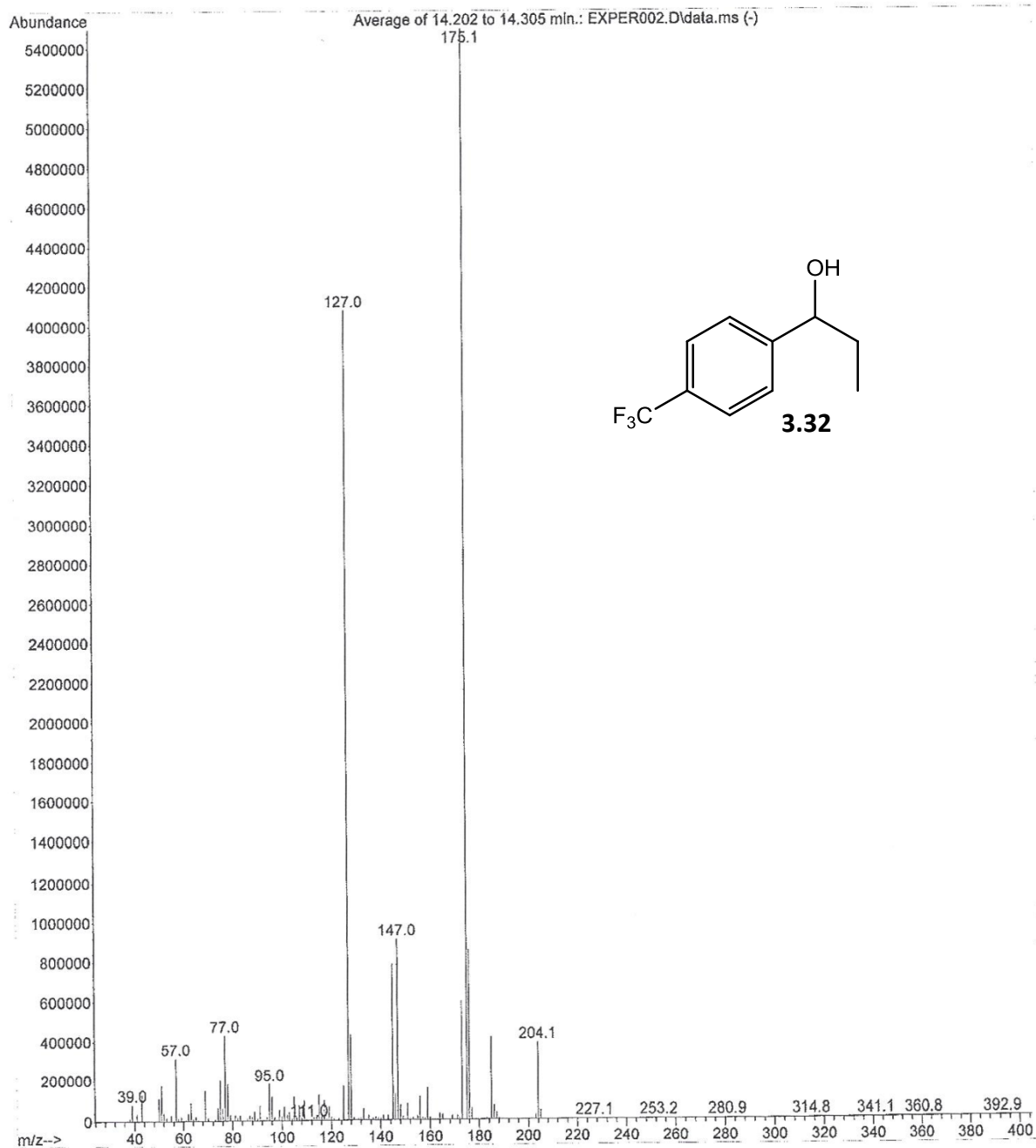


Figure A29. The mass spectrum of compound **3.32**

Chemical Formula: $C_{15}H_{16}O$
Exact Mass: 212.12
Molecular Weight: 212.29
m/z: 212.12 (100.0%), 213.12 (16.3%), 214.13 (1.3%)

#	Time	Area	Height	Width	Area%	Symmetry
1	8.284	973.1	222.8	0.0669	29.594	0.99
2	8.607	2315.1	465.8	0.078	70.406	0.823

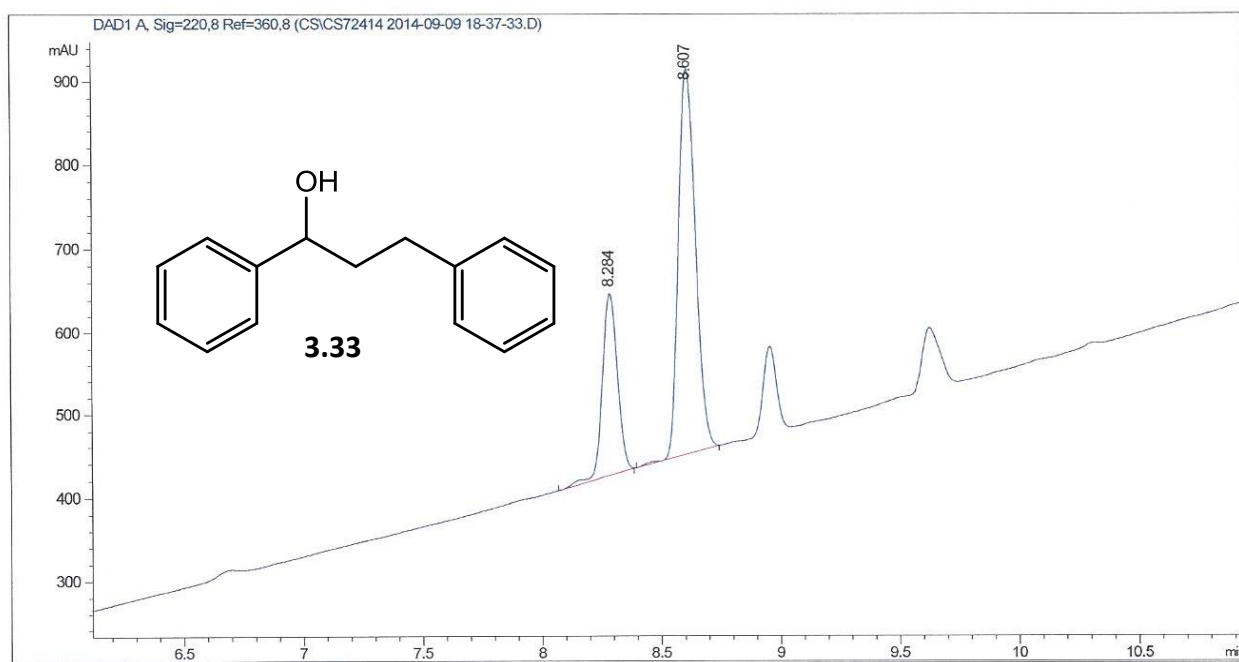


Figure A30. The chiral HPLC chromatogram of compound **3.33**



Current Data Parameters
NAME Sap29-2016-WJACSH00LA
EXPNO 2
PROCNO 1

F2 - Acquisition Parameters
Date_ 20160929
Time 11.34
INSTRUM spect
PROBHD 5 mm PABBO BB-
PULPROG zg30
TE 300.2
SOLVENT cmc13
NS 128
DS 2
SWH 6009.515 Hz
FIDRES 0.091599 Hz
AQ 5.4525952 sec
RG 90.5
DW 83.300 usec
DE 6.50 usec
TE 300.1 K
U1 1.0000000 sec
TE0 1

===== CHANNEL f1 =====
NUC1 300.1318334 MHz
P1 15.00 usec
PLW1 8.0200046 W

F2 - Processing parameters
S1 32768
SF 300.1300164 MHz
WDW EM
SSB 0
LB 0.30 Hz
GB U
PC 1.00

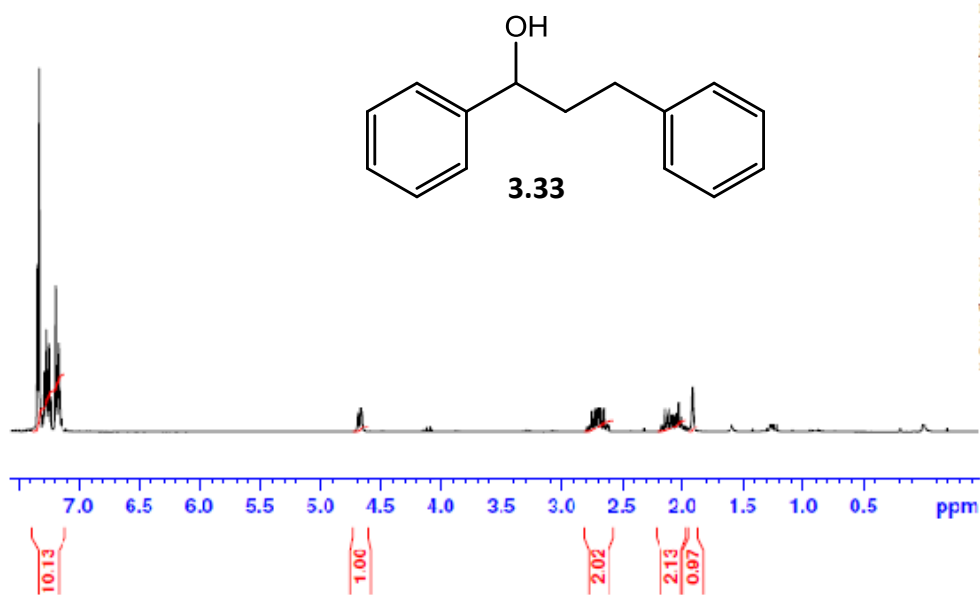
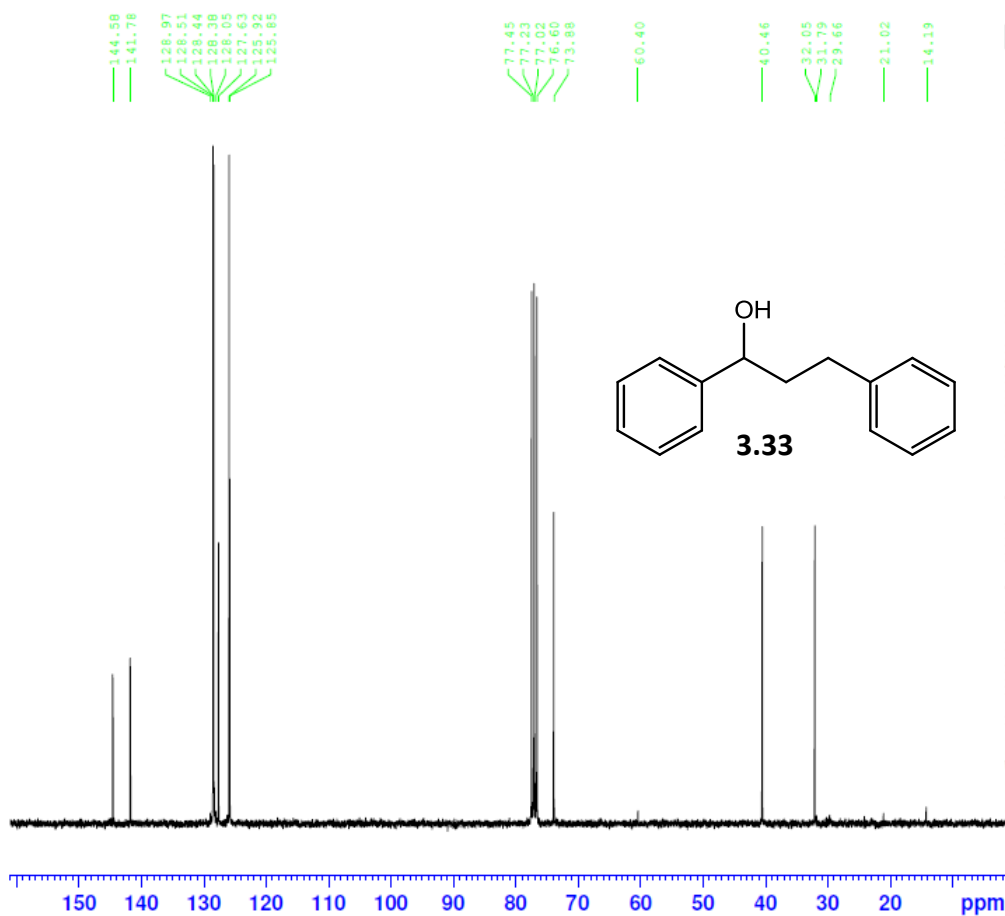


Figure A31. The ¹H NMR spectrum of compound 3.33

CS92514-2



Current Data Parameters
NAME Sep29-2014-NJACSHOOLA
EXPNO 3
PROCNO 1

F2 - Acquisition Parameters
Date_ 20140929
Time 13.09
INSTRUM spect
PROBHD 5 mm PABBO BB-
PULPROG zgpg30
TD 65536
SOLVENT CDCl3
NS 1024
DS 4
SWH 18028.846 Hz
FIDRES 0.275098 Hz
AQ 1.8175317 sec
RG 1620
DW 27.733 usec
DE 6.50 usec
TE 300.1 K
D1 2.00000000 sec
D11 0.03000000 sec
TD0 1

CHANNEL f1
SF01 75.4752949 MHz
NUC1 13C
P1 10.40 usec
PLW1 28.88699913 W

CHANNEL f2
SF02 300.1312005 MHz
NUC2 1H
CPDPRG[2] waltz16
PCPD2 90.00 usec
PLW2 8.02000046 W
PLW12 0.22278000 W
PLW13 0.18045001 W

F2 - Processing parameters
SI 32768
SF 75.4677509 MHz
WDW EM
SSB 0
LB 1.00 Hz
GB 0
PC 1.40

Figure A32. The ¹³C NMR spectrum of compound 3.33

File :C:\DATA\1408\EXPCS081014.D
Operator :
Acquired : 27 Aug 2014 11:41 using AcqMethod ZB100ND_B_MANUAL.M
Instrument : GCMS04
Sample Name: EXPERIMENT CS081014
Misc Info : ZB100ND_B, SP150:1, IN ACETONE
Vial Number: 0

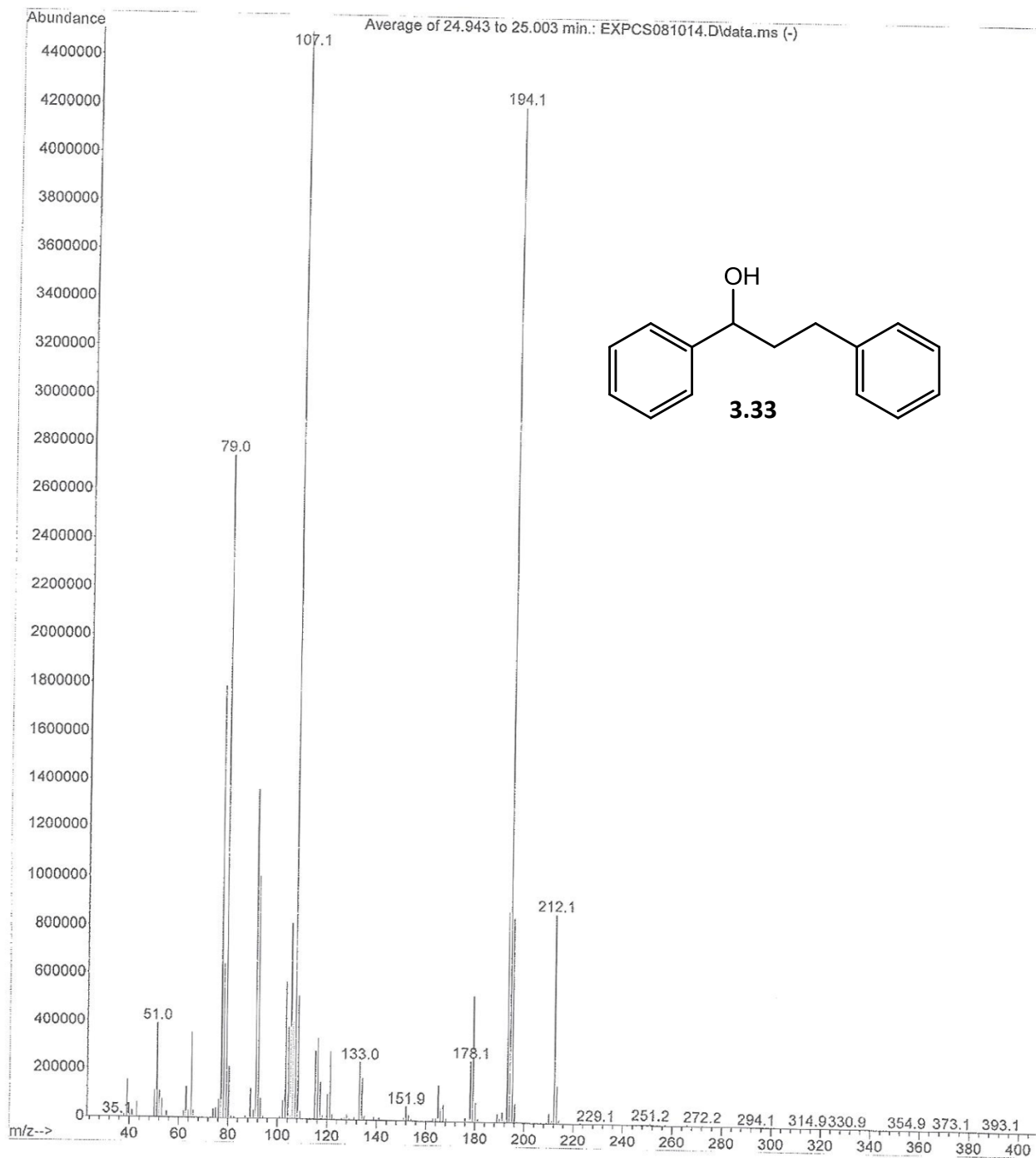


Figure A33. The mass spectrum of compound 3.33

A Final Thought....

“If you would cause your view... to be acknowledged by scientific men; you would do a great service to science. If you would even get them to say yes or no to your conclusions it would help to clear the future progress”

- Michael Faraday

To God be the glory, for His mercy endureth forever.

Christopher Olugbenga Olusegun Shoola, Ph.D.